REPUBLIC OF TÜRKİYE
HASAN KALYONCU UNIVERSITY
GRADUATE EDUCATION INSTITUTE
CIVIL ENGİNEERİNG DEPARTMENT

A MAPPING STUDY OF GEOTECHNICAL SOIL PROPERTIES OF TUNCELİ PROVINCE USING GIS

SONER KORKMAZ

M.Sc. THESIS

GAZİANTEP - 2023

GRADUATE EDUCATION INSTITUTE
THESIS ACCEPTANCE AND APPROVAL FORM

Civil Engineering Department, Civil Engineering Master Programme student Soner KORKMAZ prepared and submitted the thesis titled "**A Mapping Study of Geotechnical Soil Properties of Tunceli Province Using GIS**" and defended **successfully** at the date of 20/01/2023 and accepted by the jury as a M.Sc. Thesis.

Position	Title, Name and Surname	Departmant/University	Signature
Supervisor	Assist. Prof. Dr. Nurullah AKBULUT	Hasan Kalyoncu University	
Jury Member	Prof. Dr. Hanifi ÇANAKÇI	Hasan Kalyoncu University	
Jury Member	Assoc. Prof. Dr. M. Eren GÜLŞAN	University of Gaziantep	

This thesis is accepted by the jury members selected by institute management board and approved by institute management board.

Prof. Dr. M. Serhat YENİCE
Director

TEZ BİLDİRİMİ

Bu tezdeki bütün bilgilerin etik davranış ve akademik kurallar çerçevesinde elde edildiğini ve tez yazım kurallarına uygun olarak hazırlanan bu çalışmada bana ait olmayan her türlü ifade ve bilginin kaynağına eksiksiz atıf yapıldığını bildiririm.

DECLARATION PAGE

I hereby declare that all information in this document has been obtained and presented in accordance with academic rules and ethical conduct. I also declare that, as required by these rules and conduct, I have fully cited and referenced all material and results that are not original to this work.

Soner KORKMAZ

20.01.2023

HASAN KALYONCU ÜNİVERSİTESİ
LİSANSÜSTÜ EĞİTİM ENSTİTÜSÜ
İNŞAAT MÜHENDİSLİĞİ ANABİLİM DALI

TUNCELİ İL MERKEZİNİN GEOTEKNİK ZEMİN ÖZELLİKLERİNİN CBS İLE HARİTALANMASI CALIŞMASI

SONER KORKMAZ

YÜKSEK LİSANS TEZİ

Danışman
Dr. Ögr. Üyesi Nurullah AKBULUT

ÖZET

Coğrafi Bilgi Sistemi (CBS) teknolojisinin mühendislik projelerinde kullanılması oldukça önemlidir, çünkü verimliliği artırır, zaman kazandırır ve maliyetleri düşürür. CBS, arazi verilerini haritalama, veri depolama ve analiz etme görevlerinde kritik bir rol oynar ve bilgi paylaşımını kolaylaştırır. Haritalar, veriler ve analitik yetenekleri entegre ederek mühendislere projenin sonuçlarını daha iyi görselleştirme, erişim sağlama ve paylaşma avantajları sunar, bu da nihayetinde proje kalitesini artırır. Zemin özelliklerini anlamak, binaların ve altyapının planlanması, inşası ve uzun vadeli güvenliği açısından temel bir öneme sahiptir. Bu, zemin taşıma kapasitesi, sıvılaşma riski, kayma dalgası hızı gibi faktörlerin belirlenmesini içerir ve bu özelliklere dayalı olarak zemin seçimi hakkında bilinçli kararlar almayı içerir. Bu çalışma, şehir planlama amaçları için Tunceli Belediye İmar Müdürlügü tarafından talep edilen, farklı derinliklerdeki (3.0, 4.5, 7.5, 9.0 ve 15 m) sondaj kuyularının SPT-N değerlerinin incelenmesine odaklanılmıştır. Zemin bilgileri, laboratuvar test sonuçları ve 96 sondaj noktasından elde edilen jeolojik bilgilerin kapsamlı bir analizi gerçekleştirilmiştir. CBS yazılımı kullanılarak, sondaj verileri, laboratuvar deney sonuclari ve jeofizik test sonuçlarından türetilen hesaplamalar kullanılarak geoteknik haritalar oluşturulmuştur. SPT-N değerlerinin, taşıma kapasitesinin, kayma dalgası hızının, zemin büyütmesinin, hakim titreşim periyodunun ve ülkelerin deprem kodlarına dayalı olarak zemin sınıflandırmalarının değerlendirmeleri dahil olmak üzere çeşitli analizler, haritalama faaliyetleri ve değerlendirmeler gerçekleştirilmiştir. Çalışmanın bulguları, çalışma alanında SPT-N değerlerinin 35'i aşan bir yaygınlığını ortaya koymaktadır. Zemin taşıma kapasitesi değerlendirmeleri, Terzaghi & Peck ve Meyerhof hesaplama yöntemleri kullanılarak 300-600 kN/m^2 aralığında sonuçlar vermiştir. Özellikle Cumhuriyet, Moğultay ve Atatürk mahallelerinde 1.5 metre derinlikte daha düşük taşıma kapasitesi değerleri gözlemlenmiştir. Ayrıca, çalışma alanının merkezi bölümünde, Atatürk, Cumhuriyet ve Moğultay mahallelerini içeren sıvılaşma riski olabilecegi, diğer alanlarin sıvılaşmayacagi tespit edilmistir. 30 metre derinlikte hesaplanan kayma dalgası hızı değerleri, 286 m/sn ile 1271 m/sn arasında değişmektedir.

Anahtar Kelimeler: Tunceli, haritalandirma, CBS, SPT, geoteknik.

HASAN KALYONCU UNIVERSITY
GRADUATE EDUCATION INSTITUTE
DEPARTMENT OF CIVIL ENGINEERING

A MAPPING STUDY OF GEOTECHNICAL SOIL PROPERTIES OF TUNCELİ PROVINCE USING GIS

Soner KORKMAZ

MASTER THESIS

Supervisor
Assist. Prof. Dr. Nurullah AKBULUT

ABSTRACT

The utilization of Geographic Information System (GIS) technology is highly significant in engineering projects as it improves efficiency, saves time, and reduces costs. GIS plays a crucial role in various tasks such as mapping land data, storing and analyzing data, and facilitating information sharing. By integrating maps, data, and analytical capabilities, engineers benefit from enhanced visualization, accessibility, and shareability of project outcomes, ultimately leading to improved project quality. Understanding soil properties is fundamental in the planning, construction, and long-term safety of buildings and infrastructure. It involves determining factors like soil bearing capacity, susceptibility to liquefaction, shear wave velocity, and making informed decisions about soil selection based on these properties. In this study, a comprehensive analysis of geotechnical soil data, laboratory test results, and geological information from 96 borehole sites was conducted. The focus was on examining SPT-N values at different depths of the boreholes (3.0, 4.5, 7.5, 9.0, and 15 m) commissioned by the Tunceli Municipality Urban and City Planning Provincial Director for urban planning purposes. Geotechnical maps were created using ArcGIS software by calculations derived from borehole data, laboratory soil tests, and geophysical testing results. Various assessments, mapping activities, and analyses were carried out, including evaluations of SPT-N values, bearing capacity, shear wave velocity, soil amplification, dominant vibration period, and soil classifications based on earthquake codes such as NEHRP, EUROCODE8, and TBDY-2019. The study findings revealed a prevalence of SPT-N values exceeding 35 within the study area. Soil bearing capacity assessments were conducted using the Terzaghi & Peck and Meyerhof calculation methods, yielding a range of 300-600 kN/m^2. Notably, lower bearing capacity values were observed at a depth of 1.5 meters in certain areas such as the central, eastern, Cumhuriyet, Moğultay, and Atatürk neighborhoods. Furthermore, a liquefaction risk was identified in the central part of the study area, encompassing Atatürk, Cumhuriyet, and Moğultay neighborhoods, while the remaining areas were classified as having "non-liquefiable" soils. Shear wave velocity calculations conducted at a depth of 30 meters yielded values ranging from 286 m/s to 1271 m/s.

Keywords: Tunceli, mapping, GIS, SPT, geotechnics.

PREFACE

I am grateful to have had the opportunity to embark on this journey of academic exploration and discovery. This thesis is the result of my hard work, dedication, and perseverance, and I am proud to share it with the academic community.

I would like to extend my sincere thanks to my advisor, Assist. Prof. Dr. Nurullah Akbulut, who has been an incredible mentor, providing invaluable guidance, support, and encouragement throughout this process.

I would also like to thank my friend Bahadır Karabaş for his encouragement and support, as well as for being a source of inspiration for me.

I would like to thank the Tunceli Municipality Directorate of Reconstruction and Urbanization, for enabling us to use the necessary resources to create the database.

Last but not least, I am grateful for my family, especially my wife and children, who have been my constant source of love, support, and motivation. Their unwavering faith in me has made it possible for me to pursue my academic goals.

I hope this thesis will make a meaningful contribution to the field of study and serve as a source of inspiration for future generations of researchers.

Soner KORKMAZ
Gaziantep - 2023

TABLE OF CONTENTS

LIST OF TABLES

LIST OF FIGURES

ABBREVIATIONS OR SYMBOLS LIST

A	Relative amplification coefficient
a_{max}	Peak ground acceleration (cm/sec^2)
ASTM	American society for testing and materials
B	Short side of foundation
BS	British standard
c	Cohesion
C_B	Borehole diameter correction in SPT test
C_E	Stem bar energy ratio correction in SPT test
C_N	Overburden correction in SPT test
C_R	Stem bar (rod) length correction in SPT test
CRR	Cyclic resistance ratio
C_S	Inner tube (sampler) correction in SPT test
CSR	Cyclic stress ratio generated by average horizontal shear stress
D	Foundation depth (m)
d	Density (gr/cm^3)
D_f	Foundation depth (m)
e	Slope and eccentricity of the load
E_r	Stem bar energy ratio for SPT test
FS	Factor of safety
g	Gravity acceleration (cm/sec^2)
G_{max}	Maximum Shear Modulus
H	Layer thickness (m)
$I_{s(50)}$	Point load index
I_C	Consistency index
I_L	Liquidity index
K_o	Ground Bearing Coefficient
L	Long side of the foundation
LL	Liquid Limit
MSF	A revised magnitude scaling (correction) factor
N	SPT blow number
$N_{1,60}$	Corrected SPT blow number

NEHRP	National earthquake hazard reduction program
$\mathbf{P_{atm}}$	Atmospheric pressure 100 kPa
PI	Plasticity index
PL	Plastic Limit
$\mathbf{q}$	Bearing capacity (kN/m^2)
$\mathbf{q_{all}}$	Allowable bearing capacity (kN/m^2)
R	Radius of earth epicenter (km)
$\mathbf{r_d}$	Stress reduction factor
SPT	Standard penetration test
$\mathbf{T_o}$	Soil dominant vibration period (sec)
UCS	Unconfined compressive strength
UD	Undisturbed sample
$\mathbf{v}$	Poisson's ratio
$\mathbf{V_{30}}$	Shear wave velocity for depth of 30 meters (m/sec)
V_p	Compression wave velocity (m/sec)
V_s	Shear wave velocity (m/sec)
W_n	Water content
GWL	Groundwater level
$\mathbf{\Phi}$	Angle of friction
$\boldsymbol{\alpha}$	Coefficients to correct $(N_1)_{60}$ based on fine content values
$\boldsymbol{\beta}$	Coefficients to correct $(N_1)_{60}$ based on fine content values
$\boldsymbol{\gamma}$	Unit weight (kN/m^3)
$\boldsymbol{\sigma'_{vo}}$	Vertical effective stress (kPa)
$\boldsymbol{\sigma_{vo}}$	Vertical Total stress (kPa)
$\boldsymbol{\tau_{avg}}$	Average horizontal shear stress (kPa)

1. INTRODUCTION

1.1. General

Site investigation is a crucial step prior to constructing infrastructures. It involves collecting soil samples at varying depths below the ground surface and conducting geotechnical tests on these samples. The purpose of these tests is to determine various parameters that are commonly used by geotechnical designers to select the appropriate footing and foundation design.

In the field of geotechnical practice, the conventional method of collecting data in the actual location can be a time-consuming task. However, there are existing sources of historical data available in various formats such as hard copies, electronic files, and paper materials, including maps, reports, manuals, and even photos. These sources can be integrated and used together with a GIS digital mapping platform to save time and enhance efficiency and effectiveness in data analysis (Shaik, 2007).

Geological and geographical engineers have developed a novel method for gathering, organizing, and studying different types of site investigation data. The use of GIS allows for the presentation and analysis of digital maps and other graphical information, enabling designers to have a clear and accurate visualization of the project. This comprehensive approach facilitates effective decision-making and aids in the creation of the optimal design.

Although utilizing big data and comprehensively covering all the geotechnical characteristics of soil (including physical and mechanical properties) has not yet been achieved, doing so would provide engineers with greater accuracy during the preliminary design stage to appropriately select the most suitable foundation for their project. Creating digital maps would assist geotechnical engineers by providing useful information and an understanding of soil layers, allowing them to make informed decisions about the type of footing required in preliminary and feasibility studies.

This thesis involved the collection, classification, and analysis of extensive site investigation data from a significant number of boreholes (specifically, 96 boreholes). These data covered an area of approximately 30 km^2, spanning from the north of Tunceli governorate to the south and from the east to the west. Using ArcGIS environment facilities, a digital database was created to document the physical and mechanical properties of the soil throughout the entire investigated area. The technique utilized in this thesis, which involved 2D GIS mapping software, can also be employed in the future to encompass all soil properties in Türkiye. This methodology has proven to be beneficial for engineers and city planners, as it facilitates the easy analysis of geotechnical properties, thereby simplifying the design and planning stages of any engineering project.

1.2. Objective of the Study

This thesis focusses on the evaluation of geotechnical survey reports obtained from the Municipality of Tunceli. The study aims;

- To gather the geotechnical data from the documents and create a geotechnical database.
- To make geotechnical analysis and calculations of datas (bearing capacity, liquefaction, shear wave velocity).
- To enter the data into the ArcGIS software and,
- To transfer the geotechnical properties of Tunceli province to digital maps by using GIS.

1.3. Organization of the Study

Chapter 1: This chapter provides an overview of the study's focus, outlining the background, research objectives, significance, and research questions that guide the evaluation of geotechnical data and its integration into the Geographic Information System (GIS) for mapping applications in Tunceli province.

Chapter 2: This chapter reviews previous research on engineering soil properties, bearing capacity, and liquefaction analyses, GIS studies in geotechical engineering while identifying gaps in the existing literature.

Chapter 3: This chapter provides an in-depth exploration of the geological and geographical characteristics of Tunceli Province, encompassing its geographical location, climate, temperature, vegetation, geological features, stratigraphy, structural geology, geomorphology, and an analysis of the seismic activity within the region. This chapter lays the foundational understanding of the study area for subsequent research.

Chapter 4: This chapter serves as the foundation of the entire study, outlining the methodology used for the empirical investigations. It provides a comprehensive explanation of the techniques used for data collection and processing, highlighting the crucial role of Geographic Information System (GIS) in integrating the data for analysis.

The chapter also thoroughly describes the collection process for both fieldwork and laboratory experiments, with a focus on the spatial distribution of soil properties using GIS. It places significant emphasis on soil bearing capacity, emphasizing its importance and the creation of soil bearing capacity maps through GIS. Furthermore, it explores the critical aspect of soil liquefaction potential, presenting the methodology used and showcasing results through descriptive maps, contributing significantly to the assessment of seismic risk in the Tunceli province.

Chapter 5: This chapter presents an in-depth interpretation of the findings from the data analysis, fostering discussions on observed patterns, trends, and variations in soil properties, bearing capacity, and liquefaction potential. It also compares the results with existing literature and underscores the implications of these findings in the context of soil engineering and infrastructure planning.

Chapter 6: In this concluding chapter, the study synthesizes the main findings, draws comprehensive conclusions, highlights contributions to the field of soil engineering, acknowledges study limitations, and provides valuable recommendations for future research in Tunceli province.

Chapter 7: This chapter serves as a comprehensive list of all the sources, studies, and literature cited throughout the thesis, providing readers with a clear reference point for the sources underpinning the research.

2. LITERATURE REVIEW

In this section, previous studies related to the thesis subject are mentioned.

2.1. General

Geoinformatics, which encompasses the field of Geographic Information Systems (GIS), plays a pivotal role in the collection, analysis, and effective management of spatial data, making it an invaluable tool in various domains. This literature review delves into the diverse subjects and applications within the realm of GIS and geotechnical studies.

Today, there is much data about the Earth in spatial information systems and more complex data collection technologies. Information systems are gaining more and more importance due to the rapidly increasing number and variety of data. GIS are systems created to enter, operate, store, analyze, display, and reveal spatial original computer environments such as graphics and features in different formats. GIS can be examined in two parts according to whether they are connected to any location or not. GIS collects spatial and non-spatial data with different methods, storing them in a specific system and managing them by the purpose. Non-Spatial Information Systems are information systems in which transactions are made on information that is not dependent on location (bank, library, hotel, or flight reservation systems). Spatial Information Systems are information systems that collect, model, and analyze data in a specific location on the Earth for different purposes. In spatial information systems, coordinates indicating the geographical location of each data are also given. Many studies have been carried out in different fields related to GIS. The management of roads of different sizes providing transportation and infrastructure systems that provide maintenance, repair, and management of electricity, water, dam, and sewerage networks can be examples of spatial information systems. GIS is instrumental in creating earthquake damage maps, which provide crucial insights for disaster management and risk assessment. Furthermore, GIS is employed in land use planning and urban development, enabling the optimization of resources and infrastructure. City planning benefits significantly from GIS, facilitating spatial organization and development. Additionally, GIS plays a vital role in earthquake risk mitigation, assisting in the generation of damage maps that inform decision-making and disaster preparedness. The adaptability of GIS across these diverse fields underscores its invaluable role in spatial data management and analysis (Aranoff, 1989; Marx, 1992; Haala et al., 1998; Tecim, 1999; Anand, 2000).

Since Türkiye is placed in the earthquake zone due to its geographical location, it is essential to determine the safe and risky areas in terms of soil characteristics in planning settlement areas. For this reason, many studies are carried out to determine the engineering properties of soils and to reveal the change in soil properties in a specific region. Many different disciplinary methods are used to determine soil properties. Geotechnical, geological, and geophysical sciences come together and contribute to the completion of soil investigations. Over the last 20 years, the use of this technique has become widespread across the globe. Its effectiveness has been demonstrated in various locations with the studies from the literature (Çiftçi, 2020; Dinç, 2020).

Bargu et al. (2000) conducted a Geological-Geotechnical survey of the Gürsu (Bursa) Area. In their study, 25 boreholes and ten exploration pits were drilled in the Gürsu settlement area, and 25 seismic refraction and 25 resistivity methods were applied. In addition, the authors gave information about what precautions should be taken in the region and what should be considered in building buildings. As a result of this study, they stated that liquefaction is possible in the settlement area.

Haşimoğlu et al. (2004), Kütahya province Yoncalı region ground survey reports such as drilling, research pit, and geophysics were transferred to the digital environment by using GIS techniques.

Şen (2004) examined the liquefaction potential index distribution on the GIS platform. For this, they carried the area around the Gümüşler Municipality of Denizli province as an example. They determined the liquefaction risk by calculating the SPT values of the soils in this area.

Alparslan et al. (2006), with the help of GIS, this information such as permeability status, geology, susceptibility of soils to liquefaction, groundwater, faults, hydrology and old landslide areas, land cover, plant index, and surface temperature of the region between Büyükçekmece and Kucukcekmece Lakes were compared and analyzed in landslide susceptibility analysis. It has been used in this area, and landslide zones with high, medium, and low sensitivity have been determined.

Demirci et al. (2006), on the other hand, channeled the land use changes of the Istanbul Kucukcekmece watershed between 1963 and 2005 using GIS with the help of a comparison of water samples. They tried to determine these usage changes and the water quality of the Kucukcekmece Lake water basin.

Ergun and Sarac (2006), made an application about health geography in GIS. GIS spatial analysis of health services has been examined.

Karavul et al., (2006), produced SPT maps with two different approaches using GIS. For the SPT maps of Adapazarı city, a database was created with the SPT values pf the drillings which were made in the city center. Elastic modulus, poison ratio, wave velocity, and shear modulus maps were created using GIS.

Kargı and Sarı (2006) drew a map of the area by processing satellite images of Denizli region for mineral exploration.

Kıncal's (2006) study in the Izmir region can be given as an example of the studies in which the maps of land slope and geological data layers are created with the help of GIS.

Sert et al. (2006), emphasized the importance of data analysis, reducing the error loss of the maps, and the importance of the process while creating soil maps. In this study for geotechnical purposes of Adapazarı, bearing capacity map, liquefaction map, and damage maps were created.

Kincal et al. (2007), prepared geotechnical maps of the settlement area of Armutalanı town and added the borehole data, geophysical data, laboratory test results, bearing capacity values, and soil liquefaction analysis to the database in digital format.

Chung (2007) used geotechnical information as data in the city of Lous, and estimated engineering maps using various GIS methods. With the information received from the boreholes and soil profiles, classification maps and groundwater maps were drawn.

Karaca (2007) investigated the engineering properties of Fethiye soil and their geotechnical maps with GIS. He determined the engineering features of Fethiye and its surroundings and prepared the geological maps using GIS systems. As a result of the study, he obtained maps showing the slope, liquefaction potential, groundwater depth from the surface, groundwater level, dominant vibration period, soil earthquake amplification, and the velocity of elastic waves in soil layers.

Ayday et al. (2008), examined the geological and geotechnical properties, liquefaction potential, groundwater, and soil properties of the places within the borders of Tepebaşı Municipality and west of Eskisehir in GIS environment.

Elmasdere (2008) evaluated the area in a geotechnical point of view and conducted a microzonation and evaluation of Isparta Mavikent Area. Microzonation, wave velocity maps, ground dominant vibration period, and soil amplification maps were taken as the basis and benefited from earthquake scenario studies.

Kiyak et al. (2008) used the fuzzy logic method in the GIS environment in the study of Adapazarı province.

Yomralıoğlu, (2009) stated that GIS, like all other information systems, primarily simplifies the decision-making process and shortens the process. Furthermore, the use of attribute information in conjunction with location information sets GIS apart from other information systems.

Demir (2013) produced for the Gürsu residential area by extracting the general soil profile and determining the variation of the engineering properties of the soils and using GIS software. In his study, primarily the contour lines of the study area were digitized using the Esri ArcInfo 9.3 program. Then, the curves showing the underground level elevation of the region were digitized. Gürsu district, which is of 135 hectares, is defined by alluvial soil. Many geoengineering maps for land use were produced.

Canbolat (2016) investigated allowable bearing capacity and liquefaction potentional in Kahramanmaras by GIS.

Yılmaz (2019) investigated the engineering geology, geotechnical characteristics, and slope stability conditions of a Siirt Eruh district which is affected by landslides.

Başdemir and Dinçer (2019) assessed the geotechnical characteristics and potential for soil liquefaction in eight neighborhoods. Their evaluation was based on the geological-geotechnical survey reports derived from the zoning plan of an 8500-hectare area approved by Osmaniye Municipality in 2016.

Karabas (2019) analyzed the survey reports conducted at 192 drilling points in Malatya for creating several digital GIS maps. He made several analyses, including SPT-N, bearing capacity, groundwater level, liquefaction potential, soil classification and earthquake hazard level analysis.

Das et al. (2019) studied liquefaction caused by major earthquakes. They collected data from 97 boreholes using the SPT to determine liquefaction occurrence in Agartala, India. The findings were presented in the form of a software map called GIS-based QCBS. Based on the general liquefaction index (LPI) limit, the urban center exhibited varying levels of liquefaction potential, with the northern continental middle being classified as non-liquefiable and the southern part potentially non-liquefiable.

Ilic et al. (2020) used GIS to support urban seismic reduction policies at the urban scale.

Sartirana et al. (2020) emphasized the importance of archiving geotechnical data for settlement areas. They successfully and efficiently managed underground water management in the Milan metropolitan area by creating a GIS database for underground infrastructure such as private parking lots, public parking lots, metro lines and stations.

Calzolaria et al. (2021) used GIS to create soil type maps at a scale of 1:50,000. These maps aimed to predict the spatial distribution of soils and their liquefaction characteristics. The researchers successfully generated maps that exhibited various distribution patterns. These patterns were found to be in line with the observed relationships between soil groups and the combination of terrain features and parent materials.

Şengül and Karabaş (2021) evaluated the field and laboratory results obtained from 61 boreholes in Kütahya by GIS. GIS provided helpful information visually and numerically by producing geotechnical, SPT-N distribution, bearing capacity, liquefaction potential, and damage distribution maps.

Al Hamaydeh et al. (2021) created a risk map to reveal damage maps against seismic hazards in a network- GIS modeling system.

Demirtaş (2022) and Göksular (2022) examined the soil index properties, soil classification, and bearing capacity calculations using 210 and 178 borehole logs in Elazığ and Siirt province by GIS, respectively.

3. GENERAL GEOLOGY AND FEATURES OF THE STUDY AREA

This section mentions the study area's general features, geographical location, geology, and seismicity.

3.1. Geographical Location of the Study Area

The location of study area is shown in Figure 3.1. Tunceli is located in the west of the Eastern Anatolian region, in the Upper Euphrates section, and its lie between 38° 19' and 40° 26' east longitudes and 39° 36' and 38° 46' north latitudes. The province's total area is 7,774 km² and is surrounded by the provinces of Erzincan from the north and west, Elazığ from the south, and Bingöl from the east. The altitude of Tunceli Province is 914 meters, and Cumhuriyet Neighborhood, Esentepe Neighborhood, Moğultay Neighborhood, Alibaba, İsmet İnönü and Yeni Neighborhood are the main neighborhoods.

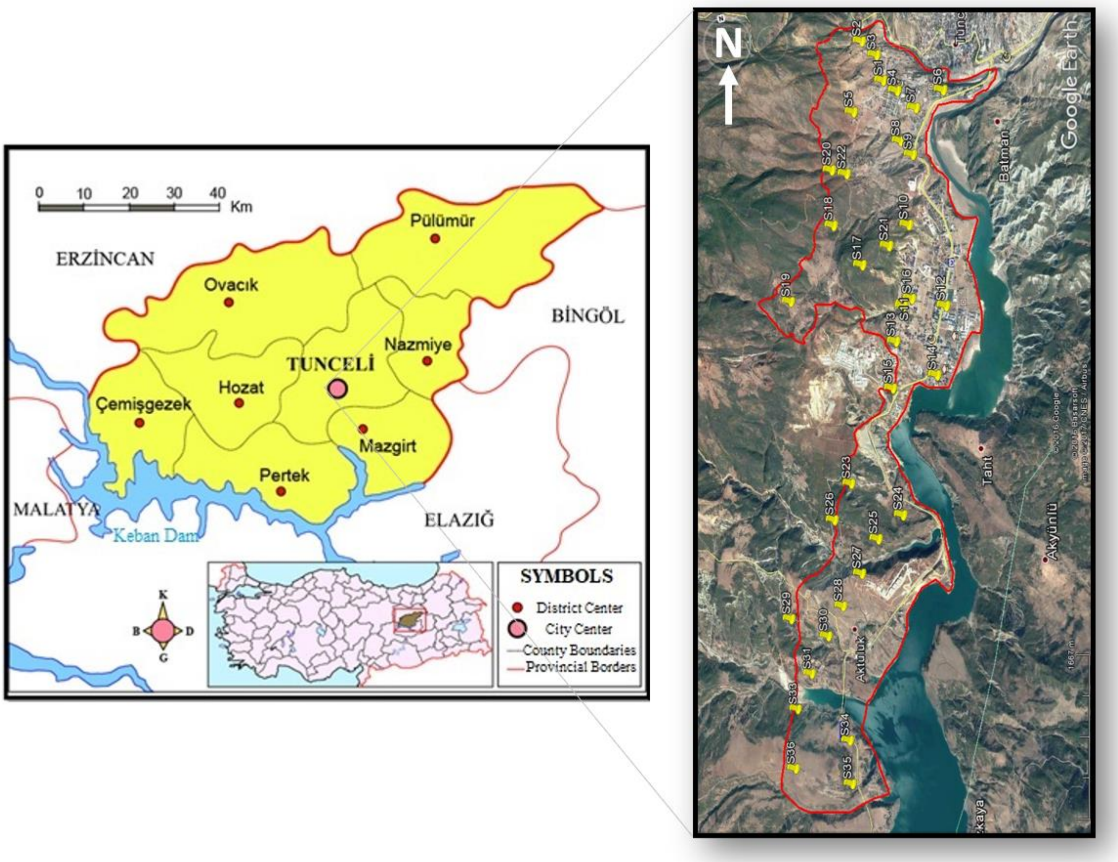

Figure 3.1. Location map of the study area

The extensions of the Eastern Taurus Mountains extend in the east-west direction and almost completely cover the province's northwest, north, and northeast. Tunceli could not integrate with the fertile depression area starting from Iğdır Plain at the eastern end of Turkey and extending to Erzincan Plain, as these mountains form insurmountable ranges. These mountains have turned into high plateaus by being eroded by surface waters and deeply carved by streams. The valleys are very narrow and steep, and there are no plains on the valley floors. Rising from the south to the north and from the west to the east, 70% of the province's lands are mountains, 25% are plateaued, and 5% are plains and plains. Most of the mountains are bare. Forests and heaths make up 30% of the provincial lands; Meadows and pastures make up 40%. The cultivated and planted area is 15%. There are more oak forests in the mountains. The plane, ash, juniper, hornbeam, and poplar trees are on the valley slopes. Grass abounds in pastures. Shrub-type maquis is common. The mountains within the provincial borders of Tunceli extend in the west-east direction as an extension of the Eastern Taurus Mountains. The Munzur Mountains and their extension, the Avcı Mountains, form the natural border in the northwest and northern parts of the province's lands, and Bağırpaşa Mountain is located in the northeast. Figure 3.2 shows the 96 boreholes examined throughout the study area.

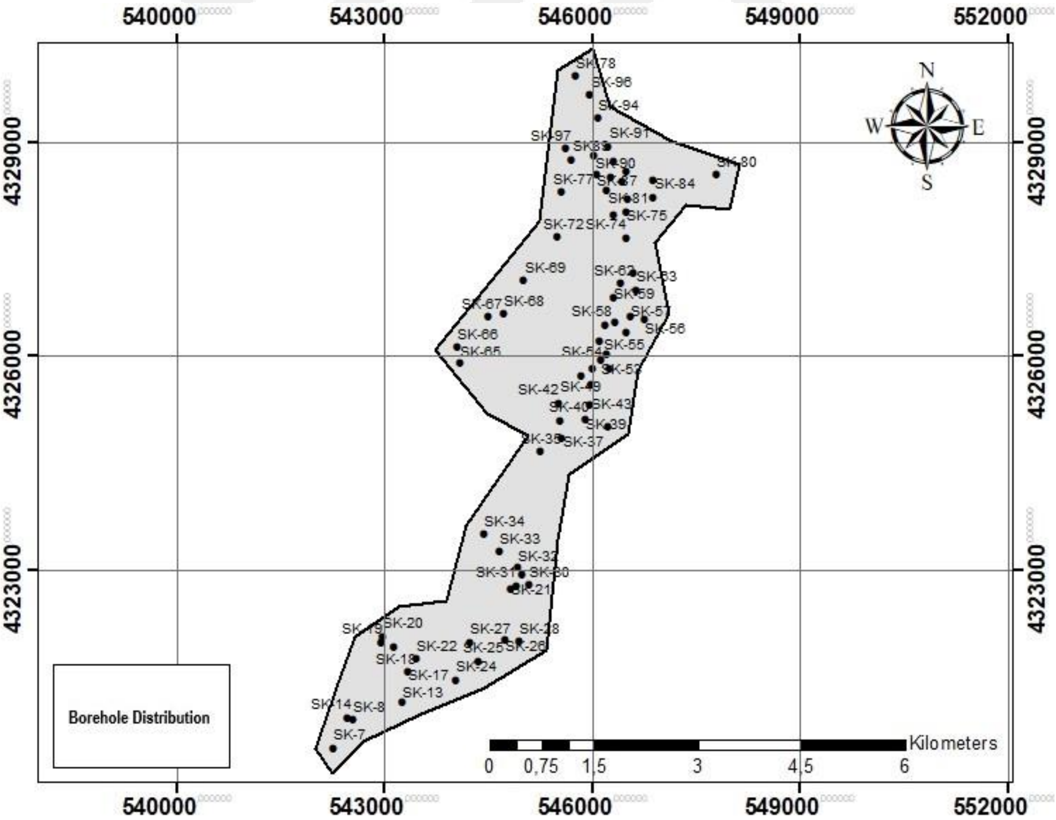

Figure 3.2. Map of the borehole points

3.2. Climate, Temperature and Vegetation of the Region

A harsh continental climate prevails in the province of Tunceli, located in the Upper Euphrates section of Eastern Anatolia. The short summer months are hot and dry, and the winters are very cold and rainy and last for a long time. Temperature differences between day and night and according to the months are very high. Annual precipitation in the province is 550-1080 mm. The lowest precipitation falls in summer and the most fall in autumn and winter. In summer, the climate is dry, with strong winds blowing from the northwest. In winter, the wind blows slightly from the southwest.

According to meteorological data, the highest temperature in summer is 42.2 °C in the southern parts, and the lowest temperature in the winter is around -26.6 °C in the mountainous parts of the north. According to the Tunceli central climate data, the average temperature is 12.5 °C. The very rough terrain of the province, from the mountainous areas at an altitude of 3500 meters in the north to 700 meters in the south, also creates significant differences in climate data, such as temperature, precipitation, wind, and sun exposure. Summers are cool and short; winters are long and very cold. The cold has been below zero degrees for months.

3.3. Geological Features of the Region

This region is located on the Taurus orogenic belt in Eastern Anatolia. The thickness consisting of flysch, tuff, basaltic-andesitic flows, and limestone forms the Lower Cretaceous, Upper Cretaceous, and Lower Eocene deposits, and the beds belonging to each period are separated from the other by a discordance. Lower Permian metasediments and Upper Permian subcrystalline limestones are the oldest formations cropping out in the region. The Lower Cretaceous flysch unconformably overlies the Upper Permian limestone, which has been partially eroded. The Lower Miocene marine limestone, unconformably overlying the Middle Eocene limestone, has passed into the lignite containing the Middle Miocene marls and the Upper Miocene red beds. After the Upper Miocene, this region was influenced by erosion and extensive extrusive volcanic activity. During the Permian, the region was included in the Tethys geosyncline, and during the Triassic-Jurassic, it was exposed to orogen, uplift, and erosion. It was considered geosynclinal from the Lower Cretaceous to the Middle Eocene and was influenced by the Varistic, Pre-Gosau, Laremian, Pyrenean, and Attic orogens (Tarhan, 2008; İlbank, 2015).

The sedimentary section above the base complex was strongly folded, faulted, affected by the volcanic intrusion, and eroded during all five orogenic episodes. The geological map of the study area and its surroundings was taken from MTA and the generalized stratigraphic section of the study area, and its immediate surroundings are given in Figure 3.3 (Tarhan, 2008; İlbank, 2015).

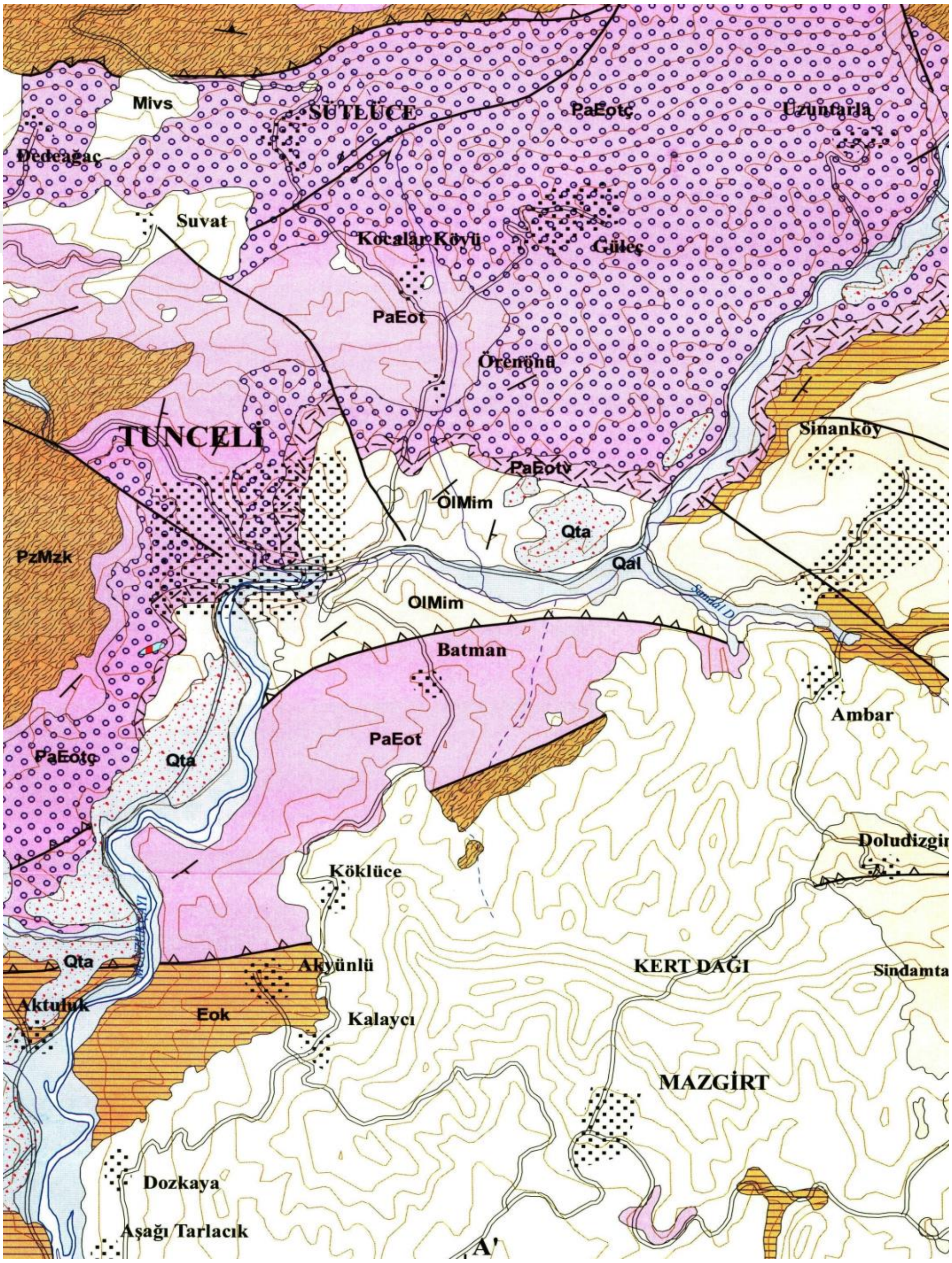

Figure 3.3. Geological map of the study area and its surrounding (Tarhan, 2008)

3.4. Stratigraphy

The 4.5-billion-year-old geological history of the Earth is generally divided into four geological periods, although there is no consensus on it. Precambrian is the oldest of these times, while the others are Paleozoic, Mesozoic, and Cenozoic. While the Cenozoic is divided into two periods, Tertiary and Quaternary, the first periods of the Precambrian are also called Hadean. When the Precambrian is taken together with the Hadean, its total duration reaches 4 billion years. This period equals eight times the duration of other geological cycles (Gradstein et al., 2012). In the study area of Tunceli province, at the bottom of Lower Permian-Upper Cretaceous Keban Metamorphics (PzMzk), Upper Paleocene-Lower Eocene aged Toraman Formation (PaEot), Oligo-Miocene Mollakulaçdere Formation (OlMim) and at the top unconformably Quaternary Alluviums (Qal). The figure below shows the formations of the study area in the Tunceli region.

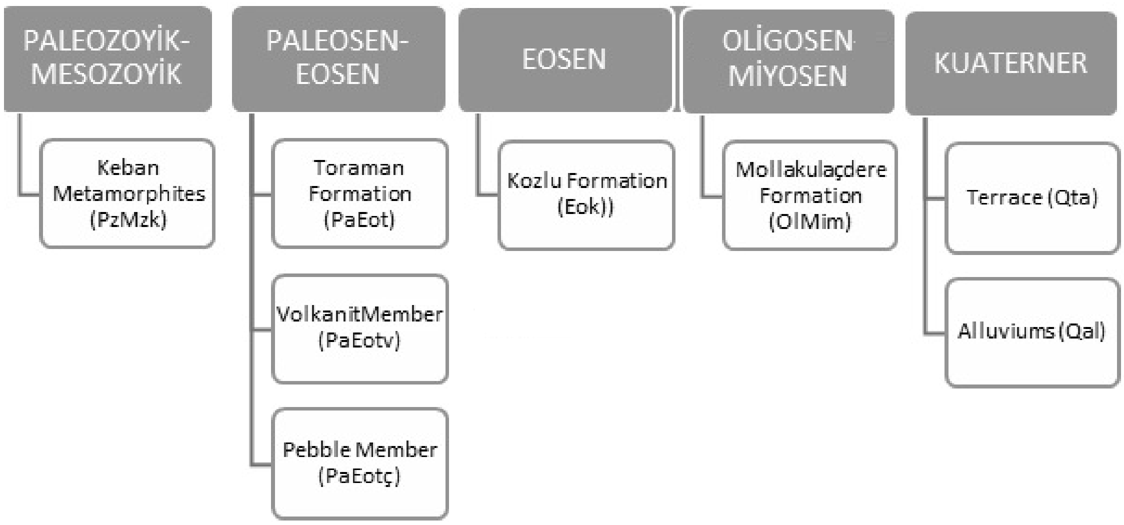

Figure 3.4. Geological periods according to Gradstein et al. (2012)

Keban metamorphites (PzMzk): The metaclastics cropping out around Tunceli-Pertek-Keban are named and described as "Keban metamorphics". In the southeast of the study area, fossils of Permo-Carboniferous and Cretaceous age from the metamorphics outcropping around Elazig, Keban, Pertek, and Nazimiye were determined by Oncel researchers. According to the region's stratigraphic and geological data, the Keban metamorphics are thought to be of the Late Paleozoic-Mesozoic age at the regional level. However, in different fields and regions, different researchers defined it with different names. Keban massif (Tolun, 1955), Keban unit (Özgül et al., 1981), Keban metamorphics (Perinçek, 1979; Özgül et al., 1981; Yazgan, 1983; Bingöl, 1982; Asutay, 1985) defined and named. The mentioned metamorphics are equivalent to the Keban metamorphics (İlbank, 2015).

Toraman Formation (PaEot): Erdoğan (1967) used Toraman for the Middle Eocene aged units. Tarhan (1989a) used the same name for the Late Paleocene-Early Eocene aged rock stratigraphic units cropping out around Toraman village (İlbank, 2015). The formation consists of gray-grey colored sandstone, conglomerate, calcarenite, limestone, clayey limestone, marl, Tuffy-clay limestone, tuffite, claystone, and tuffy marl rock types (flysch).

Conglomerate Member (PaEotç): The unit consists of red-wine colored and locally yellowish green colored conglomerate, sandstone, siltstone, and mudstone rock types (İlbank, 2015).

Volcanic Member (PaEotv): The unit consists of lava (basalt, basaltic andesite, andesite, andesitic basalt, trachyte-andesite, dacite) and pyroclastic rock (volcanic breccia, agglomerate, crystalline tuff, tuffite) types. It contains intercalations of terrestrial coarse and fine crumbs from place to place. The unit is equivalent to the Koçkar volcanic member, the Subaşı and Dedek formations (İlbank, 2015).

Kozlu Formation (Eok): The unit was named for the first time by Tarhan (1989a). The unit consists of conglomerate sandstone, mudstone, calcarenite, limestone, claystone, marl, tuffite, lava, and pyroclastic rocks (İlbank, 2015).

Mollakulaçdere Formation (OlMim): The unit was named for the first time by Özcan (1967). The formation consists of rock units representing different depositional environments (terrestrial, evaporite, marine) in the region. Marl consists of claystone, sandstone, tuff marl, limestone, tuffite, mudstone, lava, and pyroclastic rocks. The plant contains a coal crumb and its intermediates.

Terrace (Qta): Due to the active faults and uplift of the region around the riverbeds, they are old alluvial deposits that are higher than the current riverbed and correspond to the alluviums of the old stream bed. They are dense-fitting old alluvial deposits.

Alluvium (Qal): It consists of an unconsolidated block, gravel, sand, shaft, clay, and mud, containing various rock fragments and fragments in stream and stream bed. Terraces and alluviums unconformably overlie the lower units and form the youngest unit of the region. In Table 3.1, different formation names of the units found in the borehole are given (Tarhan, 2008).

Table 3.1. Different formation names and units passed in the boreholes

Borehole Number	Explanation
BH-79	Marble with clay intercalation was passed, and this well was dug in the Keban Metamorphites.
BH-31, BH-34, BH-35, BH-37, BH-39, BH-40, BH-42, BH-43, BH-45, BH-47, BH-48, BH-49, BH- 54, BH-58, BH-59, BH-65, BH-66, BH-67, BH-68, BH-69, BH-70, BH-71, BH-72, BH-73, BH-77, BH-78, BH-80, BH-81, BH-82, BH-84, BH-85, BH-86, BH-87, BH-88, BH-89, BH-90, BH-91, BH- 92, BH-93, BH-94, BH-95, BH-96 and BH-97	Conglomerate, mudstone, conglomerate, sandstone, claystone, marl, travertine, limestone and their residues take place in the formation.
BH-7, BH-8, BH-15, BH-18, BH-19, BH-22, BH-24, and BH-25	The units passing through the boreholes are sandstone, claystone, mudstone, and their residues take place in the formation.
BH-36, BH-50, BH-52, BH-53, BH-55, BH-57, BH-60, BH-61, BH-62, and BH-63	The units passing through the boreholes are andesite and conglomerate. Travertine, limestone, residuals, and the boreholes drilled in these units are located within the Mollakulaçdere Formation.
BH-1, BH-2, BH-3, BH-4, BH-5, BH-6, BH-7, BH-10, BH-11, BH-12, BH-13, BH-14, BH- 16, BH-17, BH-20, BH-23, BH-26, BH-27, BH-28, BH-38, BH-41, BH-44, BH-46, BH-51, BH-56, BH-74, BH-75, BH-76, and BH-83	These boreholes are old alluvial deposits that are higher than the riverbed and correspond to the alluviums of the old stream bed, and these boreholes were evaluated within the terrace.
BH-21, BH-29, BH-30, BH-32, and BH-33	This boreholes units consisting of clay, silt, sand, and gravel and their mixtures were passed, and the boreholes were evaluated in alluvium.

In line with the data obtained from the observational studies and drillings carried out in the northern part of the study area, it has been observed that the sandstones found here are gray, fractured-cracked, and the fracture-crack ratio decreases towards the depths.

In the studies carried out on the NE side of the study area, the Andesites were found in a small area; It was observed that they were gray, fractured, non-porous, and high in density.

The Mudstones were observed in the studies on the study area's northern side. The carbonate level increased and tightened from the upper to the lower levels, the carbonate in its composition became more dominant, and the mud ratio decreased. The red color, dominant in the upper levels, is replaced by yellowish muddy carbonate with the changing composition.

Conglomerates were observed in the studies carried out on the western side of the study area. It has been observed that it contains well-cemented carbonate and magmatic gravels with a shallow rate of fractures and cracks in gray-white color.

Travertines, seen on the side of the road parallel to the Tunceli-Elazığ highway in the study area, are white-yellowish in color, highly porous, filled with carbonate cement, and had plenty of fractures and cracks.

Travertines, seen on the side of the road parallel to the Tunceli-Elazığ highway in the study area, are white-yellowish in color, highly porous, filled with carbonate cement, and had plenty of fractures and cracks.

The Marbles observed in the studies carried out on the NW side of the study area. It was observed that it was dirty white-blackish in color, quite hard and high in density, and had a high fracture-crack rate. The cracked crack surfaces have acquired a brown color with an alteration effect.

Marls observed in the studies carried out on the western side of the study area. It has been observed that it is composed of beige-light brown colored, generally 3-10 cm thick layers, and does not present a structure that is highly fractured-cracked, fragmented, and weathered in places.

a) **b)**

Figure 3.5. Section view of a) Kozlu formation and b) Toraman formation

3.5. Structural Geology

The Tunceli Province settlement area is located within the Eastern Anatolian Fault (EAF) System and has been tectonically active since the Mesozoic time (Palutoğlu and Tanyolu, 2006).

The study area and its surroundings were shaped by the collision of Arabian and Anatolian plates in the late Miocene. The layering in the region, which has a sedimentary structure, is quite evident. The deformation started with folding first, and continued lateral pressures caused the formation of large fractures.

In the road cuts near the study area, outcrops of claystone, sandstone, marl, and limestone intercalations belonging to the Tunceli Formation are observed. The strikes of these units are approximately NE-SW and NW-SE in the form of shear fractures. In addition, there are badinage (sausage) structures in the sandstone and limestone layers of different thicknesses within the unit. Apart from these structures, there are not too large fractures with random directions that do not have a regular system. (Palutoglu, Tanyolu 2006). The plates on the earth's crust and their relative movements are shown in the Figure 3.6.

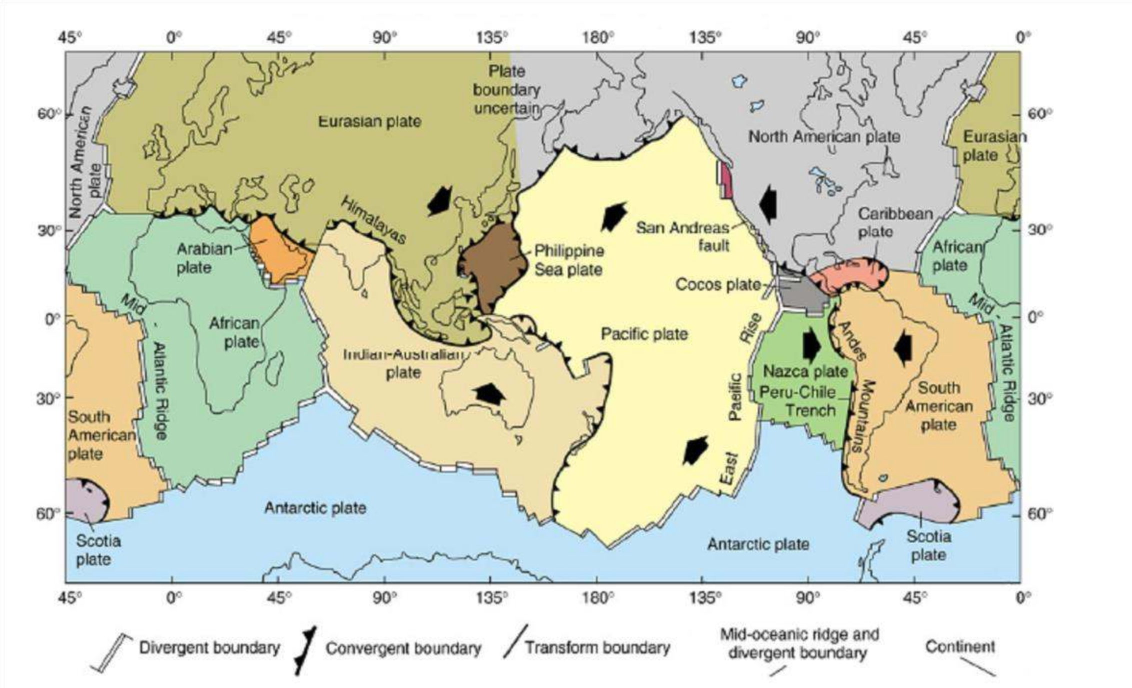

Figure 3.6 Plates on the Earth's crust and their movements relative to each other. (Palutoğlu, 2006)

The active fault map within a 100 km radius of Tunceli city center is given in Figure 3.6. The North Anatolian Fault-Yedisu segment in the north of the study area, the Nazimiye Fault nearby, the Ovacık Fault-Munzur Segment in the northwest, and the East Anatolian Fault in the south.

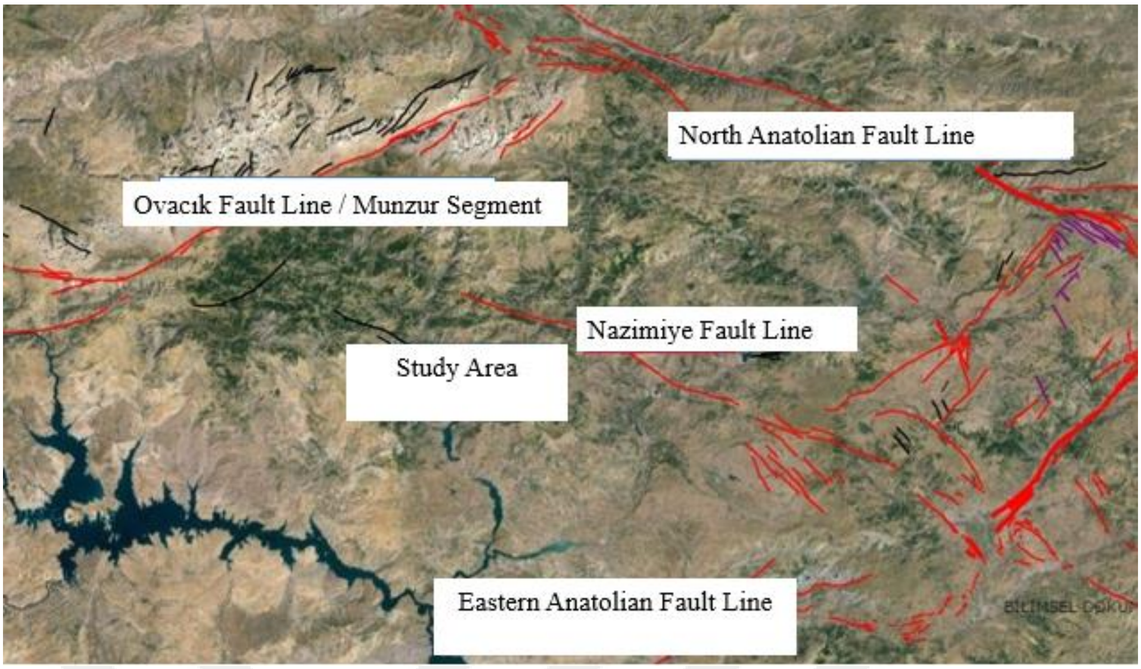

Figure 3.7. Faults in and around the study area (Şaroğlu, 1987)

East Anatolian Fault (EAF): The EAF, which is a left-sided strike-slip fault, was named by Arpat and Şaroğlu (1972). Arpat and Şaroğlu (1972, 1975) indicated the Hatay Graben, where the fault starts from Karlıova and passes through Bingöl, Palu, Hazar Lake, Sincik, Çelikhan and Gölbaşı.

Southeast Anatolia Overlay: There is a significant thrust zone in the SE of Türkiye, starting from Hakkari and extending to the west of Kahramanmaraş by drawing a concave arc towards the SW (Şaroğlu, 1987). Four points that provide essential data regarding the vitality of the thrusts in the Southeast Anatolian thrust belt are as follows: Between Siirt and Pervari, Lice Region, Cüngüş SW, and Kahramanmaraş Region. In these areas, the Late Miocene-aged rock assemblages were affected by the thrust, folded and overturned, and large morphological steeps and landslides developed in front of the thrust (Şaroğlu, 1987).

Ovacik Fault: The fact that the left-lateral strike-slip Ovacık Fault is located in this region can be considered a warning about the effectiveness of the Ovacık fault. Considering its morphological details, the Ovacık fault seems to have the potential to produce earthquakes of around 7-7.2 magnitudes. The low-velocity strain accumulation on this fault tends to be interpreted as producing large earthquakes with roughly 500-year recurrence intervals (Özener, 2006).

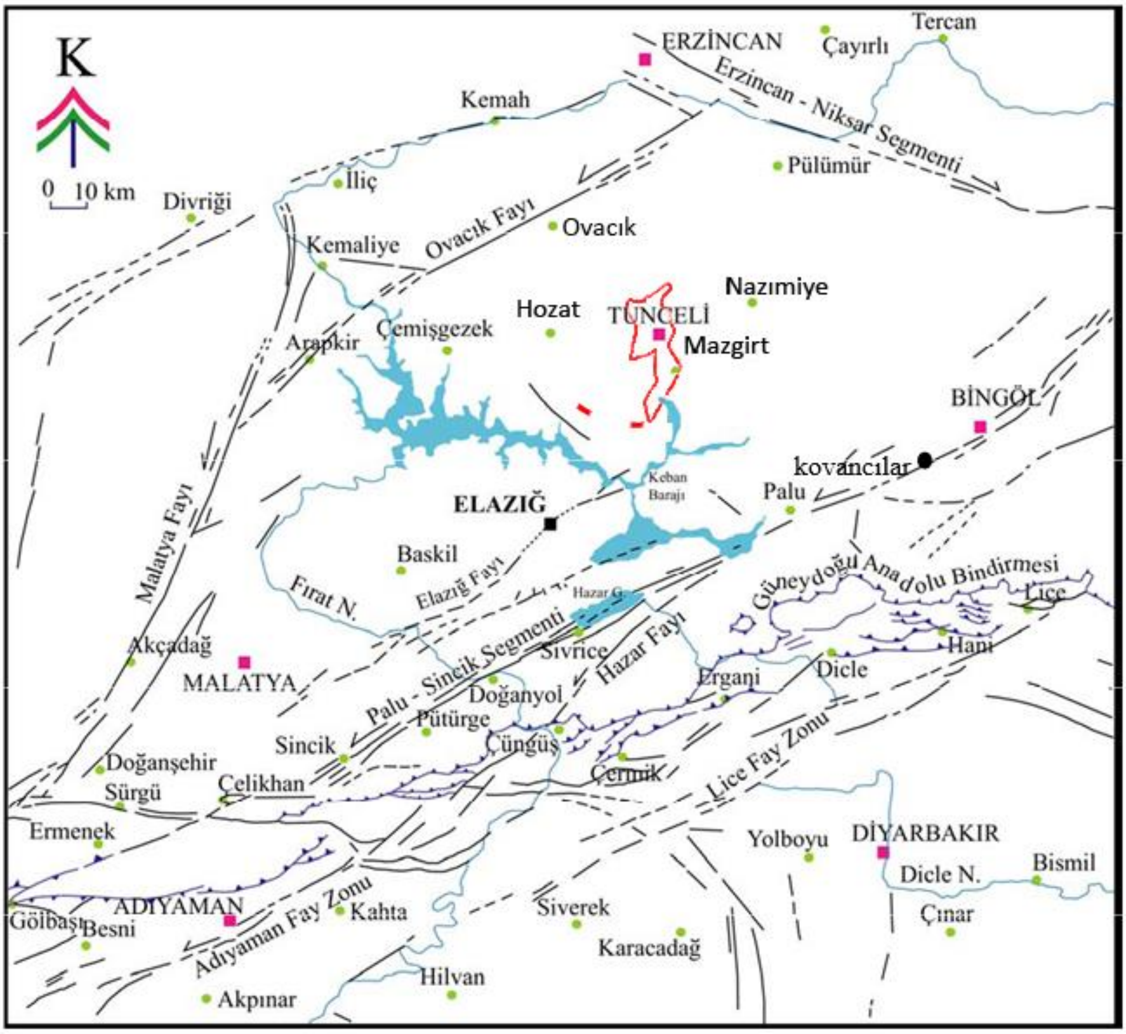

Figure 3.8. Tectonics in the southeastern anatolian region (Palutoğlı, Tanyolu 2006)

3.6. Geomorphology

It is seen that the study area is generally high sloping, and the sloping areas are seen to be between 0-20%, 20-40%, 40-60%, 60-80%, and above 80%. The slope map of the study area is given in Figure 3.9.

Tunceli is surrounded by the Bingöl mountains and Bingöl province in the east, Erzincan province in the west and north, and Keban Dam Lake and Elazığ province in the south. Its area is 7,774 km², and its height from the sea is 914 meters. 70% of Tunceli province consists of mountains, 25% plateaus, and 5% plains and plains. The most important mountain in the province has an average height of 3000 m. Munzur mountain range. Other prominent mountains are the Mercan Mountains, Gobarti Mountain, Zel Mountain, and Sevdin Mountain. There are no significant plains in the province. Ovacık plain of 74 km^2 in Ovacık district and Yeşilyazı plain of 44 km^2

located in Yeşilyazı subdistrict of the same district are the current plains of the province. Tunceli has a rich location in terms of rivers. The important rivers of the province; are Munzur, Coral, Pülümür, Tahar, and Peri. All these streams flow into the Keban Dam Lake. In the province, on the Munzur Mountains, there are four crater lakes, namely Karagöl, Koç, Şer, and Dilincik. Figure 3.9 shows the slope map of the study area.

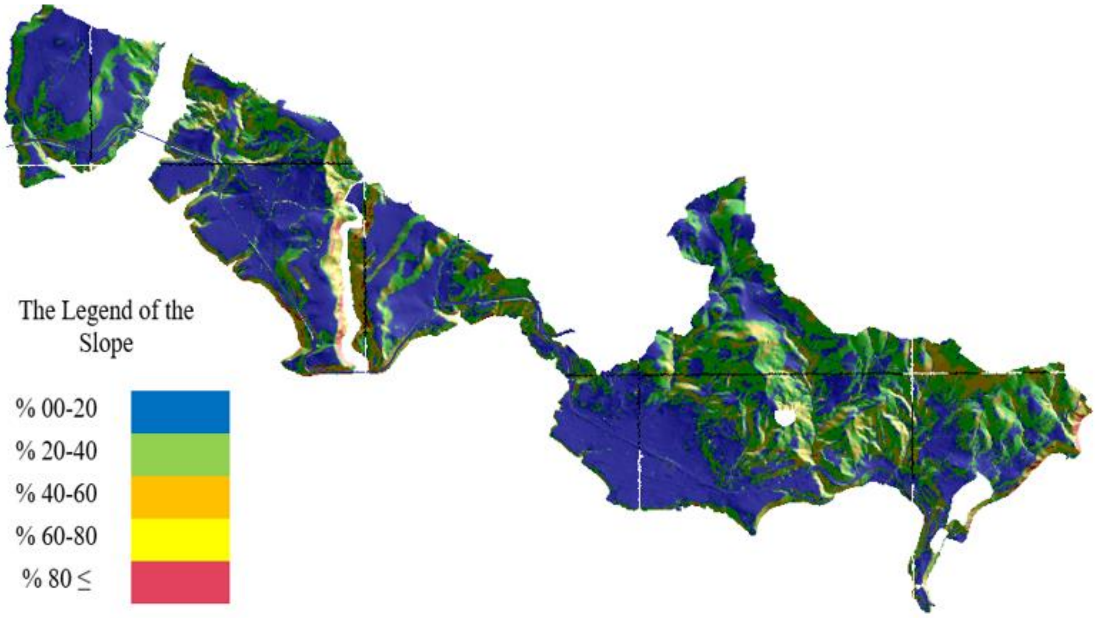

Figure 3.9. Slope map of the study area

3.7. Seismicity of the Region

Türkiye Earthquake Zone Map divides the country into five separate zones in terms of seismicity. The map shows ground acceleration values that will not be able to hang with a 90% probability in the next 50 years in Turkey. Figure 3.10 shows the seismicity map of Türkiye. In terms of seismicity:

- Region I is the most dangerous area. The areas where the ground acceleration will be 0.4g and higher are the red-colored areas marked on the map.
- Region II where ground acceleration is expected to be between 0.3–0.4g
- Region III where the ground acceleration is between 0.2–0.3g,
- Region IV where the ground acceleration is between 0.1–0.2g,
- Region V is defined as places where ground acceleration is expected to be 0.1g or less (AFAD, 2018).

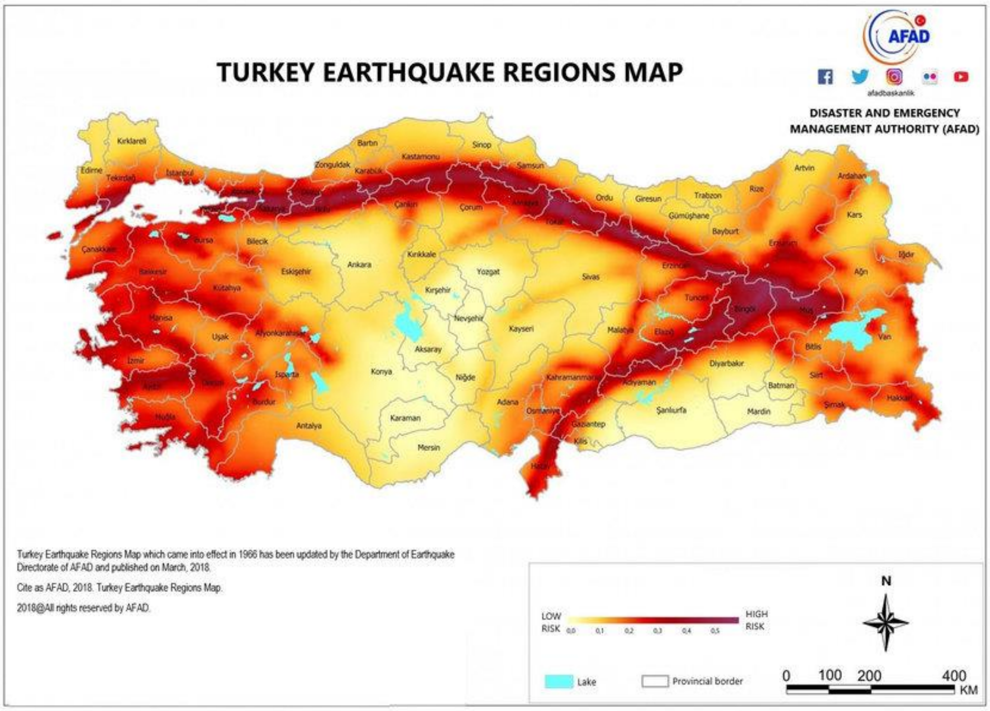

Figure 3.10. Map of Türkiye eartquake zones and active faults (AFAD, 2018)

Tunceli and its vicinity are inclusions with the East Anatolian Fault, Northeast Anatolian Fault, Ovacık Fault, and Nazimiye Fault. Since the study area is located in the 2nd-degree earthquake zone and is close to the East Anatolian Fault, Ovacık Fault, and Nazimiye Faults, the provisions of the "Regulation on Buildings to be Constructed in Earthquake Zones" must be followed before construction. In engineering terms, the determination of seismicity is based on a probability-statistical calculation. For this purpose, the older and more complete the information on past earthquakes, the more reliable the engineering approach (Büyükaşıkoğlu, 1987).

As part of the Tunceli Zoning Plan, a geological-geotechnical survey was conducted to assess earthquake hazards. The study included an analysis of seismicity and probabilistic distribution in the study area and its surrounding regions. To perform this analysis, earthquakes with a surface wave magnitude equal to or greater than 4.5 (M>4.5) that occurred between 1900 and 2018 were considered. The study area was defined as the center located at latitude 39.107555 and longitude 39.542409, within a radius of 100 km.

The earthquake data was obtained from the website of the Earthquake Department of the Prime Ministry Disaster and Emergency Management Presidency and used. The date, time, latitude (N), longitude (E), magnitude type, city, region, and magnitude values related to earthquakes used in the calculations are given in Table 3.2.

Table 3.2. Important earthquakes that occurred in Tunceli and its surroundings between the years 1900-2018

No	Date	Time	Latitude-Longitute	D	M	Location
1	04.12.1905	07.04	39.00-39.00	30	6.8	Payamdüzü-Çemişgezek
2	09.02.1909	11.24	40.00-38.00	60	6.3	Sarkoy- Su Şehri (Sivas)
3	13.09.1924	14.34	39.96-41.94	10	6.8	Emre-Köprüköy (Erzurum)
4	18.05.1929	06.37	40.20-37.90	10	6.1	Günışık-Koyulhisar (Sivas)
5	26.12.1939	23.57	39.80-39.51	20	7.9	Kurutilek (Erzincan)
6	08.11.1941	00.00	39.74-39.50	5	6.0	Erzincan
7	17.08.1949	18.44	39.57-40.62	40	6.7	Yaylım – Tercan (Erzincan)
8	14.06.1964	12.15	38.13-38.51	3	6.0	Aksu-Sıncık (Adıyaman)
9	19.08.1966	12.22	39.17-41.56	26	6.5	Çayıryolu-Varto (Muş)
10	20.08.1966	11.59	39.42-40.98	14	6.0	Kaşıkçı-Karlıova (Bingöl)
11	22.05.1971	16.43	38.85-40.52	3	6.8	Güveçli – (Bingöl)
12	06.09.1975	09.20	38.51-40.77	32	6.6	Uçdamlar-Lice (Diyarbakır)
13	13.03.1992	17.18	39.72-39.63	23	6.8	Günebakan- (Erzincan)
14	27.01.2003	05.26	39.48-39.77	10	6.1	Sağlamtaş-Pülümür (Tunceli)
15	01.05.2003	00.27	39.01-40.46	10	6.4	Kurtuluş- (Bingöl)
16	08.03.2010	02.32	38.83-40.13	5	6.1	Kovancılar – (Elazığ)

D=Deepness (km), M:Magnitude

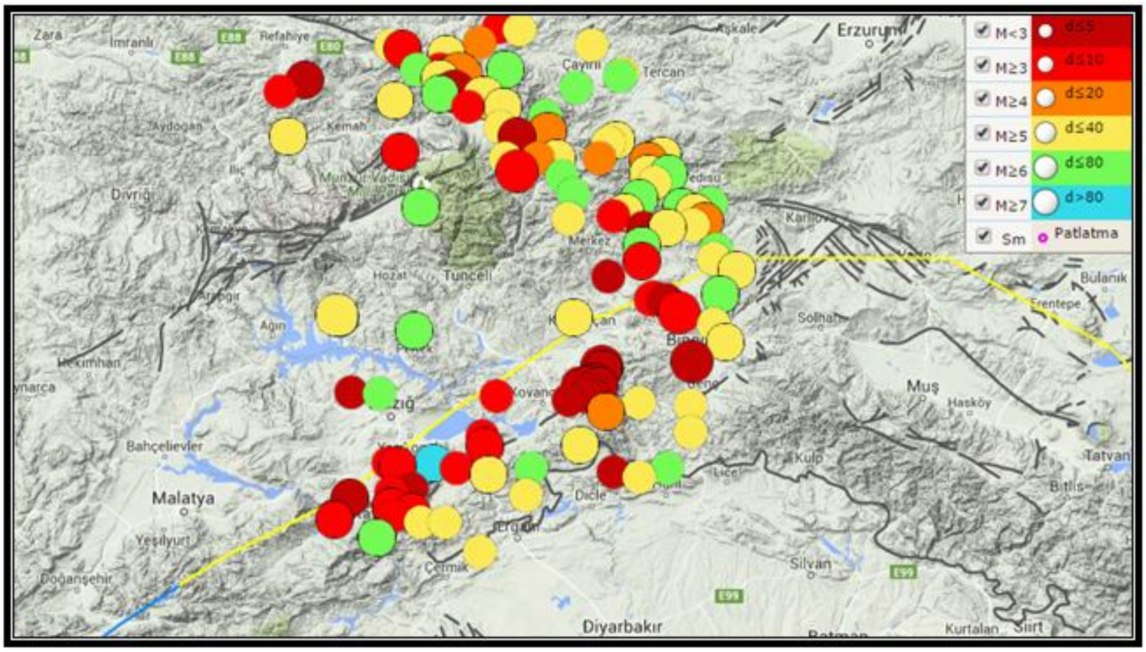

Figure 3.11. Earthquakes in and around Tunceli between the years 1900-2018 (M≥4.5)

By plotting the earthquakes listed in Table 3.2, Figure 3.11 illustrates the distribution map. The analysis reveals that the earthquakes within a 100 km radius, with the center designated as Tunceli City Center, predominantly occur along the Eastern Anatolian and North Anatolian Fault systems.

4. MATERIALS AND METHODS

This study focused on conducting a regional analysis to determine the soil characteristics within the selected project area of Tunceli province in Turkey. The study area specifically falls within the boundaries of Tunceli Municipality's settlement area, which is the city center. The study area covers approximately 1.848802 hectares as indicated on the current 1/1000 scaled map. To gather information for zoning studies, soil survey reports, laboratory test results, and formation information from 96 drilling points were examined. These drilling points were conducted by the Tunceli Municipality Provincial Directorate of Reconstruction and Urbanization. The collected data from the reports were then transferred to a GIS environment, enabling the creation of ground maps for the region.

The initial phase of the study involved a thorough examination of similar studies on the subject. Subsequently, a database was constructed in the GIS environment by modeling the GIS and inputting data obtained from fieldwork, boreholes, laboratory tests, and seismic studies. This database consisted of various data sources. In the final stage, the study was concluded by generating different maps in the GIS through various inquiries and models utilizing these datasets. The resulting maps and models are presented below. SPT maps

- Bearing capacity maps
- Liquefaction potential maps
- Shear wave velocity maps
- Soil classification maps

The study within the report's scope was carried out in 3 stages: field, laboratory, and desk studies.

4.1. Field studies

Drilling and geophysics studies carried out on samples are important to obtaining the most basic data in the study. The studies carried out in the field are 96 locations with a total depth of 1.436,8 m, varying between 05.00-30.00 m in depth in the study area, and pressiometer test examined at 42 points. From a technical view, three truck-mounted (one D-500, one D-900, and one GSM-700 truck) and two tracked Rotary drilling machines were used during the drilling of boreholes.

During drilling, undisturbed and core samples were taken with standard penetration, inclinometer, and pressuremeter tests. Undisturbed samples (UD) were taken from the well by hydraulic pressure using thin-walled tubes (Shelby tube) 500 mm long and 76 mm in diameter. After the sample was taken, both sides of the tube were paraffinized to ensure that the samples were airtight. A pressuremeter test was carried out in the boreholes that could not be sampled, and SPT could not be made. During the drilling of the boreholes, core samples were taken using double tube core barrels with water caps. Impregnated diamond drills were used as cutting bits in core barrels. Maneuver lengths were chosen as 1.50 meters, and core samples were obtained by removing the core barrel from the well at the end of the maneuver.

Considering the ground condition in the study area, the soil parameters were determined by SPT, undisturbed samples, and rock samples at suitable points. Disturbed samples were taken during SPT experiments with a 2" outer diameter and one ⅜ inner diameter slit sampler. To avoid losing their natural properties, the samples taken were put into two separate nylon bags, labeled and tightly tied in an airtight manner. An automatic type ram was used during the SPT experiments. Experiments were carried out on 354 samples of the SPT from the geotechnical drillings opened in Tunceli Central Region.

Also, Geophysical studies were carried out in order to measure the shear (S) and compression wave (P) velocities and to determine dynamic ground parameters, prevailing vibration periods, ground seismic amplification, and ground classes based on earthquake regulations.

MASW (Multi-Channel Analysis of Surface Waves) is a geophysical test used to assess subsurface soil and rock properties, particularly the shear wave velocity profile. In this context, 36 series (including P wave, reciprocating pulse), seismic refraction method (P and S waves) in 2 series, and microtremor method at 20 points to determine the ground dominant vibration period and amplification values, resistivity of units Electric resistivity method (vertical electric drilling) at 13 points in order to determine the values, groundwater level and corrosive properties of the soil, and electrical resistivity tomography method (ERT) studies in 12 profiles were carried out to determine the lateral and vertical resistivity changes.

4.1.1. Standard Penetration Test (SPT)

Standard Penetration Test (SPT), which gives information about soil's mechanical and physical properties, is a widely used field test today. SPT, a simple and economical test, was first used in different boreholes between 60 and 100 mm in diameter in the USA. The test primarily uses sandy and soft soils up to weak rocks. It is the determination of the number of blows or the energy required for the sampler at the tip of the rod to enter 300 mm into the ground by releasing the 63.5 kg hammer from a height of 760 mm during the test by freely leaving it on the anvil on the rod (Figure 4.2). After the necessary corrections of the determined data are made according to the groundwater level and drilling depth, these data give us information about the bearing capacity of the foundation soil. In addition, the liquefaction potential of the soil can be determined according to the test results (Çiftçi, 2020).

The test is usually repeated once every 1.5 m. The test stops if 15 cm penetration does not occur with 50 blows. At the end of the test, the drilling report is prepared with the help of other geotechnical features. An example of an SPT is presented in Figure 4.2 (Erol and Cekinmez, 2014).

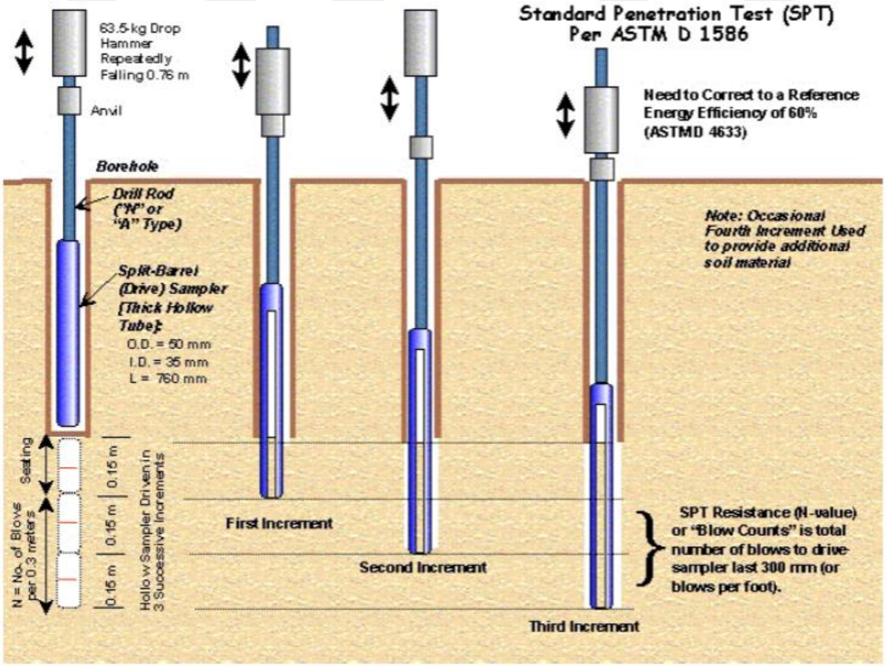

Figure 4.1. Testing Stages of SPT (Çiftçi, 2020)

Some field experiments have been widely used for 40-50 years, and some are developing with technology. The SPT is one of the oldest field tests widely used in geotechnical engineering. SPT is a more practical test compared to other field experiments. (Nixon, 1982).

- The mechanical equipment used in SPT is generally more durable.
- Since SPT can be applied in the borehole during the drilling process, the cost is lower.
- One of the important advantages of SPT is that samples can be taken from boreholes.
- SPT can be applied in all soil groups and below the groundwater level.

SPT has advantages as well as disadvantages. In some cases, it can give misleading results. Misleading results can be observed in SPT applications on gravel or stone-containing soils with an average diameter of more than 20 mm. The type of tip recommended for gravel soil can be used to eliminate this issue.

4.2. Laboratory Studies

Laboratory tests such as water content, sieve analysis, hydrometer, atterberg limits, consolidation, swelling pressure, specific gravity, natural unit weight, triaxial, point load, and unconfined compression tests have been examined on the samples from the boreholes drilled in the study area. The number of undisturbed samples used in soil mechanics experiments was 94. In order to determine the physical properties according to TS 1900-1, the water content, sieve analysis, atterberg limits tests were performed, and the samples were classified according to the combined soil classification (USCS). To determine mechanical properties according to TS 1900-2, triaxial, consolidation, swell percentage tests were carried out. Also, 476 water content, 476 sieve analyzes, 449 atterberg limits, 73 consolidations, 73 specific gravity, 72 natural unit weight, 43 triaxial, and 17 unconfined compression tests were performed in the laboratory. In addition, unconfined compression test and point loading test were performed on 104 core samples taken from the rocky samples.

4.3. Desk Studies

The geological maps created during fieldwork were generated in an office setting using the Netcad program, with a scale of 1/5000. Slope maps, calculated using a specific method, were also produced using the same program and included in the report's appendix, at a scale of 1/5000. Cross-sections were incorporated into the maps to ascertain the geological conditions in specific directions. Additionally, settlement suitability maps were created using the Netcad program to evaluate the appropriateness of the land for housing. These maps were prepared in scales of 1/1000 and 1/5000, taking into account the results of geological-geotechnical and geophysical studies.

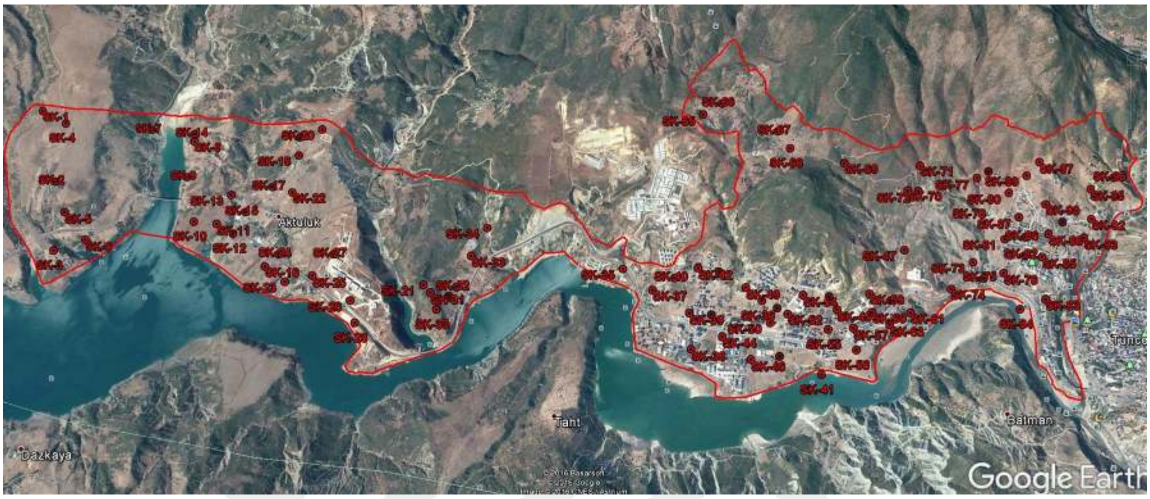

Figure 4.2. Satellite image of the borehole points in the study area.

In this study, drilling operations were conducted at 96 locations to a total depth of 1.436,8 meters, ranging from 5.00 to 30.00 meters as depicted in Figure 4.1. Pressiometer tests were performed at 42 points to examine the ground conditions. Soil parameters were determined based on Standard Penetration Test (SPT), undisturbed samples, and rock samples taken at appropriate locations in the study area. A total of 354 SPT samples from geotechnical drillings in the Tunceli Central Region 2 were subjected to experiments, investigating variables such as SPT values, liquefaction potential, water content, bearing capacity, and shear wave velocity. Other aspects examined included the depth of the groundwater table, shear wave velocity ($V_{s,30}$), soil classification according to TBDY-2018, NEHRP and EUROCODE-8, earthquake hazard level based on soil amplification, and local soil class according to dominant vibration period. The evaluations utilized GIS maps, which were created using the ArcGIS program.

4.4. Creating a Database

In the examination of the soil properties of Tunceli province, many analyzes such as SPT-N calculation analysis, bearing capacity calculation analysis, groundwater level, and water content analysis, and liquefaction calculation analysis were made, and the results of the analysis were processed into the GIS environment and evaluated. This study examined ground survey reports, laboratory test results, and reports of lands obtained from 96 drilling points, which Tunceli Municipality Provincial Directorate made of Reconstruction and Urbanization for use in zoning studies. The numerical and verbal data obtained from the report were digitized and first saved in the MS-Excel program. This information in the MS-Excel program was transferred to the Geographic Information Systems (GIS) program, and database files were created. The groundwater level was examined by mapping the region with Geographic Information Systems (GIS). If the groundwater level is high, many problems such as liquefaction in the soils arise.

4.5. Calculation Methods of Bearing Capacity

4.5.1. What is bearing capacity?

The capacity of the soil to resist the weight of a structure without failing is called bearing capacity. This refers to the ability of foundation soil to withstand the forces imposed by the superstructure without experiencing shear failure or excessive settlement. The foundation soil is the portion of the ground that is subjected to additional stress when a building is constructed. There are several key terms associated with the bearing capacity of soil, including (Civil Team, 2022).

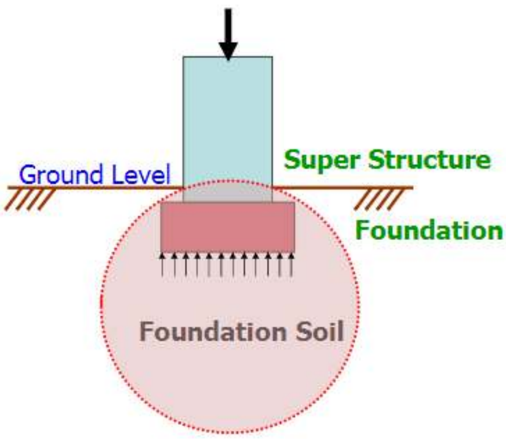

Figure 4.3. Main components of a structure including foundation soil (Civil Team, 2022).

Carrying capacity represents the load the soil particles can carry in a unit area without deteriorating their condition. Our studies compare the carrying capacity obtained using field tests (based on SPT-N) and geophysical methods (based on V_s and Vp). Seismic measurements are made in the field by measuring the velocities of longitudinal and transverse seismic wave types (V_p and V_s, respectively) propagating in the ground. The energy required for the *P* wave is the vertical direction of the 10.0 kg sledgehammer on the steel plate; The energy required for the *S* wave is obtained by the sledgehammer blowing in the horizontal direction to the plate placed in a 30 cm pit opened on the ground (Demir, 2013).There are many factors affecting the bearing capacity. Factors related to soil-profile;

- Shear strength parameters of the soil (c and ϕ)
- Soil unit weight (γ)
- Groundwater level (*GWL*)

Factors related to foundation;

- Foundation depth (D_f)
- Basic shape (square, circular, rectangular)
- Foundation dimensions (*B*, *L*)
- Short side of foundation (*B*)
- Roughness of the foundation base

Factors related to loads;

- Slope and eccentricity of the load (*e*)
- If there is GWL, the time elapsed after the construction and installation of the foundation.

Bearing capacity failures (collapse); the shear stresses of the soil depend on the net base pressure and the size of the foundation. The shear stress of soils with large base pressure and small foundation size can exceed the shear strength of the soil. This may result in a bearing capacity collapse (Sivrikaya et al., 2021). Many methods are used to determine the bearing capacity.

- Tables
- Load Experiment
- Other Field Tests (SPT, CPT, etc.)
- Theoretical Approaches

4.5.2. Bearing capacity according to Terzaghi & Peck (1967)

The method developed by Terzaghi & Peck determines the bearing capacity based on the foundation width and SPT-N values. Figure 4.4 determines the bearing capacity (Bowles, 1996). The width of the foundation was chosen as 3 m.

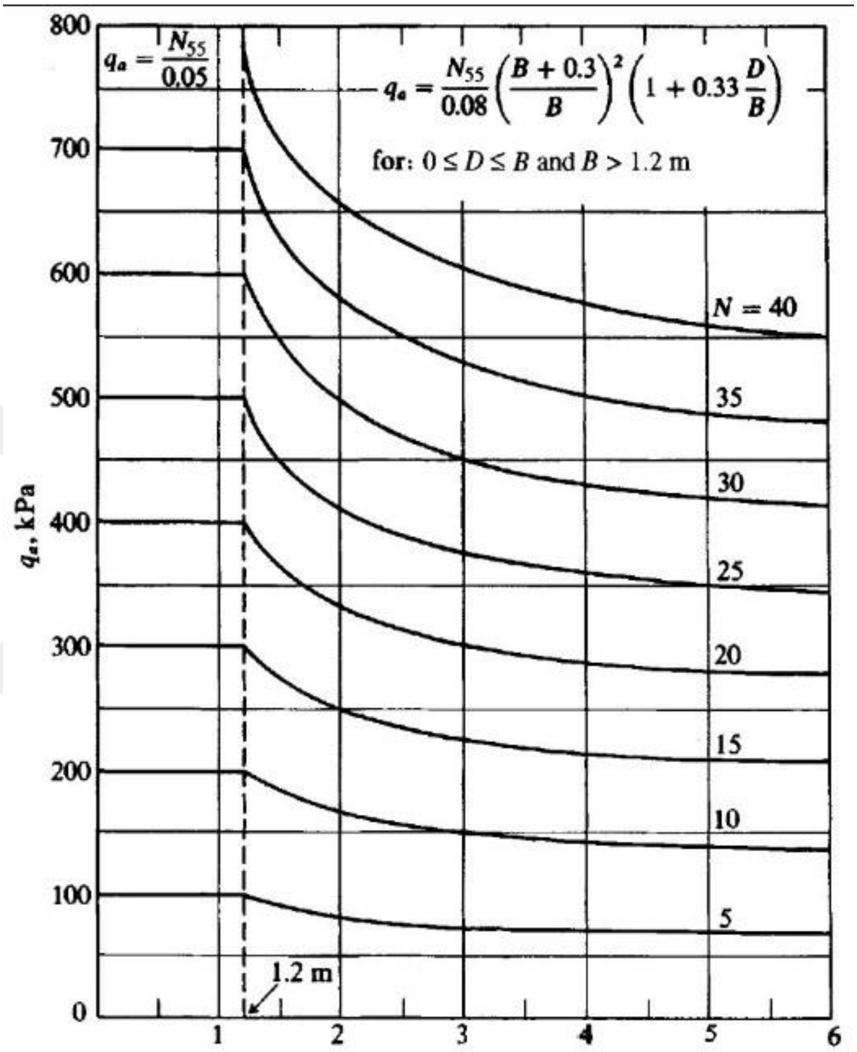

Figure 4.4. Allowable bearing capacity versus foundation width and SPT-N (Bowles, 1996).

4.5.3. Bearing capacity according to Meyerhof (1974)

The Meyerhof bearing capacity calculation is obtained by using the SPT-N value. Like Meyerhof's studies, Terzaghi and Peck also limited seating to 25 millimeters. Accordingly, the bearing capacity is calculated using the following formulas. (Bowles, 1996). The foundation width was chosen as 3 m.

$$q = 12 * N * K_d \qquad 4.1.$$

$$q = 8 * N * (\frac{B + 0{,}3505}{B})^2 \qquad 4.2.$$

$$K_d = 1 + 0{,}33 * {}^{D}/_{B} \leq 1{,}33 \qquad 4.3.$$

Here;

q : Bearing capacity (kN/m^2)

N : SPT blow number

D : Foundation depth (m)

B : Foundation width (m)

4.6. Calculation of Groundwater Level and Water Content

Earthquakes cause sudden and concise movements on the ground. When the Groundwater is close to the surface, during earthquakes, the contact forces that hold the soil grains together cause water loss, and the soil loses its strength. Under these conditions, the soil behaves like a liquid (Kurnaz, 2011). Therefore, Groundwater directly affects the layout of engineering structures and the mechanical properties of soils. (IMO, 2016)

The water content of the soil has a vital role in soil behavior and modeling. The water content is determined based on the principles outlined in TS 1900-1 (2006) or ASTM D 2216 (2010). (IMO, 2016).

4.7. Calculation of Liquefaction Potential

4.7.1. What is liquefaction?

Liquefaction was first described by Japanese researchers Mogami and Kubo in 1953. Liquefaction is the soil deformation caused by the deterioration of water-saturated cohesionless soils under conditions where water cannot be removed from the soil environment (Ulusay, 2000). Soil instabilities caused by liquefaction, the soil, which loses its strength with liquefaction, cannot bear the loads transmitted by the structure. The structures on the ground deteriorate, tilting or overturning in different directions (Şen, 2004). During liquefaction, loss of carrying capacity is observed due to the aggregation and separation of particles. For this reason, settlements on the ground surface and tilting of buildings are observed (Aydan et al., 2000). Lateral spreading can be defined as the separation of soil layers into large blocks above ground level and the lateral movement of the separated blocks. Lateral spreading develops along the surfaces with 3-5% of the slope. As a result of the movement, fractures, small depressions, and elevations occur on the ground (Sen, 2004). Flow liquefaction occurs on surfaces with a slope greater than 5%. During the movement, vast ground masses can cover a distance of kilometers in a short time (Ulusay, 2000).

Many analysis methods related to field and laboratory tests are available in the literature to determine liquefaction sensitivity. The time-consuming and costly nature of laboratory tests has led to the widespread preference for field tests investigating liquefaction potential. Within the scope of this thesis, SPT blow numbers obtained in the field were used to determine the liquefaction potential in the study area. The method used during the study is the Youd et al. (2001) method, based on the Seed and Idriss (1971) method.

Determination of the safety factor of the soil against liquefaction; is found by dividing the cyclic resistance ratio (*CRR*) by the cyclic stress ratio (*CSR*) formed by the earthquake (Youd et al., 2001). The cyclic stress rate *CSR* that occurs during an earthquake is calculated by equation 4.4.

$$CSR = \tau_{av}/\sigma'_{vo} = 0.65 * (a_{maks}/g) * \sigma_{vo}/\sigma'_{vo} * r_d \leq 1{,}33 \qquad 4.4.$$

Here,

CSR : Cyclic Stress Ratio generated by average horizontal shear as a result of earthquake

a_{max} : Peak ground acceleration (cm/sec^2)

G : Ground acceleration (cm/sec^2)

σ_{vo} : Vertical total stress (kPa)

σ'_{vo} : Vertical effective stress (kPa)

r_d : Stress reduction factor

r_d is a factor that changes with depth (z) and is 9.15 m. correlation to depth 3.10, 9.15 m. with 23 m. For the depths between, the correlation is calculated with 5.5.

$$z \leq 9.15 \text{ m for } r_d = 1.0 - 0.00765z \qquad 4.5.$$

$$9.15 < z \leq 23 \text{ m for } r_d = 1.174 - 0.00267z \qquad 4.6.$$

As mentioned in the previous paragraphs, SPT blow numbers were used to calculate the soil's cyclic resistance ratio (*CRR*) to liquefaction. As is known, the blow numbers (*N*) obtained from the SPT test are subjected to a series of corrections, and the corrected SPT blow number ($N_{1,60}$) is determined. These modifications are, load correction (C_N), rod energy ratio correction (C_E), borehole diameter correction (C_B), rod length correction (C_R), and an inner tube correction (C_S) used during the test. Youd et al. (2001) suggested SPT correction coefficients, which are given in Table 4.1.

The formula in equation 4.7 proposed by Youd et al. (2001) was used for the cover load correction (C_N).

$$C_N = 2.2/(1.2 + (\sigma'_{vo}/P_a)) \qquad 4.7.$$

Here,

P_a : Atmospheric pressure 100 kPa

σ'_{vo} : Effective stress (kPa)

The energy ratio (E_r) of the Donut type of ram used in Türkiye is 45%. T_{ij} energy ratio correction (CE) is calculated by equation 4.8

$$C_E = E_r/60 \qquad 4.8.$$

The following expression is used to find the corrected number of blow ($N_{1,60}$) for each level where the SPT test is performed. (Youd et al., 2001).

$$N_{1.60} = N * C_N * C_E * C_B * C_R * C_S \qquad 4.9.$$

Table 4.1. Coefficients used for the correction of SPT number (Youd et al., 2001)

Parameter	Definition	Coefficient
Borehole diameter (C_B)	65-115 mm	1.0
	150 mm	1.05
	200 mm	1.15
Stem bar length (C_R)	< 3 m	0.75
	3-4 m	0.8
	4-6 m	0.85
	6-10 m	0.95
	10-30 m	1.0
Inner tube use (C_S)	Standard Sample Taker	1.0
	Cases in which inner tube used	1.1 – 1.3

Youd et al. (2001) stated that the CRR increased with the increase of the acceptable grain ratio (<0.075mm) in the liquefaction analysis compared to the SPT. The corrected SPT impact values ($N_{1,60}$) were determined by the fine grain ratio (ITO) of the soil and proposed a new correction according to ($N_{1,60cs}$).

$$N_{1,60cs} = \propto + \beta * N_{1,60} \quad 4.10$$

α and β are the coefficients calculated in the following formulas.

If $FC \leq \%5$ $\alpha = 0$, $\beta=1.0$

If $\%5 < FC < \%35$ $\alpha = \exp(1.76 - (190 / FC^2))$, $\beta=(0.99 + (FC^{1.5} / 1000))$ 4.11

If $FC \geq \%35$ $\alpha = 5$, $\beta=1.2$ 4.12

Using the corrected SPT blow numbers, the soil's cyclic resistance ratio (*CRR*) is calculated using equation 4.13. This equation is valid when ($N_{1,60}$) values are less than 30, when ($N_{1,60}$) ≥ 30 soils are too dense for liquefaction and are considered non-liquefiable (Youd et al., 2001).

$$CRR = \frac{1}{34 - N_{1,60}} + \frac{N_{1,60}}{135} + \frac{50}{[10 * N_{1,60} + 45]^2} - \frac{1}{200} \quad 4.13$$

Liquefaction occurs at the depth where the shear stresses that occur during an earthquake exceed the liquefaction resistance. The security number expresses this situation by Seed and Idriss (1971).

$$\text{FS} = \frac{CRR}{CSR} \quad 4.14$$

Calculated FS values are evaluated according to the following ranges;

$FS \leq 1$ There is a risk of liquefaction.

$FS > 1$ No risk of liquefaction.

The *CRR* values calculated for an earthquake greater than 7.5 should be corrected according to the predicted earthquake magnitude in the investigated region. A revised magnitude scaling (correction) factor (MSF) has been proposed by Youd et al., (2001) for this correction.

$$\text{MSF} = \frac{10^{2.24}}{M_{W^{2.56}}} \quad 4.15$$

Here, Mw: It is the earthquake magnitude in terms of moment magnitude expected in the study area. The factor of safety (FS) against liquefaction is calculated with the following expression (4.16) (Sen, 2004).

$$\text{FS} = \frac{CRR}{CSR} * MSF \quad 4.16$$

4.8. Calculation of Shear Wave Velocity

4.8.1. What is shear wave velocity

The velocity data determined by seismic waves are used to obtain the dynamic soil variables used in soil classification and understand the engineering properties of the soil based on ground movements. Because of factors such as large depth of research, high accuracy, and resolution, the seismic method, one of the geophysics methods, is widely used in engineering studies. (Akkaya et al., 2017) One of the most important parameters to determine the local ground effect is the shear wave velocity (V_s). Many measurement methods are used to determine the shear wave velocity "V_s (m/s)" (Hunter J.A. et al., 2002). Measurement methods for the shear wave velocity can be considered as methods obtained by seismic methods and their calculation by field experiments.

Shear wave velocity provides information about soil stiffness. It is used in analyzes to determine soil behavior. It is determined or calculated by measuring in the field (depending on the SPT-N number). However, in some soil classification systems and earthquake hazard analyses, the soil's average 30 m shear wave velocity is used (Kurnaz, 2011).

4.8.2. Measurement of shear wave velocity in the field

The surface fracture method is used within the scope of measurement made in the field. It is used to determine the parameters of the soil of the study area. In this method, the propagation of the waves coming from the interfaces with fractions and waves coming directly are recorded. As a seismic energy source, an 8 kg weight sledgehammer is used. The energy in the *S* wave (shear wave) is obtained by hitting the plate perpendicular to the pit 30-40 cm deep. *S* wave records are created. Geodetic geophones (detectors) are used in the transverse wave records. A seismograph with signal accumulation is used to precisely measure *S* velocities. V_s is obtained by this method in the field. In situ measurement of the shear wave velocity can be disadvantageous in some cases; thus, shear wave velocities are often estimated from correlations associated with SPT-N numbers (Kurnaz, 2011). These correlations are given in Table 4.2.

Table 4.2. The empirical correlation based on SPT-N and V_s (Akın et. al., 2011)

Researchers	V_s (m/s) (All type of soils)
Ohba and Trauma(1970)	$V_s = 84*N^{0.31}$
Seed and Idriss(1981)	$V_s = 61*N^{0.5}$
Imai and Yoshimura (1990)	$V_s = 76*N^{0.33}$
Iyisan (1996)	$V_s = 51.5*N^{0.516}$
Hasancelebi and Ulusay(2007)	$V_s = 90*N^{0.309}$
Tsiambos and Sabatakakis (2011)	$V_s = 105.7*N^{0.327}$

V_s: Shear wave velocity, N: Uncorrected SPT number of blow

4.9. Calculation of Density Values

Depending on the density value V_p used in the equations; It is calculated with the relation.

$$P = d = 0.31 * V_p^{0,25} \quad (\text{gr/cm}^3) \qquad 4.21$$

Table 4.3. Classification according to the density values (Dursun et al., 2012)

Density (gr/cm³)	Definition
<1.20	Very low
1.20-1.40	Low
1.40-1.90	Medium
1.90-2.20	High
2.20	Very high

4.10. Calculation of Seismic Velocity Rate

It determines the density of the soil and the liquefaction of the soil. Suppose there is a geological unit suitable for liquefaction in the environment. If there is groundwater, the V_p/V_s. The ratio is checked. If this ratio is greater than 3, there is a high probability of liquefaction.

Table 4.4. Relationship between V_p/V_s ratio and soil classes.

Soil Class	V_p/V_s
Z1	1.5-2.0
Z2	2.0-2.5
Z3	2.5-3.0
Z4	3.0-10.0

4.11. Calculation of the Maximum Shear Modulus

The elastic torsion resistance indicates the flexing of the ground under shear-shear forces and describes the deflection or buckling resulting from earthquake waves or lateral pressure separations. This parameter is zero because liquids have no resistance to shear. The higher the shear modulus, the more excellent the formation's resistance to shear stresses, that is, to horizontal forces (horizontal earthquake load). Its unit is kg/cm^2.

$$G_{max} = \rho * V_s^{\,2}/100 \qquad 4.23$$

Table 4.5. Strength definition according to shear modulus (Dursun et al., 2012).

Shear Modulus (*kg/cm²*)	Strength
<400	Very weak
400-1500	Weak
1500-3000	Medium
3000-10000	Solid
> 10000	Very solid

4.12. Calculation of the Ground Bearing Coefficient

The bulk module is used to calculate the stress over settlement coefficient. The bearing coefficient is calculated from the formula below.

$$K_0 = 2.49 * \left(\frac{1}{\frac{1}{K} * 1009}\right)^{1,26} * 7 \text{ (ton/m}^3\text{)} \qquad 4.24$$

4.13. Calculation of the Soil Classes

4.13.1. Earthquake hazard by soil amplification

Sedimentary rocks that are soft can amplify the impact of earthquakes, leading to more severe damage compared to areas with hard rock layers. This is because soft sedimentary rocks increase the strength of soil movement during seismic events (Tuladhar et al., 2004). In other words, the softer sedimentary rock acts as a multiplier for earthquake waves, intensifying their effects.

Constructions erected on soft sediments are susceptible to increased harm during earthquakes due to the amplification of seismic waves. This is due to two factors. Firstly, the confinement of waves to the soft layer results in superposition between waves, and if the frequencies are similar, it can lead to resonance and the reciprocative reinforcement of the waves (Tsutomu Sato, 2004). Secondly, the local geology and the constructions themselves share similar natural frequencies (Roser & Gosar, 2010), exacerbating the effects of the earthquakes.

The resonance between constructions and local soil during earthquakes results in stronger ground vibrations and greater damage to buildings. The extent of this amplification can be predicted based on the difference in impedance between the underlying bedrock and the surface sediment (Roser and Gosar, 2010). The soil close to the surface amplifies seismic waves by increasing their amplitude as they pass through it. This is due to the low density of the soil layers. In loose soils, the earthquake waves can grow significantly during earthquakes, contributing greatly to the damages caused (Kurnaz, 2011). The soil amplification was determined using the formula proposed by Midorikawa (1987).

$$A=68V_1^{-0.6} \qquad (V_1<1100 \text{ m/s}) \tag{4.25}$$

$$A=1 \qquad (V_1>1100 \text{ m/s}) \tag{4.26}$$

Here;

A : Relative amplification coefficient

V_1 : Shear wave velocity for depth of 30 meters

Earthquake hazard level according to calculated soil amplification; for the amplification value of 0,0-2,0, hazard level C (low hazard), for the amplification value 2.0-4.0, hazard level B (medium hazard), for the amplification value of 4.0-6.5, hazard level A (high hazard) (Kurnaz, 2011).

4.13.2. Soil dominant vibration period

The soil dominant period is important for determining the frequency characteristics of ground movement. This period is specified as the vibration period corresponding to the max value of the amplitude spectrum. In addition, even for small vibrations, the soft soil layer on the solid rock layer has a dominant vibration period in nature (Kanai, 1983).

The period is expressed as the independent oscillation of the mass on the bedrock and depends on the dynamic properties of the soil layers. Soil dominant vibration period value of the soft soil layer cropping out on the bedrock (hard ground) is determined by utilizing the formula $To = \Sigma(4H/ V_{s,30})$ for small vibrations (Kanai, 1965)

$$To = \sum 4H / V_s \tag{4.27}$$

Here;

To : Dominant vibration period

H : Layer thickness (m)

V_s : Shear wave velocity (m/s)

Differences in soil layers and sections can be seen from one end to the other. Changes in earthquake waves can be seen depending on the soil layers' characteristics, type, and thickness. At the same time, dynamic properties such as soil amplification and prevailing soil period should be defined in earthquake-resistant zoning plans. (Ansal et al., 1994)

4.13.3 NEHRP (USA) earthquake code

National Earthquake Hazard Reduction Program (NEHRP) aims to increase the expected performance of important buildings during or after an earthquake in the United States of America. The soil class, according to NEHRP, is based on the average of the S-wave velocity up to 30 m depth, and these classes are given in Table 4.15 (Güzel, 2009).

Table 4.6. Soil classification criterias according to NEHRP (Güzel,2009)

Soil	Description	Properties
A	Hard rock	V_s>1500
B	Rock	760 < $V_s \leq$ 1500
C	Very dense soil/ soft rock	360 < $V_s \leq$ 760
D	Hard soil	180 < $V_s \leq$ 360
E	Soft soil	V_s <180

4.13.4 EUROCODE-8 (Europe) earthquake code

The Eurocode series are European Regulations relating to construction. "Eurocode8: Design of structures for earthquake resistance" This regulation explains how constructions in earthquake zones should be designed. Eurocode 8 applies to the design and construction of buildings and other civil engineering works in seismic regions (Halaç, 2016). The European Standards Committee has approved this regulation.

Its purpose is to ensure that human lives are protected in the event of earthquakes, the damage is limited, and structures essential for civil protection remain operational. The soil class, according to Eurocode8, is based on the average velocity ($V_{s,30}$) of the S-wave velocity up to 30 m depth, and these classes are given in Table 4.18.

Table 4.7. Soil classification criteria according to EUROCODE-8 (Güzel, 2009)

Soil	Description	Properties
A	Rock or other rock-like geological formation	$V_s > 800$
B	Very dense sand or gravel or very stiff clay	$360 < V_s \leq 800$
C	Dense sand or gravel or stiff clay	$180 < V_s \leq 360$
D	Loose to medium cohesionless soil or soft to firm cohesive soil	$V_s < 180$

$V_{s,30}$: Average shear wave velocity at 30 m depth (m/sn)

When the study area was classified depending on the NHERP conditions according to $V_{s,30}$ velocity values, it was observed that almost the entire study area was in C "Very Firm/Hard Ground or Soft Rock," and the area where S10-S15-S34 points were located in D "Compact/Hard Ground" soil class. When classified according to Eurocode-8 conditions, it was observed that almost the entire area is in B "Very compact sand, gravel or very hard clays" S10-S15-S34 points C "Compact or medium compact sand gravel or hard clays" soil class.

4.13.5. TBDY-2018 (Türkiye) earthquake code

According to the Turkish earthquake regulations, the prevailing vibration period depending on the local soil classes is given in Table 4.17. (Z1: Very dense, Z2: Hard, Z3: Medium hard, Z4: Loose, soft) (Kurnaz, 2011).

Table 4.8. Soil classification criteria according to TDBY-2018 and dominant vibration period (To) (Güzel, 2009)

Soil Type		Soil Dominant Vibration Period, To (sec)	Average To (sec)	(T_A - T_B) (sec)
Z1	a	0.20	0.25	0.10 - 0.30
	b	0.25		
	c	0.30		
Z2	a	0.35	0.42	0.15 - 0.40
	b	0.40		
	c	0.50		
Z3	a	0.55	0.6	0.15 - 0.60
	b	0.60		
	c	0.65		
Z4	a	0.70	0.8	0.20 - 0.90
	b	0.80		
	c	0.90		

5. RESULTS AND DISCUSSION

5.1. Map Analysis of SPT-N Values

In this part, the SPT-N method, widely used in field experiments, was employed to collect borehole data from soil survey reports in specific regions of Tunceli Central district. The engineering behavior of the soils was investigated by gathering SPT data from 96 drilling points within the study area. To visualize the distribution of SPT-N values and their changes with increasing depth from the surface to a depth of 15 m, maps were developed for various depths (starting from 1.5 m, including 3.0 m, 4.5 m, 7.5 m, 9.0 m, and 15 m). The ArcGIS software, utilizing the IDW (Inverse Distance Weighting) method, was utilized to generate these maps. A grid size of 10 m was used, and the SPT-N values ranged from 1 to 50. The relationship between SPT-N values and relative density for sands is presented in Table 5.2, while the relationship between clays, their consistency, and SPT-N values is provided in Table 5.1. The created maps were then evaluated based on the information in Tables 5.1 and 5.2.

Table 5.1 Correlation between q_u - SPT-N (Terzaghi & Peck 1967)

Consistency	SPT-N	q_u (kPa)
Very soft	< 2	< 25
Soft	2-4	25-50
Medium solid	4-8	50-100
Solid	8-15	100-200
Very solid	15-30	200-400
Hard	> 30	> 400

Table 5.2. Relationships between standard penetration resistance and relative density (Demir, 2013)

Soil state	N_{60}	Relative Density			
		Meyerhof (1956)	Duncan and Buchinani (1976)	Mitchell and Katti (1981)	Bowles (1968)
Very loose	< 4	< 20	< 15	< 15	< 15
Loose	4-10	20-40	15-35	15-35	15-30
Medium to dense	10-30	40-60	35-65	35-65	35-65
Dense	30-50	60-80	65-85	65-85	65-85
Very dense	> 50	> 80	85-100	85-100	85-100

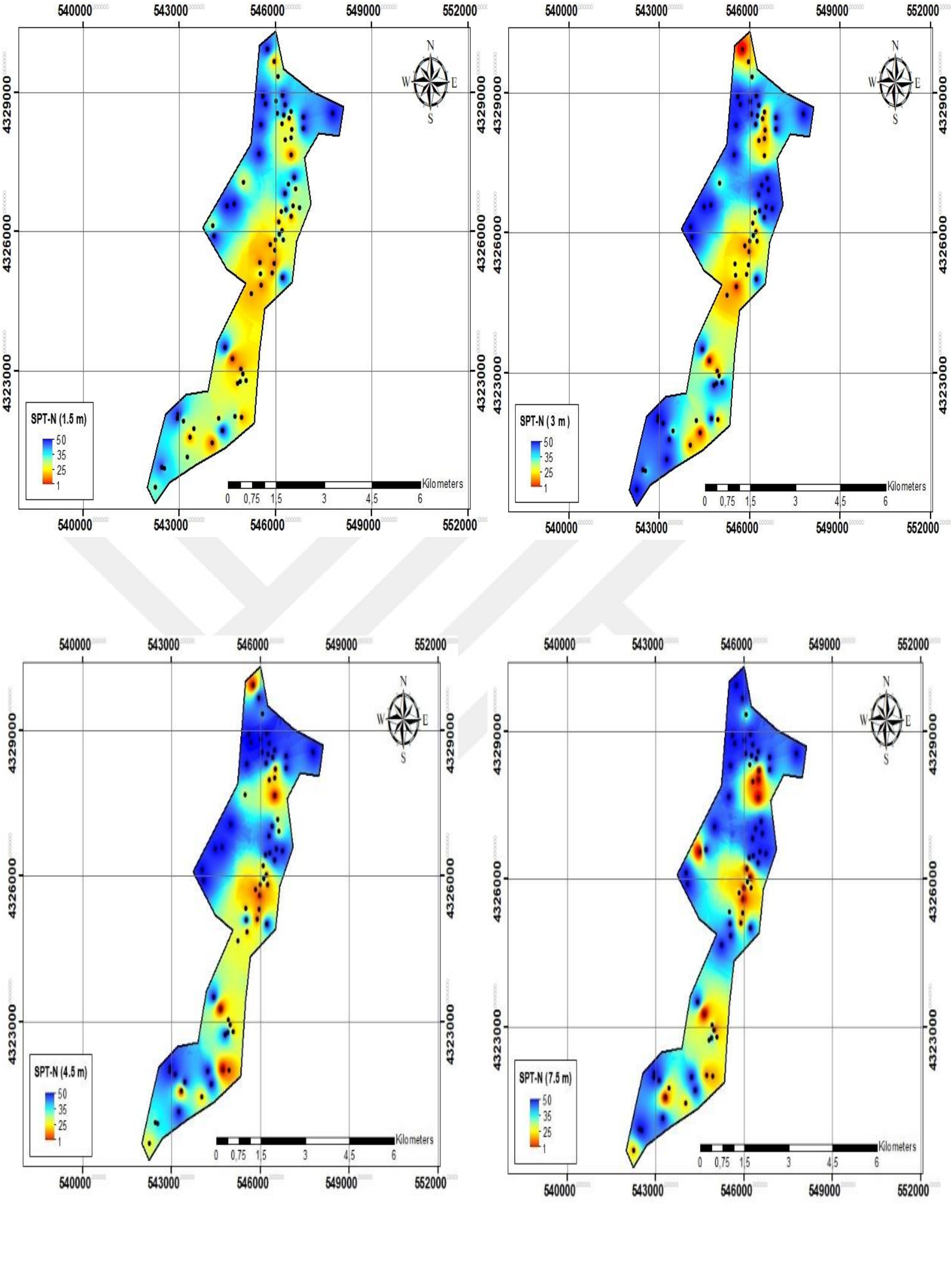
SPT-N (1.5 m)
SPT-N (3 m)
SPT-N (4.5 m)
SPT-N (7.5 m)
50
35
25
1
Kilometers
0 0,75 1,5 3 4,5 6
540000
543000
546000
549000
552000
4323000
4326000
4329000
N
S
W
E

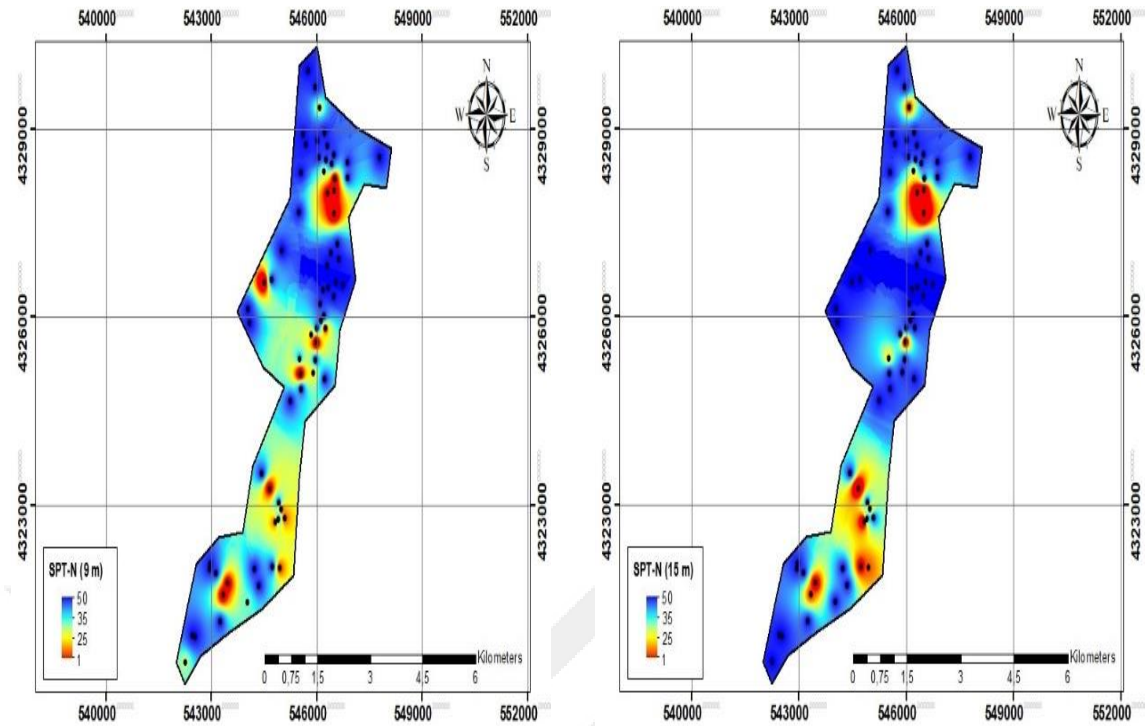

Figure 5.1. Maps of SPT-N values according to the borehole depths (1.5-3.0-4.5-7.5-9.0-15 m)

Figure 5.1 illustrates the variation of SPT-N values at different depths in boreholes. The map detailing the 3.0-meter depth reveals that the majority of the Cumhuriyet and Atatürk Districts have SPT-N values ranging from 1-25, indicating a relative density of "loose and medium dense". When examining the map displaying the SPT-N values measured at a depth of 4.5 meters, it is evident that certain areas in the Atatürk and Moğultay neighborhoods have SPT-N numbers between 1-25, suggesting a relative density of "loose and moderately dense" in these regions. In contrast, other areas exhibit a predominance of "dense" soil structure.

The SPT-N values measured at 7.5 m depth showed that, a small part of Yeni Mahallesi has an SPT-N number between 1-25 according to the map. These areas are defined as "loose" and "medium dense". A part of Atatürk and Cumhuriyet neighborhoods have SPT-N values varying between 1-25. The soils in these areas are classified as "loose" and "medium dense". In other neighborhoods, the SPT-N values are between 25-50, and in these areas, they are classified as "dense" and "very dense" in some parts of the study area.

In Figure 5.1 which is drawn according to the depth of 9 m presented that a part of Moğultay neighborhood has an SPT-N number of 1-25 according to the map. These areas are defined as "loose" and "medium dense". A part of Atatürk and Cumhuriyet neighborhoods have SPT-N values varying between 1-25. These areas are classified as "loose" and "medium dense" structures. In other neighborhoods, the SPT-N values are between 25-50, and in these areas, they are "dense" and "very dense" in places.

When the map showing the change of SPT-N values measured at a depth of 15 m is examined, according to the map, a small part of the Aktuluk Neighborhood has an SPT-N impact number of 1-25 in parts. These areas are defined as "loose" and "medium dense". Atatürk and a part of the Cumhuriyet neighborhood have SPT-N values varying between 1-25. These areas are "loose" and "medium dense" structures. In other neighborhoods, the SPT-N values are between 25-50, and in these areas, they are "dense" and "very dense" in some places. According to the SPT values at 3.0 m, 4.5 m, 7.5, 9 m, and 15 m are compared, it is seen that the ground at 15 m has a denser soil structure. In general, SPT-N values greater than 35 appear to be more common in the study area.

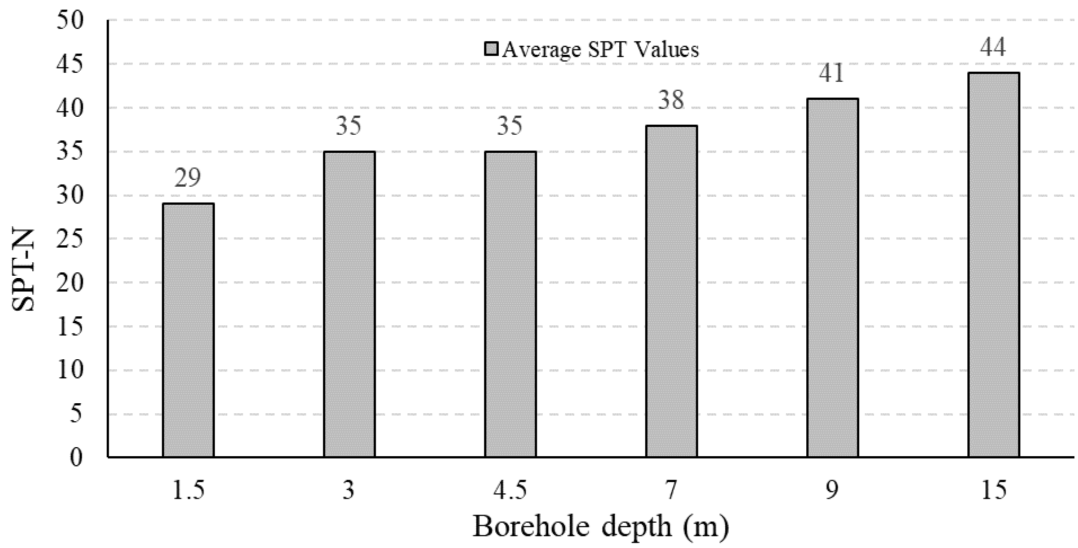

Figure 5.2. Bar chart of SPT-N values according to the borehole depth

According to Figure 5.2, the average SPT-N data from 96 boreholes were compared based on their depths (1.5 m, 3.0 m, 4.5 m, 7.5 m, 9.0 m, and 15 m). The analysis of the average SPT values revealed that the majority of the values ranged between 35-50. Comparing these values to the depths of 3 m, 4.5 m, 7.5 m, and 9 m, it is apparent that the soil structure becomes denser at a depth of 15 m. Overall, Figure 5.2 illustrates that SPT-N values exceeding 35 are prevalent in the study area.

5.2 Map Analysis of Bearing Capacity Values

The data collected from 96 drilling points in the study area was analyzed and compared to the bearing capacities derived from field experiments and geophysical methods. Maps were generated using two different methods, namely the Terzaghi & Peck and Meyerhof methods, to calculate the bearing capacities based on the values obtained from the surface to a depth of 15 m.

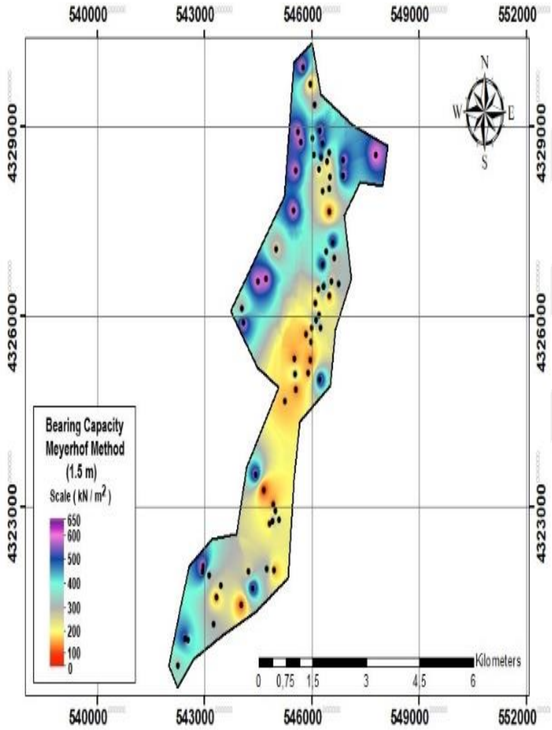

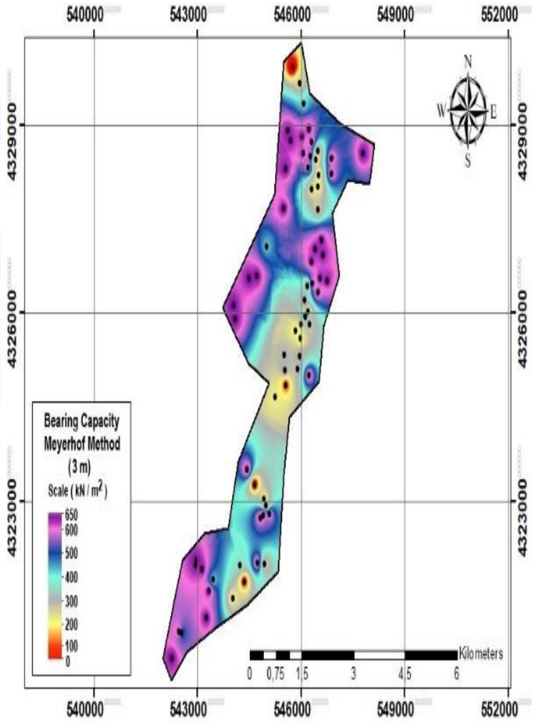

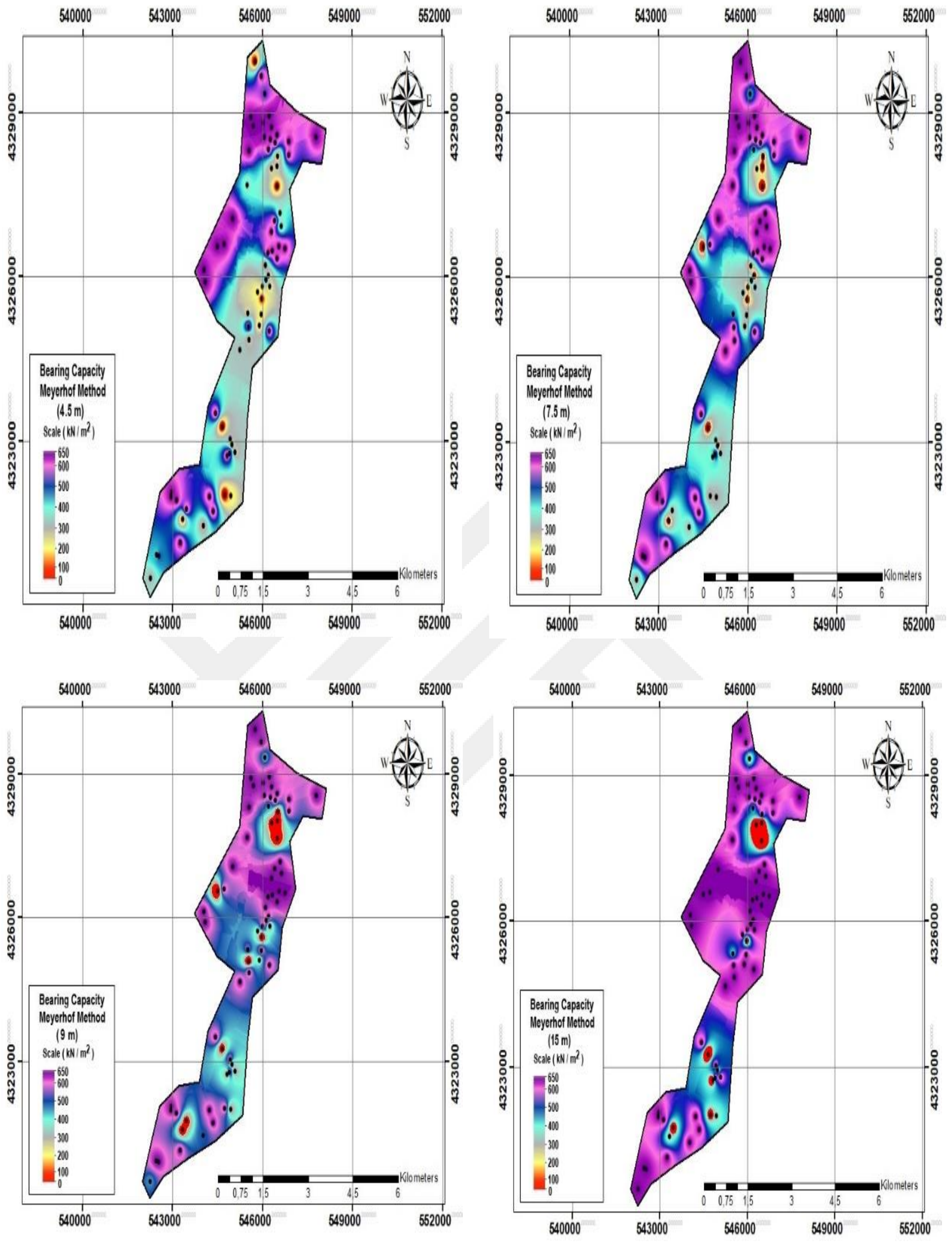

Figure 5.3. Maps of bearing capacity according to the Meyerhof method for different borehole depths (1.5-3.0-4.5-7.5-9.0-15 m)

Figure 5.3 displays the bearing capacity map created using the Meyerhof method. It is generated by averaging the SPT-N data collected from 96 drilling points at various depths (1.5 m, 3 m, 4.5 m, 7.5 m, 9.0 m, and 15 m) across the study area. The map reveals regions with low soil bearing capacity at a depth of 1.5 m, including the central part, eastern part, a portion of the Cumhuriyet neighborhood, and most of the Atatürk neighborhood. Generally, the soil consistency at this depth is considered medium solid. With the exception of the central part of the city, all neighborhoods exhibit a high bearing capacity at a depth of 1.5 m. Upon examining the soil bearing capacity at different depths (1.5 m, 3.0 m, 4.5 m, 7.5 m, 9 m, and 15 m) throughout the study area, it becomes evident that the bearing capacity increases as the depth increases. Notably, the Moğultay neighborhood has a low soil bearing capacity.

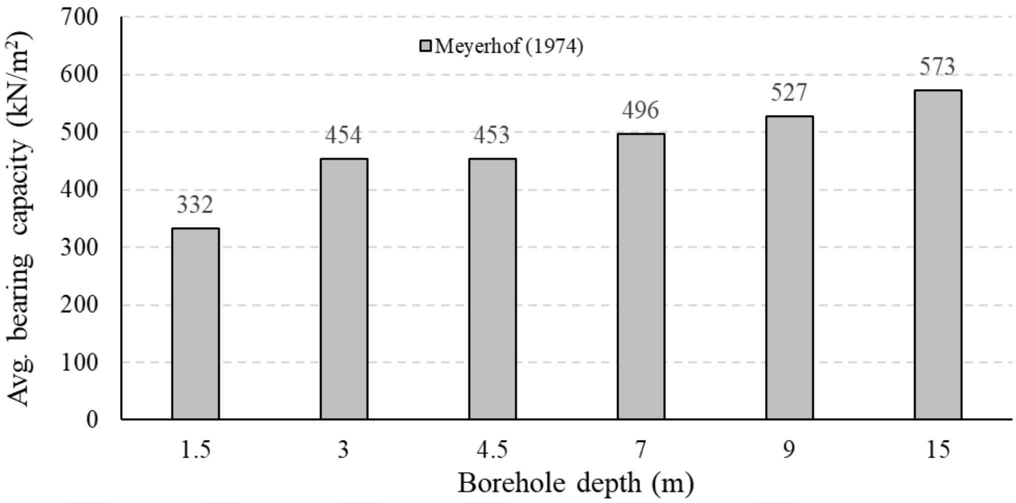

Figure 5.4. Bearing capacity results according to Meyerhof method for different borehole depths (1.5-3.0-4.5-7.5-9.0-15 m)

Figure 5.4 shows the average bearing capacity graph according to the Meyerhof method. It is seen in the graph that the bearing capacity is gradually increasing with the depths of 1.5 m, 3 m, 4.5 m, 7.5 m, 9 m, and 15 m. The bearing capacity becomes more as the depth increases.

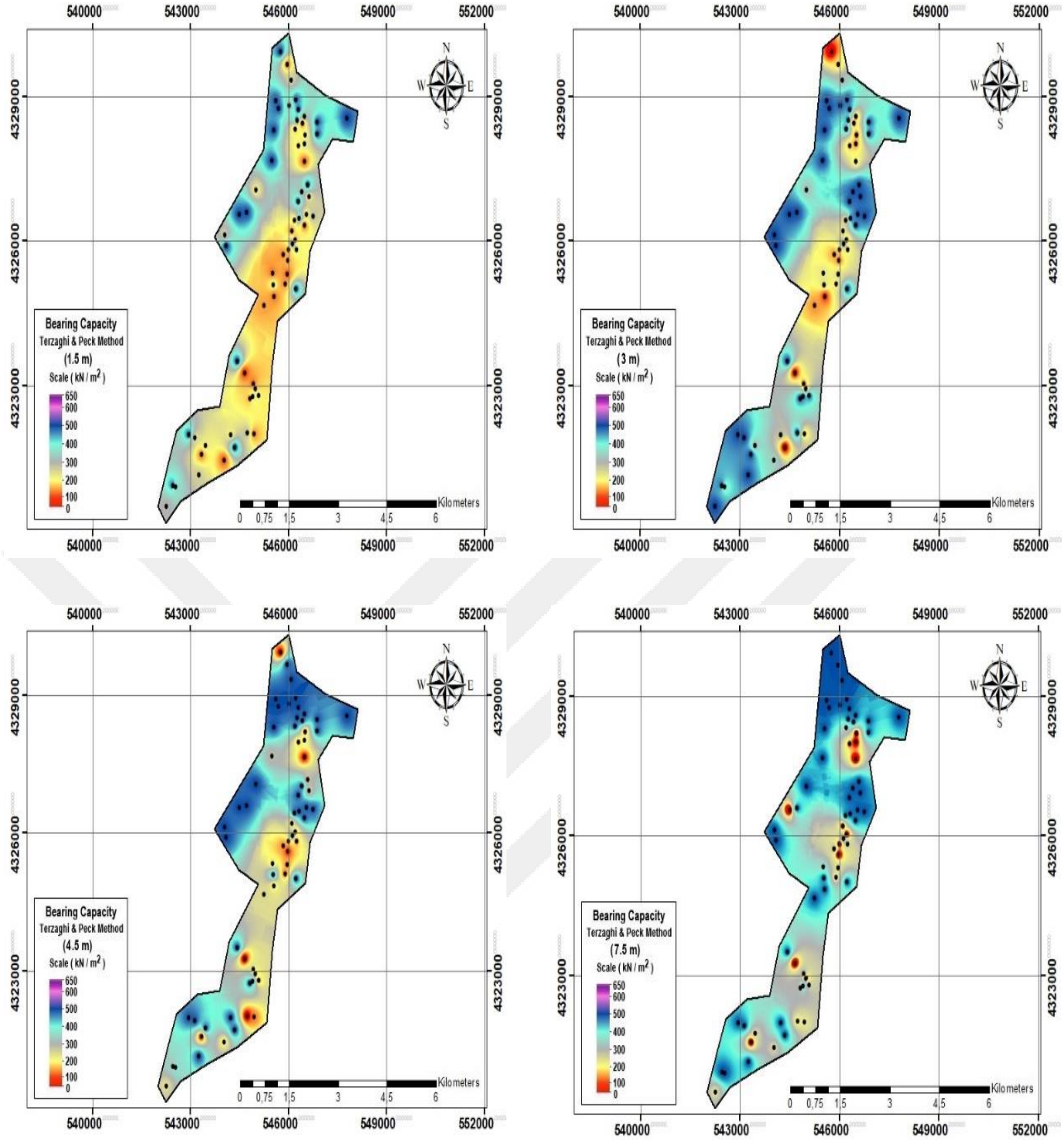
Bearing Capacity
Terzaghi & Peck Method
(1.5 m)
Scale (kN / m2)
Bearing Capacity
Terzaghi & Peck Method
(3 m)
Scale (kN / m2)
Bearing Capacity
Terzaghi & Peck Method
(4.5 m)
Scale (kN / m2)
Bearing Capacity
Terzaghi & Peck Method
(7.5 m)
Scale (kN / m2)
Kilometers

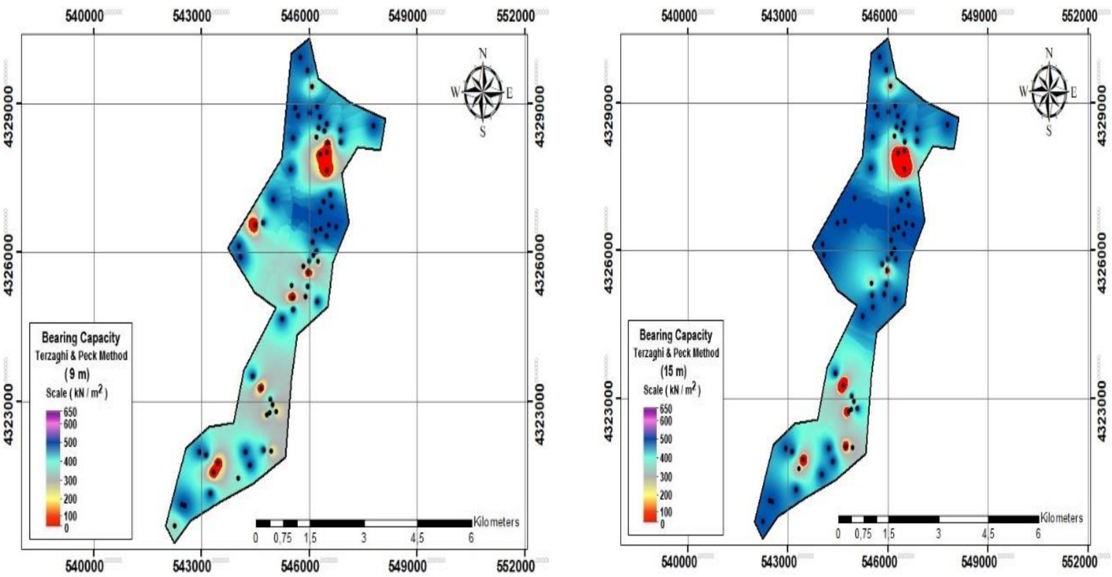

Figure 5.5. Maps of bearing capacity according to the Terzaghi & Peck method for different borehole depths (1.5-3.0-4.5-7.5-9.0-15 m)

Figure 5.5 depicts the bearing capacity map generated using the Terzaghi & Peck method. In the study area, it is observed that the soil bearing capacity is low at a depth of 1.5 m in the middle part, the eastern part, a portion of the Cumhuriyet neighborhood, and in the majority of the Moğultay and Atatürk neighborhoods. The Terzaghi & Peck method yields similar results as the Meyerhof method. The average values obtained using the Terzaghi & Peck method range from 488 kN/m^2, whereas the average values from the Meyerhof method are 646 kN/m^2.

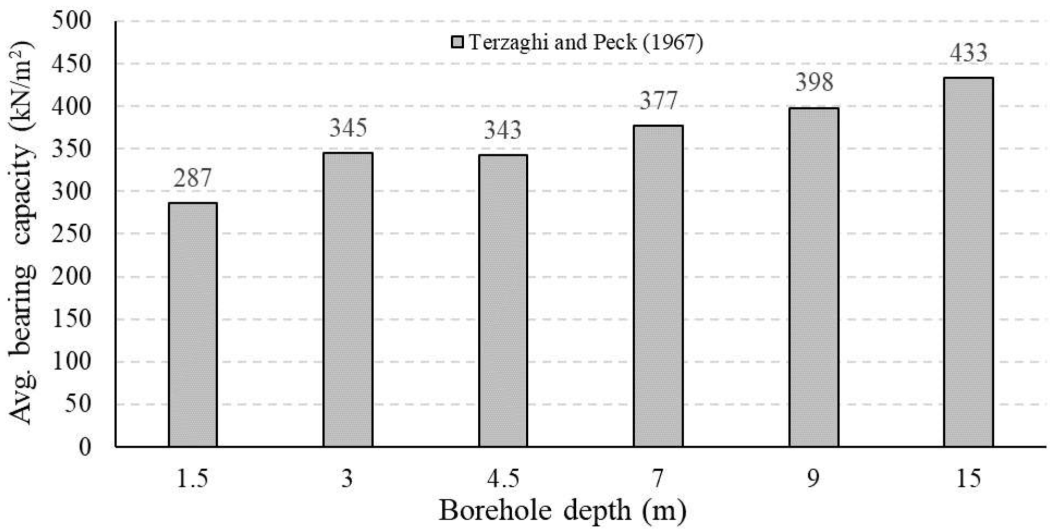

Figure 5.6. Bar chart of bearing capacity results according to Terzaghi & Peck method for different borehole depths (1.5-3.0-4.5-7.5-9.0-15 m)

The maps created using the Terzaghi & Peck and Meyerhof methods exhibit congruence, and the calculated values are similar when considering the SPT-N value and data obtained at depths of 1.5 m, 3.0 m, 4.5 m, 7.5 m, 9.0 m, and 15 m starting from a depth of 1.5 m. Nevertheless, it was observed that as the number of blows and depth increased, the Meyerhof method produced higher bearing capacity values compared to the Terzaghi & Peck method. In both approaches, the examination of the soil bearing capacity across the study area at depths of 1.5 m, 3 m, 4.5 m, 7.5 m, 9 m, and 15 m revealed an increase in capacity with greater depth. Only the Moğultay neighborhood exhibited low soil bearing capacity.

5.3. Map Analysis of Groundwater Level

Groundwater levels were assessed in 96 geotechnical boreholes within the study area, and subsequently, a map displaying the groundwater levels was generated. Figure 5.7 depicts the groundwater level in Tunceli Province. It can be observed that the central region of Tunceli has a higher groundwater level compared to the rest of the area.

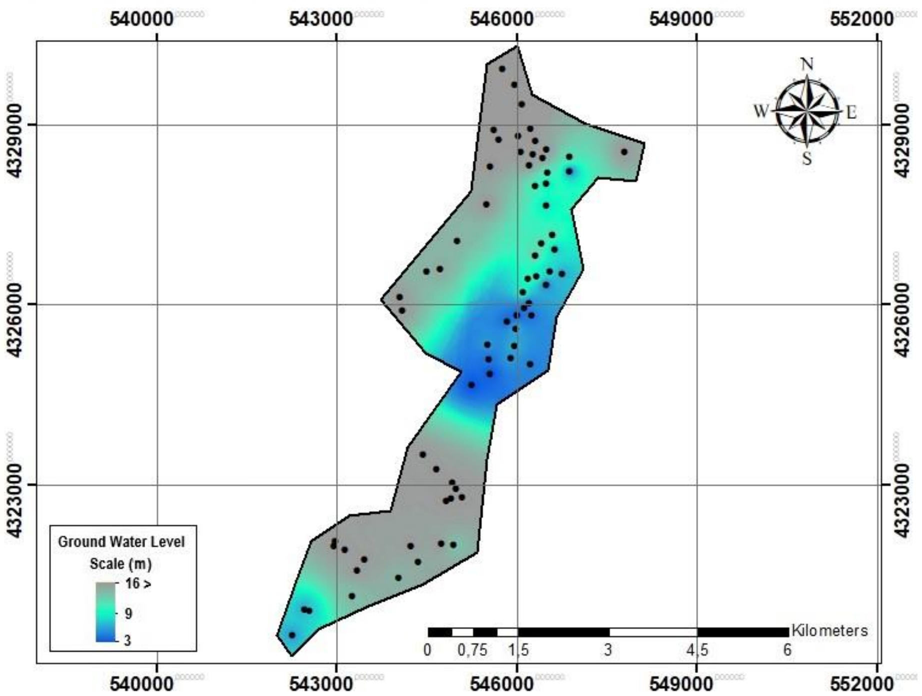

Figure 5.7. Map of groundwater level

Figure 5.8 presents the boreholes where groundwater was identified, along with their corresponding geological structures. The geological composition of Tunceli province is characterized by Quaternary Alluviums and Terraces in the southern and eastern regions, Keban Metamorphites in the northern and western areas, and rock formations including Mollakulaçdere formation, Kozlu formation, and Toraman formation, as well as residuals associated with these formations. Laboratory test results from the Toraman formation, Kozlu formation, Mollakulaçdere Formation Residuals, Alluvium, and Terrace units have provided insights into their properties.

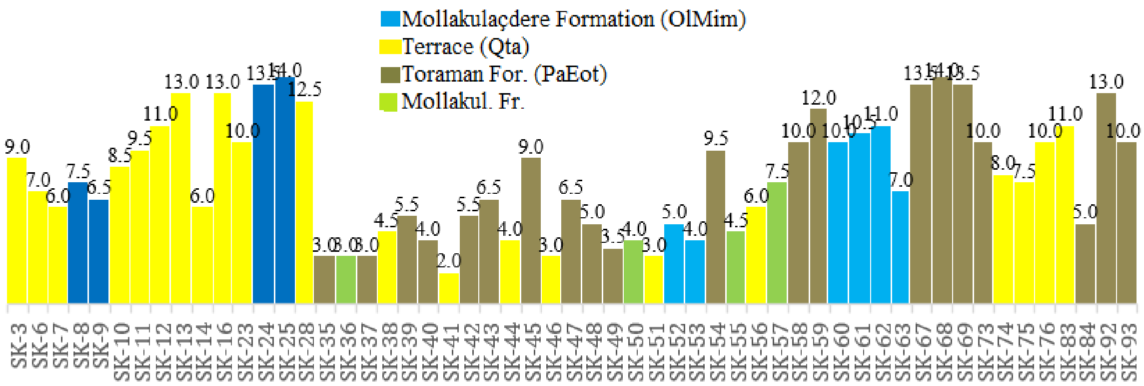

Figure 5.8. Groundwater information of different geological formations in the study area.

5.4. Map Analysis of Water Content Data

The assessment indicates that the study area has limited groundwater resources. Out of the 96 drilling points surveyed across the study area, groundwater was found at 29 points within a range of 3.5 to 29 meters. The corresponding map illustrating groundwater information is displayed in Figure 5.7.

Figure 5.9 illustrates the variations in water content at various depths, namely 1.5 m, 3.0 m, 4.5 m, 7.5 m, 9.0 m, and 15 m, starting from a depth of 1.5 m from the working front. It was observed that the water content in the Atatürk quarter of the study area remained relatively consistent across different depths, ranging between 6% to 16%. Examining the water content (w_n) values obtained from depths of 1.5 m, 3.0 m, 4.5 m, 7.5 m, 9.0 m, and 15 m within the scope of the study, the dominant w_n value was found to be 18%.

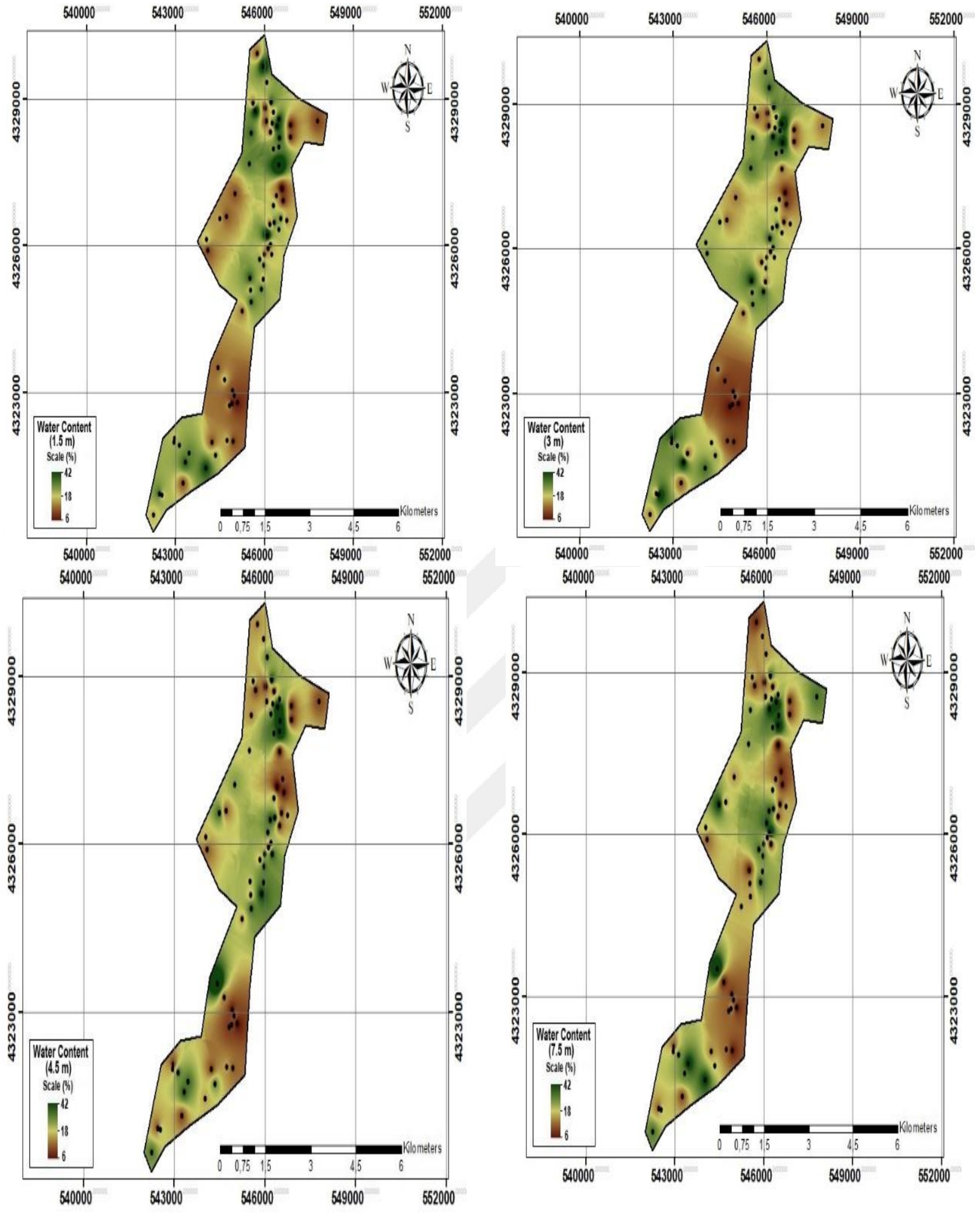
Water Content (1.5 m)
Water Content (3 m)
Water Content (4.5 m)
Water Content (7.5 m)
Scale (%)
42
18
6
Kilometers
0 0,75 1,5 3 4,5 6
N
W
E
S
540000
543000
546000
549000
552000
4323000
4326000
4329000

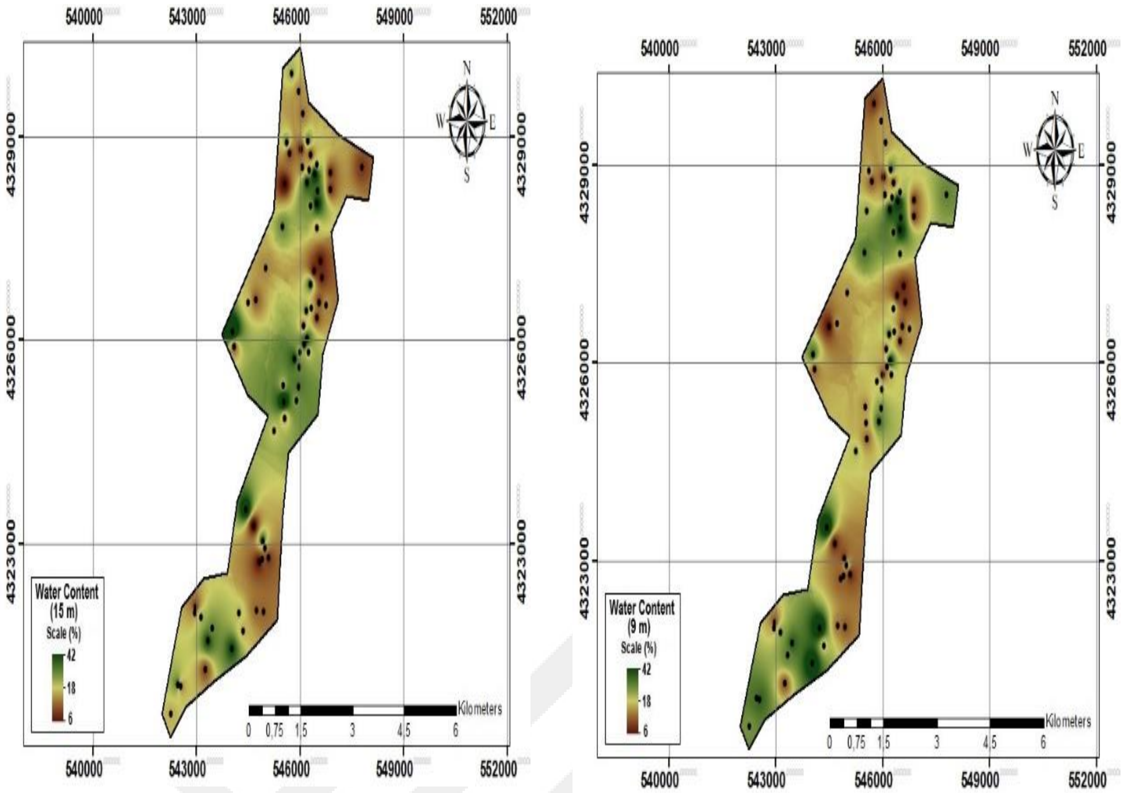

Figure 5.9. Maps of water content according to different borehole depths (1.5-3-4.5-7.5-9-15 m)

5.5. Map Analysis of Liquefaction Risk

Many analysis methods based on field and laboratory experiments are available in the literature to determine liquefaction susceptibility. Field experiments are commonly preferred in the investigation of liquefaction potential since the experiments in the laboratory are time-consuming and expensive. Among these field tests, the SPT is the most widely used one (Sen, 2004).

To determine the potential for liquefaction, SPT-N numbers obtained from 96 drilling points in the study area were utilized. In order to visualize the distribution of liquefaction probability and depth variation from the surface to a depth of 15 m, maps were created for depths of 4.5 m, 7.5 m, 9.0 m, and 15 m in the study area. These maps were generated using the ArcGIS program, with a grid size of 10 m, similar to the liquefaction potential maps. Based on the calculation and comparison method, the maps were created to indicate the risk of liquefaction. A factor of safety smaller than one indicates a risk of liquefaction, while a factor of safety greater than one suggests no risk of liquefaction.

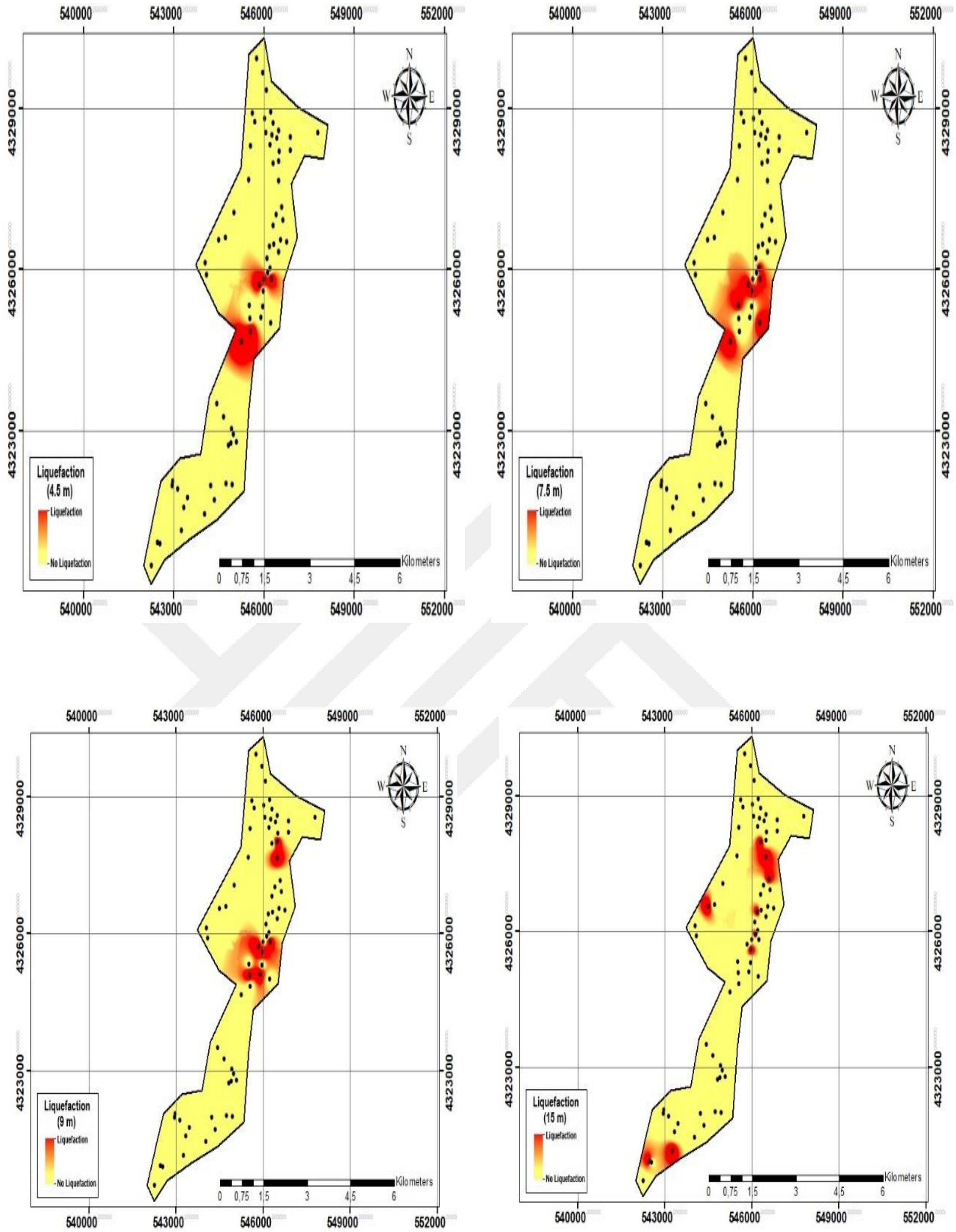

Figure 5.10. Maps of liquefaction potential for different borehole depths (4.5-7.0-9.0-15 m)

Upon analysis of Figure 5.10, it has been observed that the majority of the study area shows a factor of safety greater than one (indicating no liquefaction risk) for depths of 4.5 m, 7.5 m, 9.0 m, and 15 m. However, there is a small section in the study area where the factor of safety is smaller than one (indicating the presence of liquefaction risk). Specifically, the middle part of the study area, including the Atatürk, Cumhuriyet, and Moğultay neighborhoods, is identified as having a risk of liquefaction, while the remaining parts of the study area do not possess this risk. Based on evaluations conducted using SPT tests and laboratory data from geotechnical drilling reports, it has been determined that most of the soils in the study area are "non-liquefiable," except for areas with alluvial deposits and those with high groundwater levels, where a risk of liquefaction exists.

5.6. Map Analysis of Shear Wave Velocity

As part of the data collected from field measurements, a map was generated to analyze the shear wave velocity. This map is based on the average shear wave velocity of the soil at a depth of 30 m, which is commonly used in engineering studies, soil classification systems, and earthquake hazard analysis. During the creation of the map, it was observed that the shear wave velocity values ranged from 286 m/sec to 1271 m/sec at a depth of 30 m.

Based on field measurements conducted throughout the study area at a depth of 30 m, the data reveals that the northern segment exhibits shear wave velocity ranging between 286 m/sec and 460 m/sec, with a few locations reaching approximately 700 m/sec. Moreover, the Shear wave velocity in the Atatürk neighborhood is predominantly greater than 700 m/sec. Conversely, a section of the Aktuluk neighborhood displays shear wave velocities below 460 m/sec. The corresponding map outlining these findings can be found in Figure 5.11.

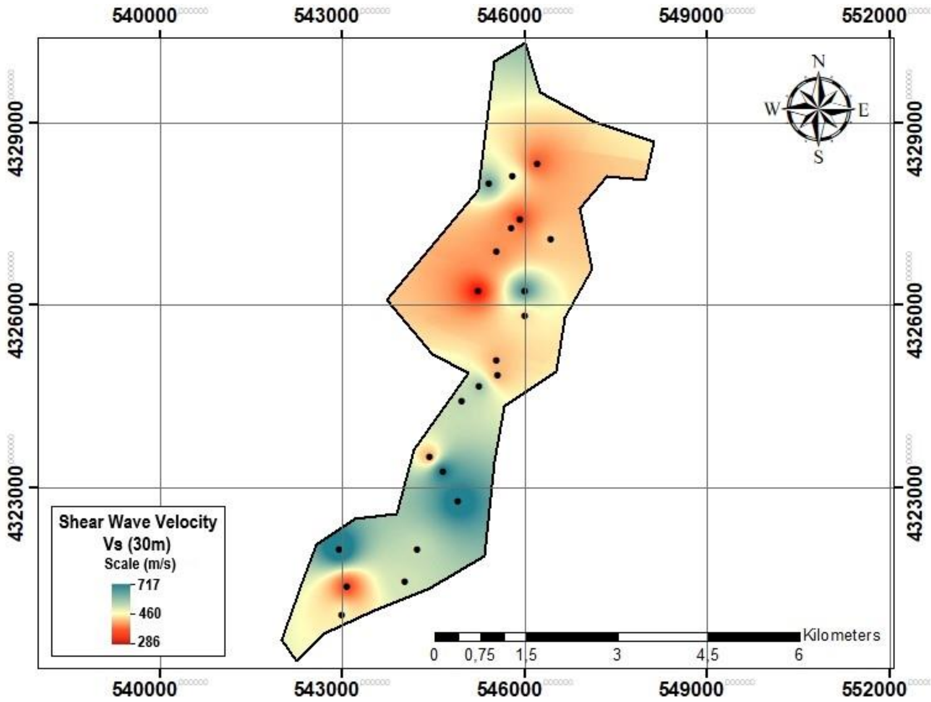

Figure 5.11. Map of shear wave velocity according to 30 m

5.4. Map Analysis of Geophysical Studies

Numerous geophysical investigations have been conducted in the area of study. These investigations include the utilization of the Multi-Channel Analysis of Surface Wave (MASW) technique, involving both P and S waves, in 36 series to determine the elastic and dynamic characteristics of the region. Additionally, the seismic refraction method was employed in 2 series, using both P and S waves, while the microtremor method was utilized at 20 locations to determine the dominant vibration period and amplification values of the soil.

5.7.1. Multi-channel analysis of surface wave (MASW) method

Due to the majority of the study area being located within the city and consisting of narrow spaces, it is not feasible to obtain field parameters for seismic refraction at the desired depth of investigation. This is because residential areas tend to have a low signal-to-noise ratio, making it difficult to determine low-velocity zones. Therefore, it is more advantageous to utilize surface waves with long wavelengths and low frequencies for data collection. Figure 5.12 shows the distribution of the MASW test locations.

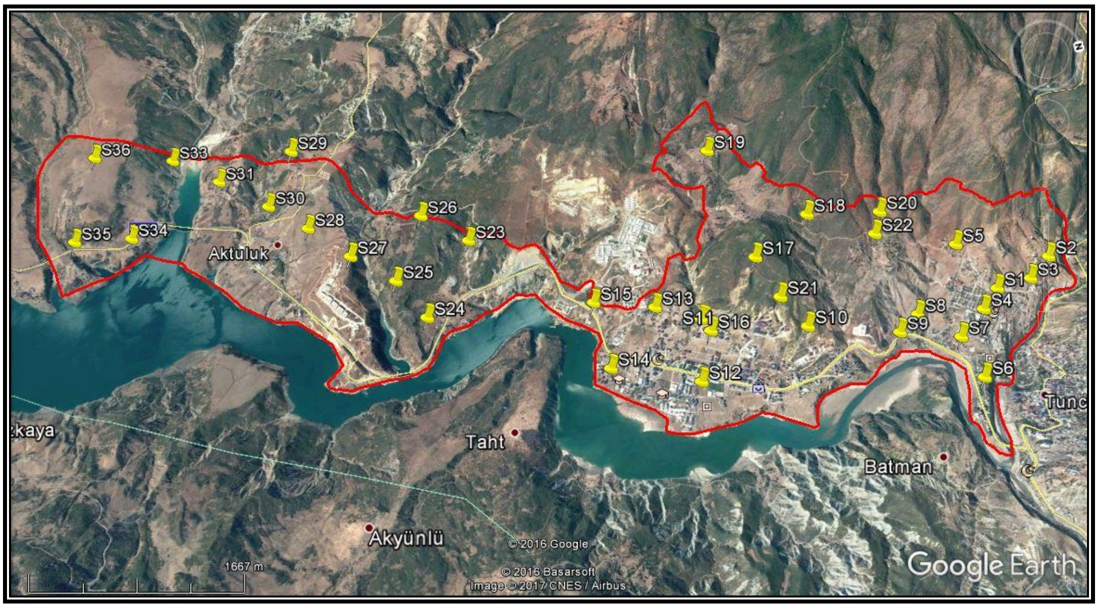

Figure 5.12. Distribution of MASW locations.

The investigation depth in the study area was set at 30 meters, and for data collection purposes, geophones were placed at intervals of 3 meters, which is one-tenth of the exploration depth. The offset distance was determined to be three times the geophone intervals. Seismic recordings were conducted using the DoReMi brand seismic recorder and 4.5 Hz surface geophones. Vertical geophones with a frequency of 14 Hz were also used in the same configuration to collect seismic data for calculating P-wave velocity with mutually shot sources. The collected field data was processed using the SeisImager/WaveEq programs to generate dispersion curves. From these curves, the fundamental mode curve was determined, and S-wave velocity values were calculated through inversion by selecting 10 initial layer models covering the entire study area. The P-wave velocity values were then combined with the S-wave velocities obtained from the mutual shot sources, which were modeled with 10 closely spaced layers.

The shear wave velocity values at a depth of 30 meters ranged from 286 to 1271 m/sec. The study presented in Figure 5.11 did not identify any low-velocity zones through the shear wave velocity investigations. However, the MASW study provided a general examination of the area and revealed that the lowest $V_{s,30}$ velocity values in the city center varied from 250 to 450 m/sec. The residential areas bounded by the S9-S17-S15 and S14 testing locations exhibited the lowest velocity values. Notably, sudden velocity transition zones were observed in the northwestern part of the study area. Figure 5.13 displays the shear wave velocity based on the results obtained from the MASW testing.

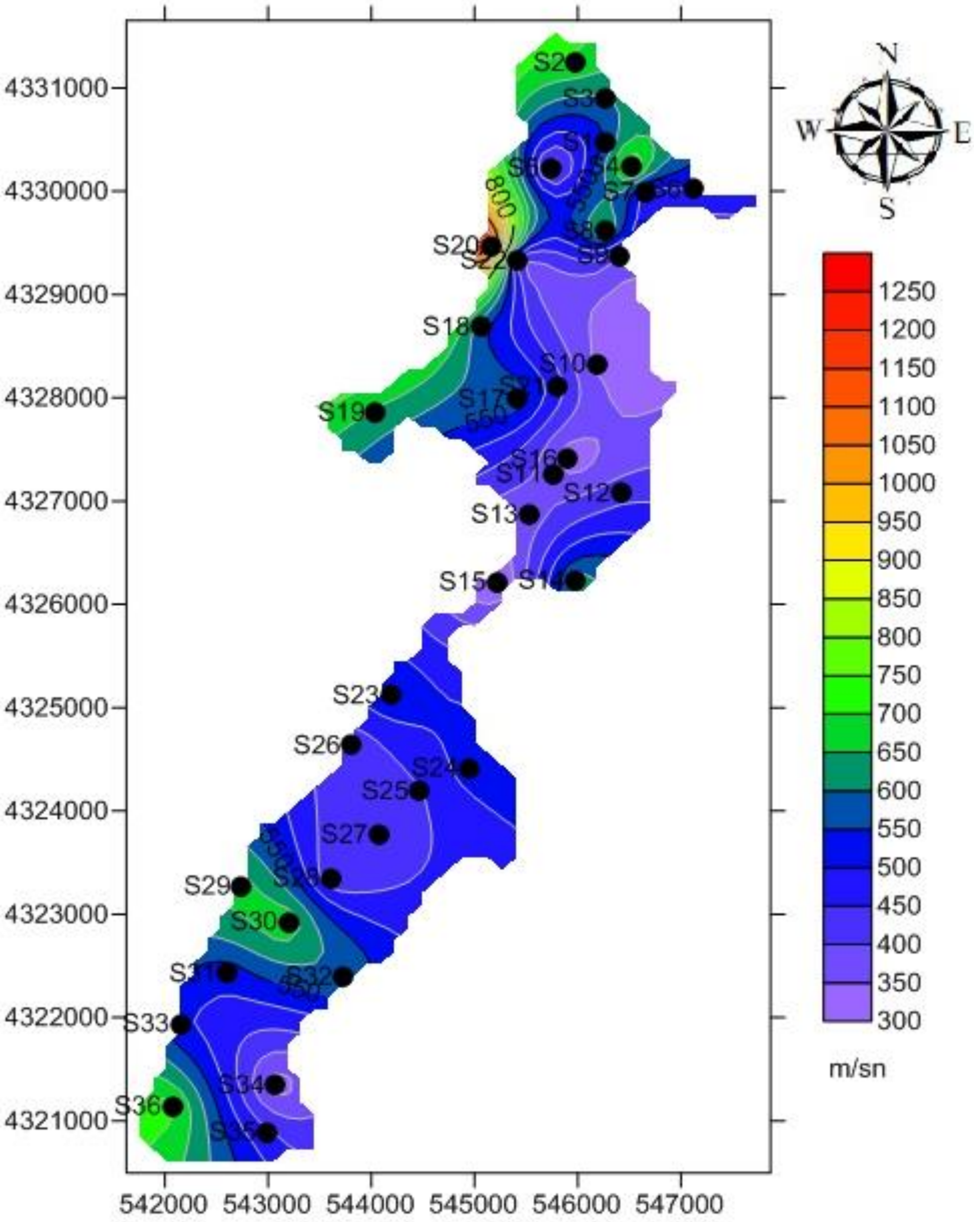

Figure 5.13. Map of $V_{s,30}$ obtained from MASW values.

5.7.2. Seismic refraction method

The method relies on measuring the time it takes for refracted seismic waves to travel across the boundaries between different soil layers with varying propagation velocities. These refracted waves follow a favorable path along the ground and typically have a frequency range of 5 to 25 Hz. The seismic refraction technique is illustrated in Figure 5.14, showcasing the two locations where testing was conducted.

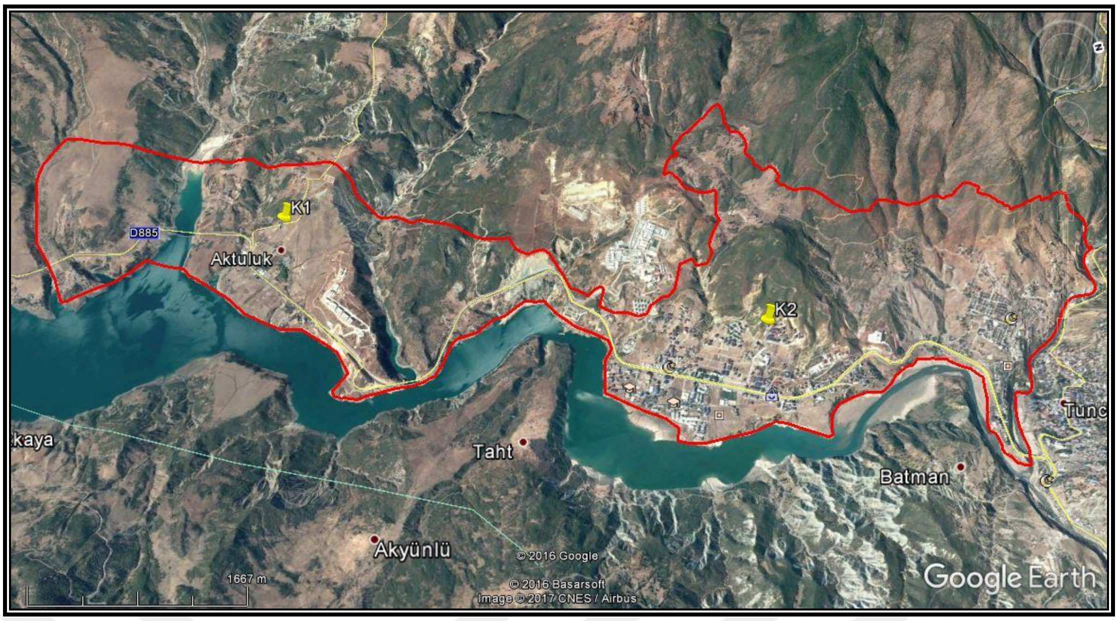

Figure 5.14. Distribution of seismic refraction locations.

Seismic refraction data were collected using a 12-channel DoReMi seismic recorder, equipped with 14 Hz vertical and horizontal geophones. The recordings had a length of 0.25 to 0.50 ms and a sampling time of 0.5 ms. The field parameters were determined based on the characteristics and objectives of the study area, and recordings of reciprocating P and S waves were obtained in two separate series. In the study area, the geophone intervals were set at 5 meters, while an offset distance of 2.5 meters was chosen. Empirical relationships were employed to calculate the V_p and V_s values of the soil based on the measured parameters. Table 5.3 is showing the testing results of seismic refraction.

Table 5.3 Velocities measured according to the seismic refraction test

Point No	Layer No	V_p (m/sec)	V_s (m/sec)	h (m)	d (m)	Formation
K1	1. Layer	445	213	7	7	Tunceli Fm. Residual
	2. Layer	1907	959	-	-	Tunceli Formation
K2	3. Layer	349	119	6	6	Tunceli Fm. Residual
	4. Layer	1448	779	-	-	Tunceli Formation

As can be seen on Table 5.3, K1 and K2, two distinct seismic layers were identified with an approximate depth of 6 meters. In the first layer, the velocity values of V_p ranged from 349 to 445 m/sec, while the velocity of V_s ranged from 213 to 959 m/sec. In the second layer, V_p values varied between 1448 and 1907 m/sec, whereas V_s values were observed to be between 119 and 779 m/sec. The second layer exhibited shear wave velocity values (V_s) that exceeded 760 m/sec, which can be referred to as the seismic bedrock.

5.7.3. Microtremor method

The ground, which vibrates at small amplitudes continuously, vibrates by increasing its amplitude at specific frequencies. The microtremor method is the best way to determine the parameter known as the ground dominant vibration period. Microtremor studies were carried out at 20 points with the SR04S3-10 microtremor device developed by Sara Instrument. The accelerometer device with a natural vibration frequency of 1-100Hz has three components X-Y-Z. Since the measurements were taken during the hours of the cultural activity, the recording times were kept for 15 minutes. At some points in the city center, measurements were taken in the morning when the activity was the least. Evaluations were made with the GEOPSY package program, and full windowing of 15-20 seconds was made. Figure 5.15 shows the distribution of the microtremor testing locations. Shear wave velocity values have been used for the determination of soil classes of the country earthquake codes.

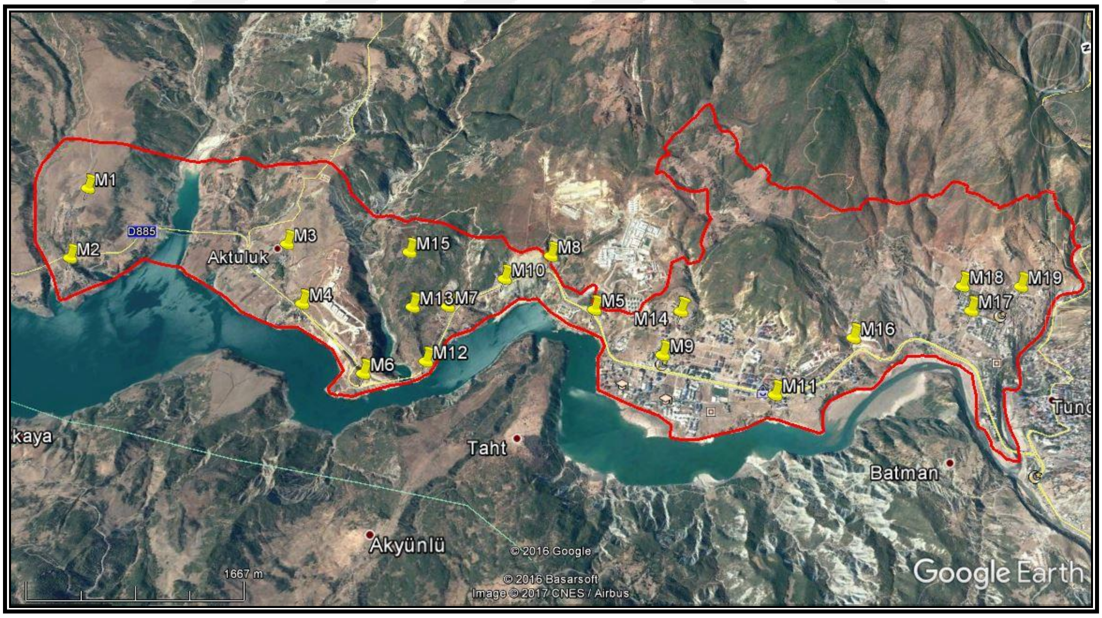

Figure 5.15. Distribution of Microtremor locations.

5.8. Map Analysis of Soil Classes according to Earthquake Codes

A map illustrating the soil classification was generated based on the field measurements of shear wave velocity. The analysis of these measurements revealed that the majority of the study area falls under soil class C, with a small portion classified as

D. The corresponding map can be found in Figure 5.16. It is worth noting that the soil classes align between NEHRP and TBDY-2018, whereas there are discrepancies in the classifications under EUROCODE-8 due to limitations in the earthquake regulations of Europe.

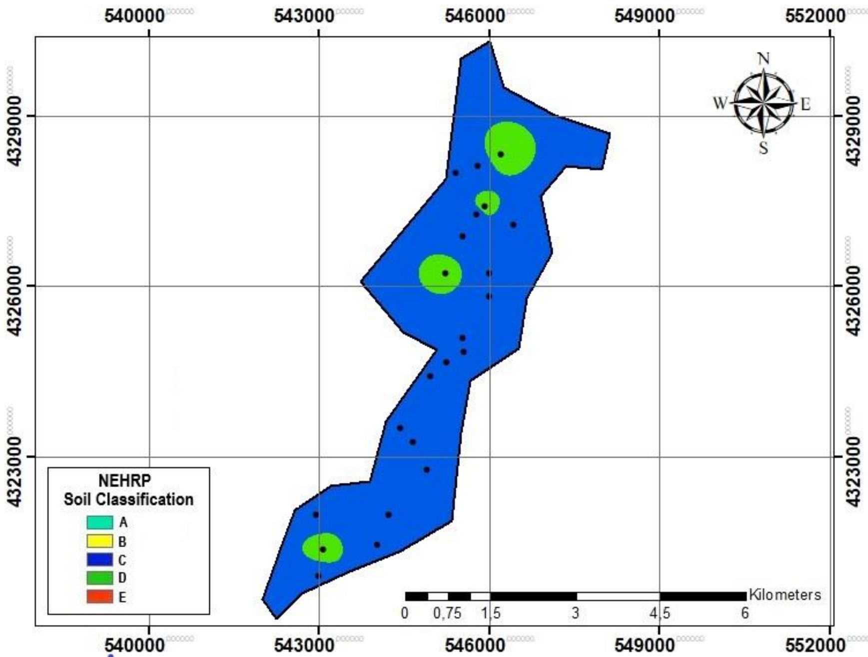

Figure 5.16. Map of soil classification according to earthquake regulations.

Based on the NEHRP earthquake code's classification, the majority of the study area falls under the C category, denoting "Very Firm/Hard Ground or Soft Rock." However, the location of points S10, S15, and S34 within the area corresponds to soil class D, which is categorized as "Hard Ground." The Turkish earthquake code TBDY-2018 also shares similar soil classifications, given the same limitations.

On the other hand, when considering the EUROCODE-8 earthquake code classification, it is observed that almost the entire area is classified as B, representing "Very compact sand, gravel, or very hard clays." The remaining points (S10, S15, S34) are classified as class C, which corresponds to "Compact or medium compact sand gravel or hard clays."

5.9. Map Analysis of Density Values

The density has been determined using Equation 4.21, as provided in chapter 4, and evaluated based on Table 4.3 by Dursun et al. (2012). The values obtained for d in the study area are presented in Figure 5.17, where the unit of measurement is g/cm^3. The density values have been calculated depending on V_p.

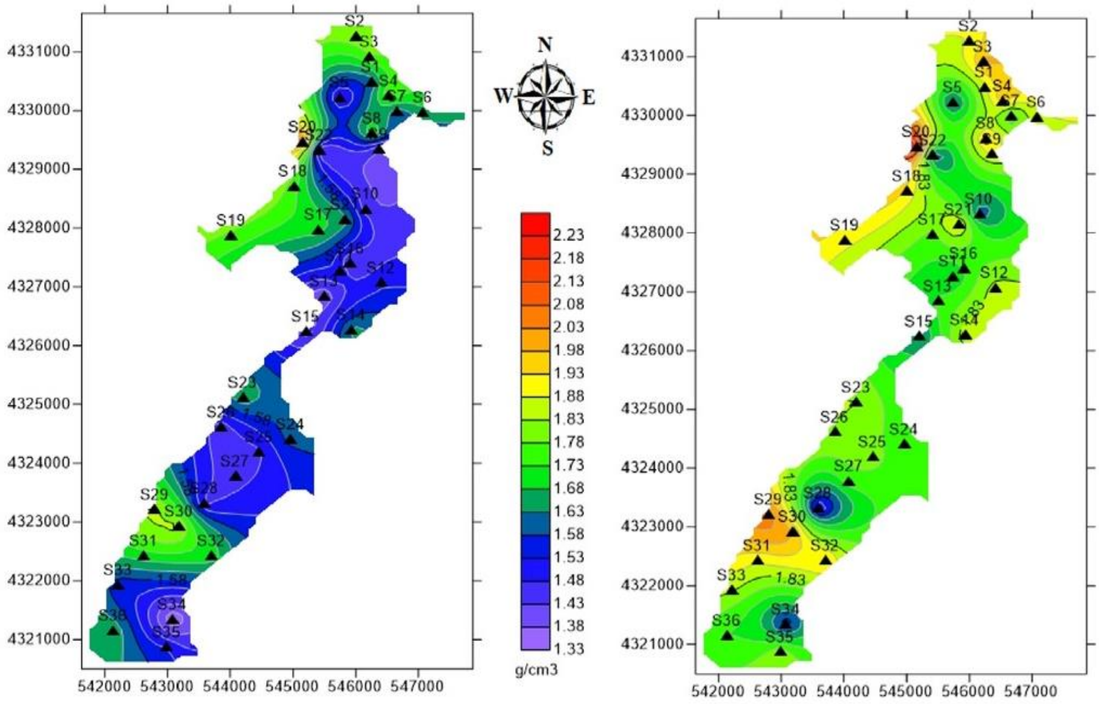

Figure 5.17. Maps of density values (left: 1st layer, right: 2nd layer)

5.10. Map Analysis of Seismic Velocity Rates

According to the seismic velocity rates, the density of the soil and the liquefaction risk of the soil can be estimated. Suppose there is a geological unit suitable for liquefaction in the environment. If there is groundwater, the V_p/V_s ratio is checked. If this ratio is greater than 3, there is a high probability of liquefaction risk. The V_p/V_s ratio has been classified according to the Table 4.4 in chapter-4 and the map of this analysis is shown on Figure 5.18.

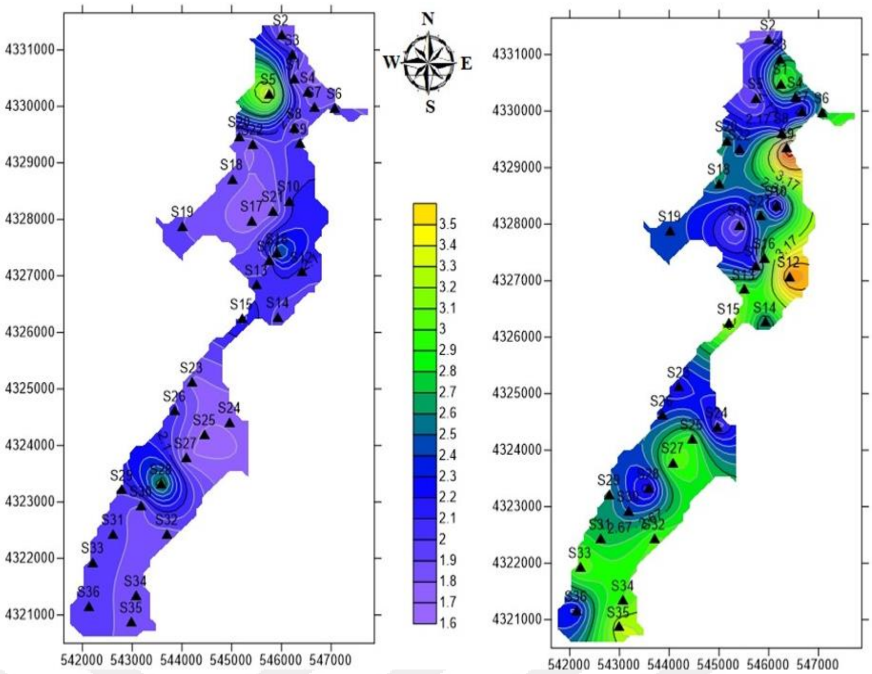

Figure 5.18. Maps of V_p/V_s values (left: 1[st] layer, right: 2[nd] layer)

5.11. Map Analysis of Maximum Shear Modulus

The maximum shear modulus (Gmax) has been determined using Equation 4.23, as provided in chapter 4, and evaluated based on Table 4.5 by Dursun et al. (2012). Generally speaking, the higher the shear modulus, the greater the strength of the formation in resisting shear stresses, such as those caused by horizontal forces. The values obtained for G_{max} in the study area are presented in Figure 5.19, where the unit of measurement is kg/cm^2.

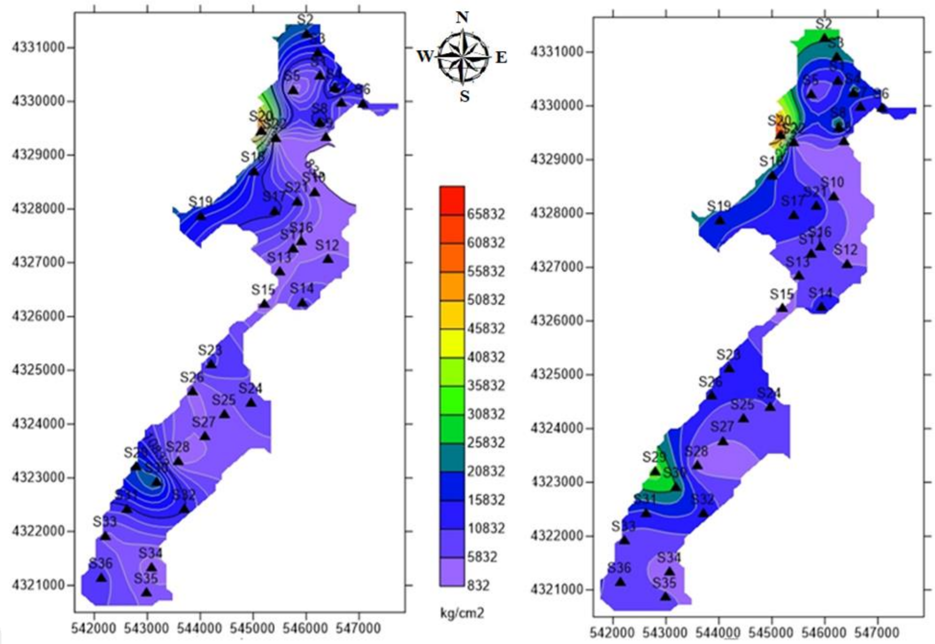

Figure 5.19. Maps of G_{max} values (left: 1[st] layer, right: 2[nd] layer)

5.12. Map Analysis of Ground Bearing Coefficient

The bulk module (*K*) is used to calculate the stress over settlement coefficient. The bearing coefficient is calculated from the equation 4.24 in chapter-4. Figure 5.20 shows the results of the bulk module values of the study area.

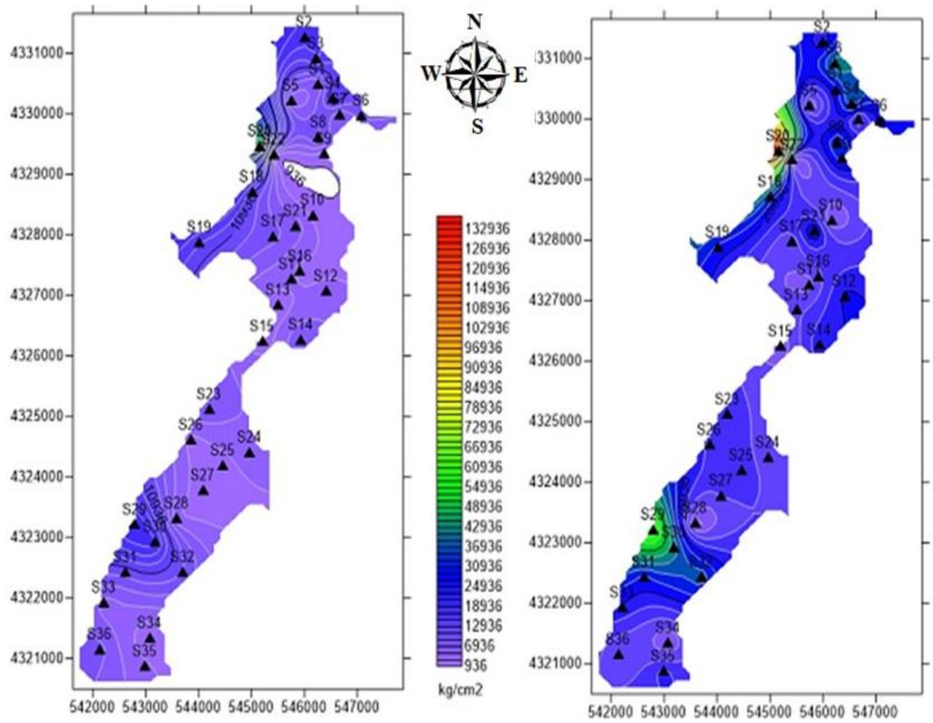

Figure 5.20. Maps of *K* values (left: 1[st] layer, right: 2[nd] layer

6. CONCLUSIONS

In this thesis, a database was constructed by utilizing field and laboratory test data extracted from geotechnical reports found in the Tunceli Municipality archive, enabling the generation of various maps, such as SPT-N values at different depths, bearing capacity, liquefaction potential, shear wave velocity, soil classes based on different earthquake codes, soil amplification, dominant vibration period, water content, and groundwater levels. These maps offer a visual assessment of geotechnical information within the Tunceli Municipality study area, facilitated by a GIS-based program.

GIS maps play a crucial role in determining soil properties. These maps provide a comprehensive overview of the physical and geotechnical characteristics of an area, including bearing capacity, liquefaction, soil classes and seismic aspect. By analyzing this information, engineers can evaluate the risk of soil behaviours.

There are several benefits to using GIS maps for determining soil properties. Firstly, it allows for a quick and efficient analysis of large areas, making it easier to identify high-risk zones. Secondly, integrating various data sources, like topographical maps, geology maps, and geotechnical data, into a single GIS map offers a comprehensive understanding of the area and helps identify potential uncertainties. Lastly, GIS maps are easily accessible, user-friendly, and can be regularly updated to reflect changes in soil properties and conditions. Overall, incorporating GIS maps in assessing soil properties is vital in geotechnical engineering and ensures the safety and stability of structures. The advantages of this method, including speed, efficiency, and accessibility, make it an indispensable tool for engineers and geologists. The study's findings are summarized below in bullet points.

- Atatürk and a part of the Cumhuriyet neighborhood have SPT-N values varying between 1-25. These areas are "loose" and "medium dense" structures.
- SPT values at 3.0 m, 4.5 m, 7.5, 9 m, and 15 m are compared, it is seen that the ground at 15 m has a denser soil structure. In general, SPT-N values greater than 35 appear to be more common in the study area.
- In the study area, it is observed that the soil bearing capacity is low at a depth of 1.5 m in the middle part, the eastern part, a portion of the Cumhuriyet neighborhood, and in the majority of the Moğultay and Atatürk districts.

- The Terzaghi & Peck method yields similar results as the Meyerhof method. The average values obtained using the Terzaghi & Peck method range from 488 kN/m^2, whereas the average values from the Meyerhof method are 646 kN/m^2.
- Mogultay neighborhood has a low soil-bearing capacity in Tunceli province.
- It is observed that the central region of Tunceli has a higher groundwater level compared to the rest of the area.
- In the study area, the groundwater was found at 29 points within a range of 3.5 to 29 meters.
- The water content in the Atatürk quarter of the study area remained relatively consistent across different depths, ranging between 6% to 16%. Examining the water content (w_n) values obtained from depths of 1.5 m, 3.0 m, 4.5 m, 7.5 m, 9.0 m, and 15 m showed that the dominant w_n value was found to be 18%.
- It has been observed that the majority of the study area shows no liquefaction risk for depths of 4.5 m, 7.5 m, 9.0 m, and 15 m.
- A small section in the study area is indicating the presence of liquefaction risk Specifically, the middle part of the study area, including the Atatürk, Cumhuriyet, and Moğultay neighborhoods, is identified as having a risk of liquefaction.
- Based on evaluations conducted using SPT tests and laboratory data from geotechnical drilling reports, it has been determined that most of the soils in the study area are "non-liquefiable".
- It was observed that the shear wave velocity values ranged from 286 m/sec to 1271 m/sec at a depth of 30 m in the study area.
- The data reveals that the northern segment exhibits shear wave velocity ranging between 286 m/sec and 460 m/sec, with a few locations reaching approximately 700 m/sec.
- The shear wave velocity in the Atatürk neighborhood is predominantly greater than 700 m/sec. Aktuluk neighborhood displays shear wave velocities below 460 m/sec.
- The lowest $V_{s,30}$ velocity values were conducted in the city center varied from 250 to 450 m/sec. The residential areas exhibited the lowest velocity values. The sudden velocity transition zones were observed in the northwestern part of the study area.

- Based on the NEHRP earthquake code's classification, the majority of the study area falls under the C category, and a small part corresponds to soil class D,
- According to EUROCODE-8 earthquake code classification, it is observed that almost the entire area is classified as B, and a small part is as classified as soil class C.

REFERENCES

AFAD (2018), Deprem Haritası. https://deprem.afad.gov.tr/depremkatalogu/deprem-bolgeleri-haritasi.

AlHamaydeh, M., Al-Shamsi, G., Aly, N., & Ali, T. (2021). Seismic risk quantification and GIS-based seismic risk maps for Dubai-UAE_Dataset. Data in brief. 39, 107566.

Alparslan, E., Yuce, H., Erkan, B., İnan, S., Ergintav, S. and Saatcılar, R. (2006). Analysis of landslide sensitivity between the region Buyukcekmece and Kucukcekmece Lakes with remote sensing and detailed analysis with geographical information systems. Proceedings of the 4th GIS days in Turkey, Fatih University. Istanbul, Turkey, 558.

Alpaslan, N. (2013). Zemin sıvılaşması ve mekanizması. Batman Üniversitesi Yaşam Bilimleri Dergisi. 3(2), 67-89.

Anand S.A. (2000). Recent developments toward earthquake risk reduction India. Current Science. 79, 1270-1277.

Arranoff S (1989). Geographic Information Systems: a management perspective. WDL Publications, Ottawa Canada.

Asutay, HJ., 1985, Baskil çevresinin jeolojik ve petrografik incelenmesi,, A.Ü.F.F. Müh. Fak. Doktora tezi. (yayımlanmamış), 156, Ankara.

Aydan, Ö., Ulusay, R., Hasgür, Z. and Taşkın, B. (2000). Site investigation of Kocaeli earthquake of August 17 1999. Turkey Earthquake Foundation. TDV/DR 08-49, 176.

Ayday, C. (2008). Research report of earthquake hazard mapping update and change under the boundaries of Eskisehir Tepebasi Municipality, Eskisehir, Türkiye

Bargu, S. (2000). Osman Şahin ve Öztoprak S. Gürsu (Bursa) Alanının Jeolojik ve Jepteknik Araştırma Raporu. İstanbul Üniversitesi Araştırma ve Yardım Vakfı Eğitim Faliyetleri İşletmesi.

Başdemir, S. E., & Dinçer, İ. (2019). Osmaniye ili alüvyal zeminlerin jeoteknik incelemesi Master's thesis.

Bingöl, A.F. (1982). Elazığ–Pertek–Kovancılar arası volkanik kayaçların petrografik ve petrolojik incelenmesi: F.Ü. Fen Fak. Dergisi, 1, 9–21.

Boulanger, R. W., & Idriss, I. M. (2006). Liquefaction susceptibility criteria for silts and clays. Journal of geotechnical and geoenvironmental engineering. 132(11), 1413-1426.

Bowles, J. E. (1996). Foundation analysis and design 5th. The McGraw-Hill Companies Inc. New York, USA.

Burmester, M. A. H. (1951). The construction and validation of a test to measure some of the inductive aspects of scientific thinking. Michigan State University.

Burmister, D. M. (1951). Identification and classification of soil an apprasial and statement of principles. ASTM STP, 113.

Büyükaşıkoğlu, S. (1987). Sismoloji Ders Notları. İstanbul Teknik Üniversitesi Jeofizik Mühendisliği Bölümü.

Calzolari, C., Ungaro, F., and Vacca, A., Effectiveness of a soil mapping geomatic approach to predict the spatial distribution of soil types and their properties, Catena, 196, 104818, 2021.

Chung, J. W. (2007). Development of a geographic information system-based virtual geotechnical database and assessment of liquefaction potential for the St. Louis Metropolitan area. University of Missouri-Rolla.

Çiftçi, R. (2020). Nevşehir il merkezi güneyinin jeoteknik değerlendirmesi ve coğrafi bilgi sistemi ile modellenmesi (Master's thesis, Nevşehir Hacı Bektaş Veli Üniversitesi).

Civil Team, July 21, 2022. Bearing Capacity of Soil, https://studylib.net/doc/8477708/bearing-capacity-of-soil---civil-team

Deere, D. U., Miller, R. P. (1966). Engineering classification and index properties for intact rock. Illinois Univ at Urbana Dept of Civil Engineering.

Das, S, Ghosh, S., and Kayal, J. R., Liquefaction potential of AgartalaCity in Northeast India using a CBS platform, Bulletin of EngineeringGeology and the Environment, 78 (4), 2919-2931, 2020.

Demir Gökçe, (2013). Gürsu (Bursa) yerleşim alanındaki temel zemininin jeo-mühendislik özelliklerinin coğrafi bilgi sistemleri (CBS) kullanılarak değerlendirilmesi (Master's thesis, Balıkesir Üniversitesi Fen Bilimleri Enstitüsü).

Demirci et al. "The relationship between land use change and water quality in Küçükçekmece Lake watershed." CBS Bilişim Günleri Bildiriler Kitabı 27 (2006): 34.

Dinç Göğüş, Ö. (2020). 3D discrete analysis of damage evolution of hard rock under tension. Arabian Journal of Geosciences, 13(14), 661.

Dursun, E., Ünver, S., & Hafız, A. C. A. R. (2012). Orman Yolu Güzergahlarının Sismik Zemin Etüdü Metodu ile Belirlenmesi Üzerine Bir Çalışma. Süleyman Demirel Üniversitesi Fen Bilimleri Enstitüsü Dergisi, 16(1).

Elmasdere, E. (2008). Isparta Mavikent yerleşim bölgesinin sismik mikrobölgelemesi ve değerlendirilmesi. Doctoral dissertation, SDÜ Fen Bilimleri Enstitüsü.

Erdoğan, T., 1967, Erzurum - Karayazı bölgesi İ47-c2, c3,İ48-d4, paftalarına ait jeolojik rapor : MTA Rap., 4193 (yayımlanmamış), Ankara

Ergun, S. and Sarac, İ. (2006). Use of GIS in health geography Samsun health center example. National Geographic Information Systems Congress Karadeniz Technical University, Trabzon.

Erol, O. and Çekinmez, Z. (2014). Field tests in geotechnical engineering. High Project Publications, Nu: 14-01, Ankara.

Gradstein, F. M., Ogg, J. G., Schmitz, M., & Ogg, G. (Eds.). (2012). The geologic time scale 2012. elsevier.

Gökçe, A. (2013). The dynamic impacts of oil price shocks on Turkey's economic growth. Journal of economics and sustainable development, 4(8), 181-192.

Gökçe, Demir (2013). Gürsu (Bursa) yerleşim alanındaki temel zemininin jeo-mühendislik özelliklerinin coğrafi bilgi sistemleri (CBS) kullanılarak değerlendirilmesi (Master's thesis, Balıkesir Üniversitesi Fen Bilimleri Enstitüsü).

Gücek S., Zorluer İ. (2021). Bir Boyutlu Analiz Yöntemiyle Sahaya Özel Sıvılaşma Risk Haritalarının Oluşturulması: Karahisar Örneği. Afyon Kocatepe Üniversitesi Fen Ve Mühendislik Bilimleri Dergisi. 21(4), 908-921.

Güzel, M. (2009). Integrated use of geological, geophysical and geotechnical data in microzonation studys (northern adana case), Department Of Geological Engineering Instıtute of Natural and Applıed Scıences Unıversıty of Çukurova, PhD.Thesis, Adana.

Haala, N., Brenner, C. Anders and K.H. (1998). 3D urban GIS from laser altımeter and 2D map data. Proceedings of ISPRS Commission III Symposium, Columbus, Ohio, USA.

Halaç, B. (2016). Review of the soil classification criteria in earthquake regulations with respect to amplification, İstanbul Technical University Institute of Science, M.A. Thesis, İstanbul.

Haşimoğlu, A., Ünal, M., & Daban, Y. (2004). Zemin Etüd Bilgi Sisteminin Oluşturulmasının Önemi Yoncalı (Kütahya) Örneği. 3. İmar İşleri Müdürlüğü, Planlama Servisi.

Hossain, M. B., Roknuzzaman, M., & Rahman, M. M. (2022). Liquefaction Potential Evaluation by Deterministic and Probabilistic Approaches. Civil Engineering Journal, 8(07).

IAEG, R. (1981). soil description and classification for engineering geological mapping. Report by the IAEG Commission on Eng. Geol. Mapping. Bull. of the IAEG, (24), 235-274.

İlbank. (2015). Tunceli Belediyesi Merkez (2. Bölge) İmar Planına Esas Jeolojik-Jeoteknik Etüt Raporu. Tunceli.

Ilic, J. M., Bento, R., ve Cattari, S., 3DCBS representation for supporting seismic mitigation policies at urban scale: The case study of Lisbon, Journal of Cultural Heritage, 45, 265-278, 2020

İyisan, R., Ansal, A. (1994). Geoteknik mühendisliğinde sismik yöntemler ile dinamik özelliklerin belirlenmesi. Zemin Mekaniği ve Temel Mühendisliği, 5, 173-183.

Kanai, K. (1983). Engineering seismology. IIESEE Lecture Note, IEESS Japan.

Kanai, K., “Semi Empirical Formula for the Seismic Characteristic of the Ground”, Bull. Earthq. Res. Ins., Vol.35, Part 2, 1965

Karaca, Ö. (2007). Fethiye yerleşim alanı zeminlerinin mühendislik özelliklerinin belirlenmesi ve jeoteknik haritalarınnın coğrafi bilgi sistemleri (CBS) kullanılarak hazırlanması (Doctoral dissertation, Süleyman Demirel Üniversitesi Fen Bilimleri Enstitüsü).

Karavul, C., Kurnaz, T. F., & Kıyak, A. (2006). Coğrafi Bilgi Sistemleri (Cbs) Kullanılarak İki Farklı Yaklaşımla Adapazarı Kenti Spt (Standart Penetrasyon Testi) Haritalarının Oluşturulması, 4. Cografi Bilgi Sistemleri Bilişim Günleri, İstanbul, Türkiye.

Kargı, H., and Sarı, N. (2006). Determination of landsat tm images of the alteration zones. Proceedings of the 4th GIS days in Turkey. Fatih University Istanbul, Turkey, 558.

Keçeli, A. 1990. Sismik Yöntemlerle Müsaade Edilebilir Dinamik Zemin Taşıma Kapasitesi ve Oturmasının Saptanması. Jeofizik Dergisi, 4, 9, 55-91

Kıncal, C. (2006). The use of gis in field use oriented studies. Proceedings of the 4th GIS days in Turkey, Fatih University, Istanbul, Turkey, 558.

Kıncal, C., Koca, Y. M., Özyalın, Ş. (2007). Armutalanı (Marmaris-Muğla) Beldesi Sahasının Yerleşim Amaçlı Arazi Kullanım Haritasının Coğrafi Bilgi Sistemleri (CBS) Destekli Hazırlanması. TMMOB Harita ve Kadastro Mühendisleri Odası Ulusal Coğrafi Bilgi Sistemleri Kongresi, 145-160.

Kıyak, A. (2008). Coğrafi bilgi sistemleri kullanılarak adapazarı ilinin mikro zemin parametre haritalarının hazırlanması (Master's thesis, Sakarya Üniversitesi).

Koçak, B., Naimi, S. (2020). Vp Hızıyla Elde Edilen Birim Hacim Ağırlık Değerinin Katsayı Atanarak Belirlenmesi. Journal of the Institute of Science and Technology, 10(4), 2704-2713.

Kurnaz, T.F. (2011). Geotechnical microzonation of Istanbul Esenler soils based on geographical information systems, Sakarya University Graduate School of Natural and Applied Sciences, Ph.D. Thesis, Sakarya.

Marx, C. (1992). Applications of earthquake hazard maps to land-use planning and regulations in Seattle. Seattle Planning Department, 25.

Midorikawa, S. (1987). Prediction of isoseismal map in Kanto plain doe to hypothetical earthquake. Journal of Structural Dynamics, 33B, 43-48.

Nixon, I.K., “Standard penetration test: State-of-the-art report”, Proceedings of the 2nd Europen Symposium on Penetration Testing, Amsterdam, Netherlands, 3-21, May 1982.

Patra, S., Mishra, P., Mahapatra, S. C. (2018). Delineation of groundwater potential zone for sustainable development: A case study from Ganga Alluvial Plain covering Hooghly district of India using remote sensing, geographic information system and analytic hierarchy process. Journal of Cleaner Production, 172, 2485-2502.

Perinçek, D., 1979. Guidebook for Excursion (B), Interrelations of the Arab and Anatolian plates: First Geology Congress on Middle East Tecknical University, Ankara

Rodell, M., Velicogna, I., & Famiglietti, J. S. (2009). Satellite-based estimates of groundwater depletion in India. Nature, 460(7258), 999-1002.

Rošer, J., & Gosar, A. (2010). Determination of $V_{s,30}$ for seismic ground classification in the Ljubljana area, Slovenia. Acta Geotechnica Slovenica, 7(1), 60-76.

Sartirana, D., Rotiroti, M., Zanotti, C., Bonomi, T., Fumagalli, L., & De Amicis, M., A 3D Geodatabase for Urban Underground Infrastructures: Implementation and Application to Groundwater Management in Milan Metropolitan Area, ISPRS International Journal of Geo-Information, 9 (10), 609, 2020.

Seed, H.B., and Idriss, I.M., (1971), Simplified procedure for evaluation soil liquefaction potential. Journal of the Soil Mechanics and Foundations Division ASCE, 97, 1249-1273.

Şen, G. (2004). Gümüşler Belediyesi mücavir alanının sıvılaşma analizi ve coğrafi bilgi sisteminde uygulaması (Master's thesis, Pamukkale Üniversitesi Fen Bilimleri Enstitüsü).

Şengül, T., Karabaş, B. 2021. Kütahya Merkez İlçesinde Sıvılaşma Potansiyelinin Coğrafi Bilgi Sistemi ile İncelenmesi. Bilecik Şeyh Edebali Üniversitesi Fen Bilimleri Dergisi, 8(2), 817-825.

Sert, S., Ozocak, A. and Ural N. (2006). Use of geographic information systems with geotechnical purposes in Adapazari. Geographic Information Systems Forensics Days, Fatih University, Istanbul, Turkey, 8.

Sivrikaya, O., Aydin, E., Turker, H. (2021). Improvement of dynamic response of structures on sandy soil by means of viscous dampers. Iranian Journal of Science and Technology, Transactions of Civil Engineering, 45(2), 741-756.

Tarhan, N.(1989a). Hınıs-Varto (Erzurum-Muş) dolayının jeolojisi ve petrolojisi (Yayımlanmamış Doktora Tezi), İ.Ü Fen Bilimleri Enstitüsü, İstanbul.DEM

Tarhan, N., 2008, 1/100.000 scaled Turkey Geological Map Series with Distortion, Erzincan-J43 map: MTA General Manager, Department of Geological Studies, Ankara.

Taylor, R. G., Scanlon, B., Döll, P., Rodell, M., Van Beek, R., Wada, Y., ... & Treidel, H. (2013). Ground water and climate change. Nature climate change, 3(4), 322-329.

Tecim, V. (1999). Bilgi Teknolojilerinde Yeni Bir Gelişme: Coğrafi Bilgi Sistemleri Ve Bilgi Sistemleri Arasindaki Yeri. Dokuz Eylül Üniversitesi İktisadi İdari Bilimler Fakültesi Dergisi, 14(1), 1-12.

Terzaghi, K. P., & Peck, P. (1967). RB (1967). Soil mechanics in engineering practice.

Tuladhar, R., Yamazaki, F., Warnitchai, P., & Saita, J. (2004). Seismic microzonation of the greater Bangkok area using microtremor observations. Earthquake engineering & structural dynamics, 33(2), 211-225.

Ulusay, R. (2000). Soil liquefaction, Blue Planet Popular Science Magazine, TMMOB Chamber of Geological Engineers Publication, 1, 34-45.

Velazquez, H. A. (2018, May). Cálculo por método simplificado para evaluación de licuefacción en suelos limosos, inducidos por cargas cíclicas y gravitacionales (Método simplificado de Presas SEED-IDRISS, 1982, Wang, 1979). Comité Argentino De Presas–IX Congreso Argentino de Y Aprovechamientos Hidroeléctricos, Mendoza. 16-19 de mayo de 2018.

Yazgan, E. V. R. E. N., Michard, A. N. D. R. É., Whitechurch, H. U. B. E. R. T., & Montigny, R. (1983). Le Taurus de Malatya (Turquie orientale) élément de la suture sud-téthysienne. Bulletin de la Société géologique de France, 25, 59-69.

Yılmaz, H. (2019). Siirt ili Eruh ilçesi heyelan alanının jeolojik, jeoteknik incelenmesi ve şev stabilite analizi (Master's thesis, Batman Üniversitesi Fen Bilimleri Enstitüsü).

Yomralioglu, T., Colak, E. H., & Aydinoglu, A. C. (2009). Geo-relationship between cancer cases and the environment by GIS: A case study of Trabzon in Turkey. International journal of environmental research and public health, 6(12), 3190-3204.

Youd, T. L., Idriss, I. M., Andrus, R. D., Arango, I., Castro, G., Christian, J. T., Dobry, R., Liam Finn, W. D., Harder Jr., L. F., Hynes, M. E., Ishihara, K., Koester, J. P., Liao, S. S. C., Marcuson III, W. F., Martin, G. R., Mitchell, J. K., Moriwaki, Y., Power, M. S., Robertson, P. K., Seed, R. B. and Stokoe II K. H. (2001). Liquefaction resistance of soils: summary report from the 1996 NCEER and 1998 NCEER/NSF workshops on evaluation of liquefaction resistance of soils, Journal of Geotechnical and Geo-Environmental Engineering ASCE, 127, 817-832.

EKLER

EK-1 Tunceli Belediyesi Merkez (2. Bölge) İmar Planına Esas Jeolojik-Jeoteknik Etüt Raporu izin belgesi

T.C.
TUNCELİ BELEDİYE BAŞKANLIĞI
İmar ve Şehircilik Müdürlüğü

Sayı : 19984903-060.04-7075 2.9..09..202
Konu : Dilekçe

Sayın Soner KORKMAZ
Çaydaçıra Mh. Adnan Kahveci Bul. No:24/15
ELAZIĞ

İlgi : 14.09.2021 tarih ve 6813 sayılı yazınız.

Tunceli İlinin ilçelerinin imar planına esas jeolojik-jeoteknik etüt raporlarını Hasan Kalyoncu Üniversitesi İnşaat Mühendisliği Yüksek Lisans çalışmalarında kullanmak üzere izin istemektesiniz.

Belediyemiz sınırları dahilinde yer alan Merkez Mahallelerimizin bir kısmını kapsayan alanda yapılan imar planına esas jeolojik-jeoteknik etüt raporları 2017 yılında onaylanmış olup, ilgili çalışmadan faydalanmanızda Belediyemizce herhangi bir sakınca görülmemiş olup, çalışma ile ilgili istenilen dökümanlar CD ortamında yazımız ekinde sunulmuştur.

Bilgilerinizi ve gereğini rica ederim.

Fatih Mehmet MAÇOĞLU
Belediye Başkanı

Ek: 1 Ad. CD

Moğultay Mahallesi Okullar Caddesi No : 3 Tunceli
Telefon No: (428)212 13 27 Faks No: (428)212 10 17
e-Posta: malihizmetler@tunceli.bel.tr İnternet Adresi: https://www.tunceli.bel.tr
Kep Adresi: tuncelibelediyesi@hs01.kep.tr

Bilgi için: Berrak YILMAZ
Belediye İşçisi
Telefon No: